


2014

Chmp1 negatively regulates Epidermal Growth Factor signaling in the *Drosophila* wing

Meagan Elisabeth Valentine
lester64@marshall.edu

Follow this and additional works at: <http://mds.marshall.edu/etd>

 Part of the [Biological Phenomena, Cell Phenomena, and Immunity Commons](#), [Cell and Developmental Biology Commons](#), and the [Genetic Processes Commons](#)

Recommended Citation

Valentine, Meagan Elisabeth, "Chmp1 negatively regulates Epidermal Growth Factor signaling in the *Drosophila* wing" (2014). *Theses, Dissertations and Capstones*. Paper 802.

CHMP1 NEGATIVELY REGULATES EPIDERMAL GROWTH FACTOR SIGNALING IN
THE DROSOPHILA WING

A dissertation submitted to
the Graduate College of
Marshall University

In partial fulfillment of
the requirements for the degree of Doctor of Philosophy

in

Biomedical Sciences

by
Meagan Elisabeth Valentine

Approved by
Dr. Simon Collier, Committee Chairperson
Dr. Beverly Delidow
Dr. Richard Egleton
Dr. Todd Green
Dr. Guo-Zhang Zhu

Marshall University
May 2014

ACKNOWLEDGEMENTS

Thanks to the Biomedical Sciences program for not only funding my education, but for providing the outstanding resources and teachers to promote my education and scientific training. Within this program there are numerous faculty and staff members who are friendly and willing to help wherever they can.

I especially extend my gratitude to my committee, Drs. Beverly Delidow, Todd Green, Richard Egleton, and Guo-Zhang Zhu. They were consistently supportive and encouraging. Their advice was invaluable and when I needed help, be it teaching a class in which I was the only student, or writing last minute recommendation letters, they were reliable and always came through. I thank my committee for listening to me talk during meetings and seminars, for being approachable, and for being critical without being harsh.

Special thanks to my advisor, Dr. Simon Collier. Without his guidance my educational career would have taken a different route. As an undergraduate, he encouraged me to pursue a Master's degree, and then as a Master's student, he encouraged me to pursue a PhD. He has supported me academically, financially, and personally throughout my scientific training. I thank him for giving me my space, for weekly meetings, for weekend conferences, for being interested in my ideas, and for editing numerous powerpoints, lots of posters, a few grant applications, multiple papers, and my dissertation. I especially appreciate his not abandoning me when he got a job at the University of Cambridge. He worked with me, Marshall University, and the University of Cambridge to get me to England for the incredible experience of working overseas for 6 months to finish my PhD. I would also like to thank the University of Cambridge, especially Drs. Cahir O'Kane and Steven Russell, for inviting me to Cambridge to finish up my PhD work with Simon, and for also providing resources and space for my research and writing.

I would like to thank all who have been through the Collier lab, especially Justin Hogan, Andrea Belalcazar, Shaimar Gonzalez, David Neff, and Jared Galloway, for being such great listeners and for all of their help and advice in the lab.

Last but certainly not least, I would like to thank my family and friends – they made this possible, supporting me throughout my entire education. Thanks to my father, Jim Lester, for sparking my interest in science as a kid. Thanks to my mother, Dreama Lester, for being a friend and work-out partner when I needed to get away from the lab. Thanks to my brothers, J.R. and Cameron Lester, for being good friends and for listening to me ramble about science that they didn't care a thing about. Thanks especially to my wonderful husband, Michael. He has been my rock. He brings me joy. He listens when I am frustrated, encourages me when I am insecure, gives me perspective when I'm bogged down in the details, and is patient when I'm stressed and irritable. Thanks to Michael's family too, who make me laugh so hard, and have shown a genuine interest in me and my research.

TABLE OF CONTENTS

Acknowledgements.....	ii
List of Figures.....	viii
List of Tables	xi
List of Abbreviations	xii
Abstract.....	xvi
Chapter 1. Background and Introduction.....	1
I. Fly development	2
A. Life cycle.....	2
B. Wing development	3
C. Eye development.....	6
II. Fly genetics	7
A. Balancer chromosomes.....	8
B. UAS-Gal4.....	9
C. RNAi in flies.....	11
D. FLP/FRT.....	12
E. Variations of FLP/FRT.....	14
F. Fly crosses.....	15
III. The DER pathway	18
IV. The ESCRT machinery.....	21
V. Structure and function of Chmp1	24
A. Chmp1 structure.....	24
B. Chmp1 and survival.....	25

C. Control of growth.....	26
D. Chmp1 in the nucleus	28
E. Chmp1 in the cytoplasm.....	30
F. Chmp1 and mitosis.....	31
G. Conserved binding partners of Chmp1	31
H. Binding partners of Drosophila Chmp1	33
Chapter 2: Rationale, Specific Aims, and Hypotheses	35
I. Rationale.....	35
II. Specific Aims and Experimental Design	37
III. Hypotheses	40
Chapter 3: Materials and Methods.....	42
I. Alignment of Chmp1 sequences.....	42
II. Generation of transgenic fly lines	42
III. Fly stocks and genetics	43
IV. Mounting fly wings	45
V. Measurements and statistics.....	45
VI. Immunohistochemistry of embryos	46
VII. Immunohistochemistry of imaginal discs	47
VIII. Antibodies used	49
IX. Eye preparation and sectioning	49
Chapter 4: Results.....	51
I. Chmp1 is conserved and essential.....	51
II. <i>Chmp1</i> knockdown produces a cell fate change in the wing.....	55

III.	Chmp1 interacts with regulators of DER signaling	71
IV.	Chmp1 negatively regulates DER signaling.....	78
V.	Over-expression of <i>Chmp1</i>	85
VI.	Investigation into Chmp1 regulation of Notch-Delta signaling.....	91
VII.	Testing for interactions between <i>Chmp1</i> and regulators of the DER using <i>Chmp1</i> over-expression fly lines.....	104
VIII.	<i>Chmp1</i> knockdown in the eye disrupts ommatidia	107
IX.	Drosophila Chmp1 localizes apically and to the cell membrane	111
X.	Chmp1 localizes to the late endosome	115
Chapter 5: Discussion.....		118
I.	Chmp1 is essential.....	119
II.	Chmp1 regulates wing vein cell fate decision	120
III.	Chmp1 and DER signaling	121
IV.	Clones of <i>Chmp1</i> knockdown in the wing.....	125
V.	Chmp1 and Notch signaling.....	127
VI.	HM-Chmp1 localization.....	128
VII.	Concluding remarks	131
X.	Possible future studies	132
Chapter 6: Projects investigating Frizzled Planar Cell Polarity Signaling in Drosophila..		136
I.	Background on PCP.....	136
II.	The Fz PCP pathway in the Drosophila wing.....	137
III.	The Fz PCP pathway in the Drosophila eye	138
IV.	Project 1: Chmp1 may regulate Fz PCP signaling.....	140

V.	Project 2: Expression of <i>pk</i> and <i>sple</i> in pupal wings	146
VI.	Project 3: Pk and Sple protein isoforms in patterning of the <i>Drosophila</i> eye	149
VII.	Project 4: Localization of the Sple isoform in pupal wing cells	151
Appendix		156
	IRB approval letter	156
References		157

LIST OF FIGURES

Figure 1.1 Timeline of major developments in <i>Drosophila</i> research	2
Figure 1.2 Development of the <i>Drosophila</i> wing.....	5
Figure 1.3 Development of the <i>Drosophila</i> eye	7
Figure 1.4 The UAS-Gal4 System	10
Figure 1.5 The Inducible FLP/FRT System: generate homozygous clones in heterozygous tissue.....	13
Figure 1.6 Variation of the FLP/FRT system with UAS-Gal4.....	15
Figure 1.7 Examples of crosses in <i>Drosophila</i>	18
Figure 1.8 A simplified diagram of the DER pathway.....	20
Figure 1.9 ESCRT-III function on the endosome	23
Figure 1.10 Chmp1 protein structure in <i>Drosophila</i>	25
Figure 2.1 Experimental Design.....	40
Figure 3.1 Orientation of fly heads in resin block for eye sectioning	50
Figure 4.1 Chmp1 is conserved.....	52
Figure 4.2 Cross design to test ubiquitous <i>Chmp1</i> knockdown	54
Figure 4.3 Expression patterns of wing drivers.....	56
Figure 4.4 <i>Chmp1</i> knockdown cross design	57
Figure 4.5 <i>Chmp1</i> knockdown at 30°C.....	59
Figure 4.6 Cross design for <i>Chmp1</i> knockdown in <i>Chmp1</i> heterozygous background	60
Figure 4.7 <i>Chmp1</i> knockdown results in thickened wing veins.....	62
Figure 4.8 <i>Chmp1</i> knockdown in wings heterozygous for the <i>Chmp1</i> gene: wing vein measurements.....	63

Figure 4.9 Cross design for rescue of <i>Chmp1</i> knockdown with <i>Chmp1</i> over-expression.....	66
Figure 4.10 <i>Chmp1</i> over-expression rescues the <i>Chmp1</i> knockdown phenotype	69
Figure 4.11 <i>Chmp1</i> over-expression rescues <i>Chmp1</i> knockdown: wing vein measurements	71
Figure 4.12 Cross design testing for interaction between <i>Chmp1</i> and DER regulators	73
Figure 4.13 <i>Chmp1</i> interacts with regulators of DER signaling in <i>Drosophila</i>	76
Figure 4.14 <i>Chmp1</i> knockdown and DER signaling regulators wing vein measurements	78
Figure 4.15 Cross design for <i>Chmp1</i> knockdown marked with GFP in the posterior wing disc	79
Figure 4.16 Cross design for generating <i>Chmp1</i> knockdown clones marked with GFP in wing discs.....	80
Figure 4.17 <i>Chmp1</i> knockdown reduced Bs staining in imaginal discs	82
Figure 4.18 Cross design for <i>Chmp1</i> and <i>forked</i> knockdown clones in the adult wing.....	83
Figure 4.19 Clones of <i>Chmp1</i> and <i>forked</i> knockdown in the adult wing.....	85
Figure 4.20 Cross design for achieving <i>Chmp1</i> over-expression in the <i>Drosophila</i> wing	86
Figure 4.21 <i>Chmp1</i> over-expression with <i>MS1096-Gal4</i> in the <i>Drosophila</i> wing causes vein deltas	88
Figure 4.22 <i>Chmp1</i> over-expression in the <i>Drosophila</i> wing causes deltas	90
Figure 4.23 Rare phenotypes caused by <i>Chmp1</i> over-expression in the <i>Drosophila</i> wing	91
Figure 4.24 Cross design to test for an interaction between <i>Chmp1</i> and Notch using the <i>MS1096-Gal4</i> driver	93
Figure 4.25 Cross design to test for an interaction between <i>Chmp1</i> and Notch using the <i>dpp-Gal4</i> driver	96
Figure 4.26 Variable notching phenotypes associated with various genotypes.....	98

Figure 4.27 Control cross design to show interaction between Car and Deltex	101
Figure 4.28 Cross design to test for an interaction between Chmp1 and Deltex.....	102
Figure 4.29 Interaction between Chmp1 and Deltex	104
Figure 4.30 Cross design using <i>Chmp1</i> over-expression transgenes to test for an interaction between Chmp1 and DER regulators	105
Figure 4.31 <i>Chmp1</i> over-expression and DER regulators	107
Figure 4.32 Cross design for <i>Chmp1</i> knockdown in <i>Drosophila</i> eye.....	108
Figure 4.33 <i>Chmp1</i> knockdown and over-expression in the <i>Drosophila</i> eye.....	110
Figure 4.34 Cross design for HM- <i>Chmp1</i> expression in both the anterior of embryonic parasegments and the posterior wing disc in larvae	112
Figure 4.35 Localization of HM- <i>Chmp1</i> in wing imaginal discs	114
Figure 4.36 Cross design for HM- <i>Chmp1</i> and YFP-Rab9 expression in the anterior of embryonic parasegments	116
Figure 4.37 Relative subcellular localizations of HM- <i>Chmp1</i> with endosome markers and Vps4	117
Figure 5.1 Model for <i>Chmp1</i> regulation of the DER through the MVB pathway.....	132
Figure 6.1 The Fz PCP pathway polarizes cells of the <i>Drosophila</i> wing and eye	140
Figure 6.2 <i>Chmp1</i> may regulate Fz PCP signaling.....	145
Figure 6.3 Genetic structure of the <i>prickle</i> gene	146
Figure 6.4 Amplification of <i>pk</i> , <i>sple</i> , and <i>actin</i> cDNA fragments.....	149
Figure 6.5 Pk and Sple in Fz PCP signaling in the <i>Drosophila</i> eye.....	151
Figure 6.6 Sple localization in the <i>Drosophila</i> pupal wing.....	155

LIST OF TABLES

Table 1.1 The effect of temperature on life cycle length in <i>Drosophila</i>	3
Table 1.2 Summary of balancer chromosomes and dominant markers used in this research.....	9
Table 1.3 Protein interactions with <i>Drosophila</i> Chmp1	34
Table 3.1 Fly stocks used	44
Table 3.2 Fly lines generated in this study.....	45
Table 3.3 Antibodies used for immunostaining	49
Table 4.1 <i>Chmp1</i> over-expression can rescue the <i>Chmp1</i> knockdown phenotype	70
Table 4.2 Notching frequencies of individual genotypes.....	99
Table 6.1 Primers used to amplify <i>pk</i> , <i>sple</i> , and <i>actin</i> cDNA	147

LIST OF ABBREVIATIONS

A498	Renal Cell Carcinoma cell line
Act5c	Actin5c
acv	Anterior Cross Vein
AMSH	Associated Molecule with the SH3-domain of STAM
Aos	Argos
AP	Anteroposterior
ATM	Ataxia Telangiectasia Mutated
ATRA	All-trans Retinoic Acid
B ¹	Bar
Bc	Black Cell
BMI1	B Lymphoma Moloney Murine Leukemia Virus Insertion Region 1 Homolog
Bs	Blistered
BSA	Bovine Serum Albumin
Car	Carnation
CCT	Phosphocholine Cytidylyltransferase
ce	Columnar Epithelium
Chmp1	Chromatin Modifying Protein, Charged Multivesicular Protein
CRBP-1	Retinol Binding Protein-1
Cy	Curly
CyO	Curly of Oster
D ¹	Dichaete
DER	Drosophila Epidermal Growth Factor Receptor
Dgo	Diego
DNA	Deoxyribonucleic acid
Dox	Doxycycline
DPiM	Drosophila Protein Interaction Map
Dpp	Decapentaplegic
Drk	Downstream of Receptor Kinase
Ds	Dachsous
Dsh	Dishevelled
DSOR1	Downstream of Ras1
DSRF	Drosophila Serum Response Factor
dsRNA	double stranded RNA
Dx	Deltex
EcR-293	Human Embryonic Kidney cell line, expresses Ecdysone Receptor
EGFR	Epidermal Growth Factor Receptor
en	Engrailed

ESCRT	Endosomal Sorting Complex Required for Transport
F1	First Filial Generation
F2	Second Filial Generation
F3	Third Filial Generation
FLPase	FLP recombinase
FM	First Multiple
Fmi	Flamingo
FRT	FLPase Recombination Target
Ft	Fat
Fz	Frizzled
GFP	Green Fluorescent Protein
Gla	Glazed
GMM	Gary's Magic Mountant
GOI	Gene of Interest
hAPF	hours After Pupal Formation
HEK-293T	Human Embryonic Kidney cell line, non-tumorigenic
Hh	Hedgehog
HM	His-Myc
hpRNA	hairpin RNA
Hrs	Hepatocyte Growth Factor Receptor Substrate
hs	heat shock
hs-flp	heat shock FLP recombinase
If	Irregular Facets
ILV	Intralumenal Vesicle
INK4	Inhibitor of CDK4
kD	kiloDaltons
Kek-1	Kekkon-1
LIP5	Lyst-Interacting Protein 5
m	Myoblast
MAPK	Mitogen-Activated Protein Kinase
MF	Morphogenetic Furrow
MIM	MIT-Interacting Motif
MIT	Microtubule Interaction and Transport
mPcl1	mammalian Polycomblike
mRNA	messenger RNA
MVB	multivesicular body
NICD	Notch Intracellular Domain
NLS	Nuclear Localization Sequence
P	Parental Generation
PanC1	Human Pancreatic Ductal Tumor cell line

PBS	Phosphate Buffer Saline
PBST	Phosphate Buffer Saline with Triton-X
PcG	Polycomb Group
Pcl	Polycomblike
PCP	Planar Cell Polarity
PCR	Polymerase Chain Reaction
pcv	Posterior Cross Vein
Pk	Prickle
pm	Peripodial Membrane
PM	Plasma Membrane
ptc	Patched
qPCR	Quantitative real-time PCR
Rho	Rhomboid
RISC	RNA Induced Silencing Complex
RNA	Ribonucleic Acid
RNAi	RNA interference
RT	Reverse Transcription
RTK	Receptor Tyrosine Kinase
Sal1	Supernumerary Aleurone Layers 1
Sb	Stubble
Ser	Serrate
shRNA	short hairpin RNA
siRNA	short interfering RNA
SKD1	Suppressor of K ⁺ Transport Growth Defect
SM	Second Multiple
SOS	Son of Sevenless
Sple	Spiny Legs
Stan	Starry night
Stbm	Strabismus
Sty	Sprouty
Tb	Tubby
TM	Third Multiple
TRiP	Transgenic RNAi Project
Tsg101	Tumor Susceptibility Gene 101
UAS	Upstream Activating Sequence
UBPY	Ubiquitin-specific processing Protease Y
Vang	Van-gogh
VDRC	Vienna Drosophila Resource Center
Vn	Vein
Vps4	Vacuolar Protein Sorting 4

Vtalp

Wg

Wg^{Sp1}

YFP

Vps Twenty Associated 1 Protein

Wingless

Sternopleural

Yellow Fluorescent Protein

ABSTRACT

A critical step in cellular signaling through transmembrane receptors is the down-regulation of activated receptors through the multivesicular body (MVB) pathway to the lysosome. MVB generation is mediated by the highly conserved ESCRT (0, I, II, and III) protein complexes. Though the ESCRT-III complex provides the core function of the ESCRT machinery, it is the least characterized of the ESCRT complexes. The Chmp1 protein is an ESCRT-III component and a putative tumor suppressor that has been linked to pancreatic and renal cancers in humans. However, published data on Chmp1 activity are conflicting and its role during tissue development is not well defined.

Drosophila melanogaster (the common fruit fly) provides a powerful model system for investigating the function of genes involved in human development and disease. In this study, knockdown and over-expression techniques were used to investigate the function of Chmp1 in *Drosophila*. RNAi was used to reduce *Chmp1* expression, and transgenic fly lines that allow for expression of either wild-type or epitope tagged Chmp1 were used to investigate over-expression, as well as the subcellular localization of Chmp1.

Knockdown of *Chmp1* expression using RNAi was lethal in the fly, suggesting that *Chmp1* is an essential gene for *Drosophila* development. In the wing, loss of Chmp1 activity caused a cell fate change from intervein to vein, which was likely a result of de-regulation of the *Drosophila* Epidermal Growth Factor Receptor (DER) pathway. Genetic interactions between Chmp1 and regulators of DER signaling suggest that Chmp1 negatively regulates DER signaling. Furthermore, *Chmp1* knockdown also decreased Blistered expression, which is repressed by DER signaling.

Over-expression of *Chmp1* had mild phenotypic effects, suggesting that dosage of Chmp1 is not critical for cellular function. Some of the epitope tagged Chmp1 protein was detected at the late endosome in *Drosophila* embryonic epithelial cells. This is consistent with Chmp1 functioning as an ESCRT-III component during MVB formation. Therefore, *Drosophila* Chmp1 may negatively regulate DER signaling through its role in MVB formation as an ESCRT-III component.

CHAPTER 1

BACKGROUND AND INTRODUCTION

For over 100 years *Drosophila melanogaster*, or the common fruit fly, has been used as model for biological and medical research (Figure 1.1). From Thomas Hunt Morgan's fly room at Columbia University in the early 1900's to the sequencing of the genome in 2000, the fruit fly has become one of the most studied organisms around the world. The sequencing of the fly genome provided an important resource to biologists and identified about 14,000 genes [4]. After many years of work on *Drosophila*, today's researchers are supplied with an extensive base of knowledge of this species, along with many sophisticated genetic and molecular tools that have been developed for studying gene and protein function, many of which are unique to this organism [2]. Although *Drosophila* is particularly useful in the fields of genetics and developmental biology, it is increasingly becoming a useful model for human disease, especially neurodegenerative disorders [5, 6]. Importantly, there is a great deal of homology between human genes and *Drosophila* genes; it is thought that about 75% of human disease genes have homologues in *Drosophila* [7, 8].

In the research presented in this dissertation, *Drosophila* was used as a model organism to study proteins involved in human development and disease. Therefore, it is appropriate to describe relevant aspects of *Drosophila* research, including the fly life cycle, the development and anatomy of the eye and wing, and the genetic tools and techniques used in these studies.

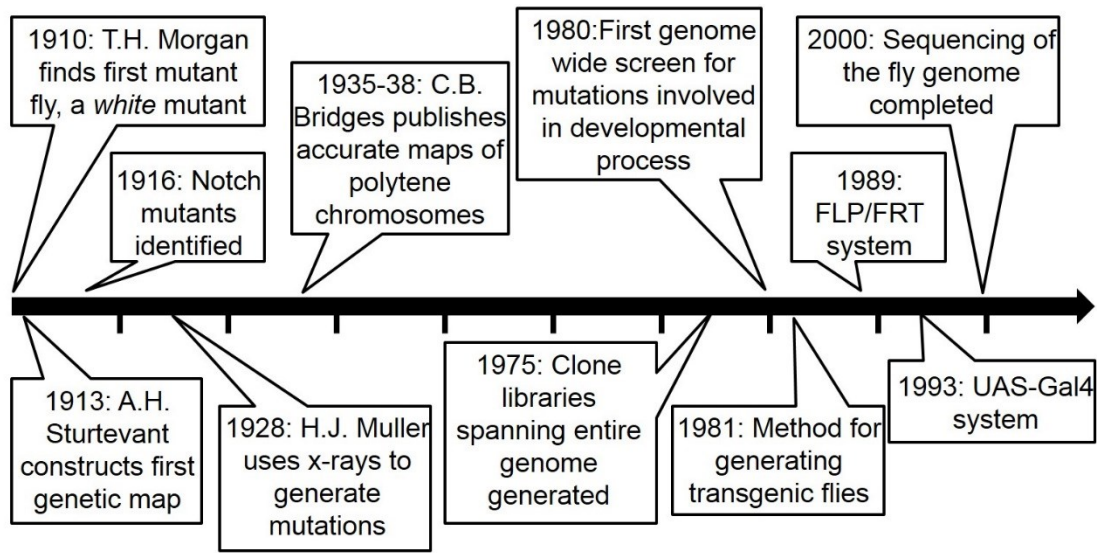


Figure 1.1 Timeline of major developments in *Drosophila* research [9, 10]

I. Fly development

The short life cycle of the fruit fly is one of the attributes that make it such a fine model organism. *Drosophila* development is well studied and includes multiple stages: embryogenesis, three instar larval stages, the pupal stage, and adult. Under ideal conditions, the entire life cycle is completed in 9-10 days, allowing for the analysis of multiple generations over a short period of time.

A. Life cycle

The length of the *Drosophila* life cycle is temperature dependent, completing in only 10 days at room temperature (Table 1.1) [11]. The life cycle begins with embryogenesis (described in [12]). There are 17 well documented stages of embryogenesis that take place in 21-22 hours at 25°C [13]. Early embryonic cellular divisions are synchronous and rapid, occurring nearly every 10 minutes. Division of the cytoplasm does not occur at this early stage, and consequently a single multinucleate cell, or syncytium, is formed. After 13 divisions forming about 6000 nuclei,

cellularization begins, which is followed by gastrulation and segmental patterning along the anteroposterior axis of the embryo. Embryogenesis is followed by three instar larval stages, each with a molt in between. The larval stages are followed a very short prepupal period before progressing on to the pupal stage. Morphogenesis from larva to fly takes place in the pupal stage.

During embryogenesis, tissues called imaginal discs form. These tissues will become most of the external adult structures, e.g., the eyes, antennas, wing, legs, etc. Imaginal discs grow and become patterned throughout the larval and pupal stages.

Temperature	Length of life cycle
18°C	19 days
25°C	9-10 days
28°C	8-9 days
30°C	7-8 days

Table 1.1 The effect of temperature on life cycle length in *Drosophila*

B. Wing development

In most of the studies presented in this dissertation, the developing or adult *Drosophila* wing was used to investigate the function of the *Drosophila* Chmp1 protein. The adult *Drosophila* wing is a cuticular structure that is quite a lot like a flattened balloon (wing development reviewed in [14, 15]). It has opposing dorsal and ventral surfaces, both decorated with a regular array of distally-pointing hairs (Figure 1.2A and B). The major cell types that compose the adult *Drosophila* wing are vein cells and intervein cells. The vein cells form conduits called wing veins that span the surface of the wing. The wing veins provide rigidity and support for the wing, and also carry trachea and neurons. There are four longitudinal wing veins (L2-L5), two marginal wing veins (L1 and L6), and two shorter transverse veins (anterior cross vein [acv] and posterior cross vein [pcv]) (Figure 1.2A). The longitudinal veins L3, L5, and

distal portion of L4 are positioned on the dorsal surface of the wing, while L2 and the remainder of L4 are on the ventral surface of the wing.

Wing development begins in the embryo, when imaginal disc precursor cells are specified. As the larva grows, the wing disc becomes larger through cell proliferation, and cell fates become established through activation of and interaction between many signaling pathways, including Decapentaplegic (Dpp, Bone Morphogenetic Protein [BMP] in humans) signaling, Wingless (Wg, Wnt in humans) signaling, Hedgehog (Hh) signaling, the Drosophila Epidermal Growth Factor Receptor (DER) pathway, Notch signaling, and the Frizzled (Fz) Planar Cell Polarity (PCP) pathway. The mature wing disc is a pear shaped tissue that can be divided into three parts, each giving rise to different structures of the adult fly: the wing pouch, which will form the wing blade; the hinge region, which will form the wing hinge; and the body wall region, which is composed of cells that will become part of the thorax (Figure 1.2C). The wing disc is composed of three major types of cells: disc proper cells, which are columnar epithelial cells that give rise to the epidermis in the adult fly and make up the majority of the disc, including the wing pouch; peripodial cells, which are squamous cells that form a thin membrane overlaying the wing disc; and adepithelial cells, which are myoblasts that will form the trachea and flight muscles (Figure 1.2D).

DER, Notch, Wg, Hh, and Dpp signaling pathways interact to form an adult wing with the wild-type wing vein pattern (reviewed in [14, 15]). First, provein and intervein territories are established in the imaginal wing disc. The proveins are broad stripes, 5-6 cells in width that are vein competent, i.e., they have the potential to differentiate into wing vein [16]. The DER and Notch signaling pathways interact extensively during wing vein specification. DER signaling is activated in the center of the provein and promotes vein cell fate, while Notch signaling is

activated in the cells bordering the provein and represses vein cell fate [17-20]. The fate of vein and intervein cells is refined to produce a narrow stripe of vein cells as development progresses through the pupal stage. In fact, some genes involved in vein specification are active quite late in pupal development, suggesting that the final choice between differentiation into vein and intervein cells is not settled until late developmental stages [15, 21].

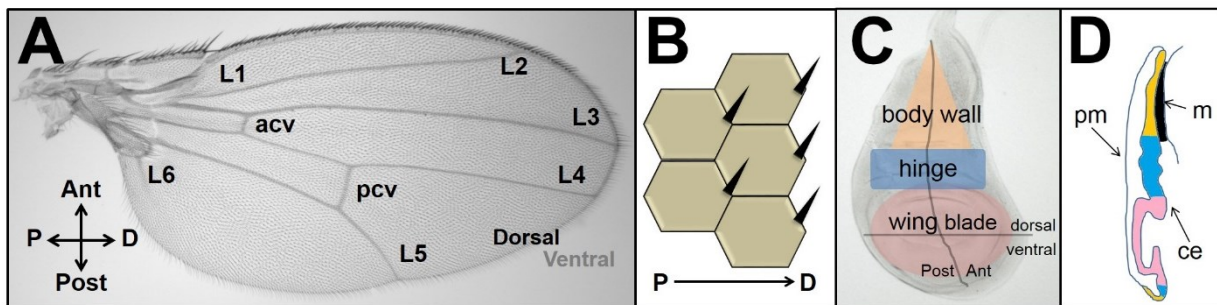


Figure 1.2 Development of the *Drosophila* wing. **A.** Light microscope image of an adult female fly wing. Wing veins are labeled: L2-L5 (longitudinal), L1 and L6 (marginal), acv and pcv (transverse). Dorsal and ventral surfaces are in the plane of the page. **B.** Individual wing cells are hexagonally packed and each cell produces a distally pointing hair. **C.** The wing imaginal disc gives rise to cells of the body wall (orange), the wing hinge (blue) and the wing blade (pink). **D.** A schematic side view of the wing disc shown in C. There are three cell layers. Cells that give rise to the body wall, wing hinge, and wing blade are ce cells. The pm is composed of squamous cells. The apical surfaces of the pm and ce cells are adjacent. m form a third layer. P is posterior, D is distal, Ant is anterior, Post is posterior, acv is anterior cross vein, pcv is posterior cross vein, pm is peripodial membrane, m is myoblast, ce is columnar epithelium. Images generated by M. Valentine. Panels C and D modified from [1].

At the pupal stage of development the wing disc undergoes major structural changes in which the layer of epithelial cells of the wing pouch everts (pushes out) to form a folded layer of epithelial cells. The basal surfaces of these cell layers adhere to one another and form the dorsal and ventral surfaces of the wing. Each wing cell produces a hair and secretes a layer of cuticle on its apical surface. When metamorphosis has completed and the fly emerges, the intervein

wing cells delaminate, die, and are cleared out of the wing, leaving behind the cuticle of the adult wing.

C. Eye development

The *Drosophila* eye was also used in these studies to investigate the function of the *Drosophila* Chmp1 protein. Like the wing, the development and structure of the eye are well understood, making it a suitable tissue for investigating protein function. The adult *Drosophila* eye is a typical insect eye, composed of around 800 hexagonal ommatidia, or facets (Figure 1.3A). Each ommatidium is composed of eight photoreceptors (R1-R8) in an asymmetric pattern, four cone cells, pigment cells, and a sensory bristle, totaling 22 cells. The ommatidia are arranged in a symmetrical fashion with respect to the equator, or the dorsal/ventral boundary of the eye, so that cells of the dorsal and ventral halves are mirror images (Figure 1.3B).

The *Drosophila* eye, like the wing, begins as a set of precursor cells specified in the embryo and grows into the eye-antennal disc during larval development (eye development reviewed in [3]). This disc gives rise to the adult eye and antenna, as well as the head capsule and mouthparts (Figure 1.3C). Throughout the first and second instar larval stages, the cells of the eye disc proliferate in an undifferentiated state. During the third instar larval stage, the cells of the eye begin to differentiate from posterior to anterior of the disc. This process appears as a wave of differentiation traveling from posterior to anterior, called the morphogenetic furrow, and is visible as an indentation in the disc (Figure 1.3C). As the morphogenetic furrow passes, ommatidial cells are recruited and specified sequentially. The first cell to differentiate is the R8 photoreceptor, followed in pairs by R2 and R5, R3 and R4, R1 and R6, and lastly R7. As differentiation occurs, the photoreceptor clusters rotate 90° away from the equator (clockwise in the dorsal half of the eye, counter-clockwise in the ventral half), producing the symmetrical

arrangement of the eye (Figure 1.3B and C). Morphogenesis occurs during the pupal stage of development, and the eye-antennal discs evert and fuse to form the head.

As in the wing disc, the development of the eye disc requires the work of many signaling pathways. For example, DER signaling is required for differentiation of all of the photoreceptor cells, except R8, and is important for proper rotation as well [22, 23]. Additionally, Fz PCP and Notch signaling are required for the R3 and R4 photoreceptor cell fate decision, which determines the chirality, or handedness, of the photoreceptor clusters, and likely direction of rotation as well [24, 25].

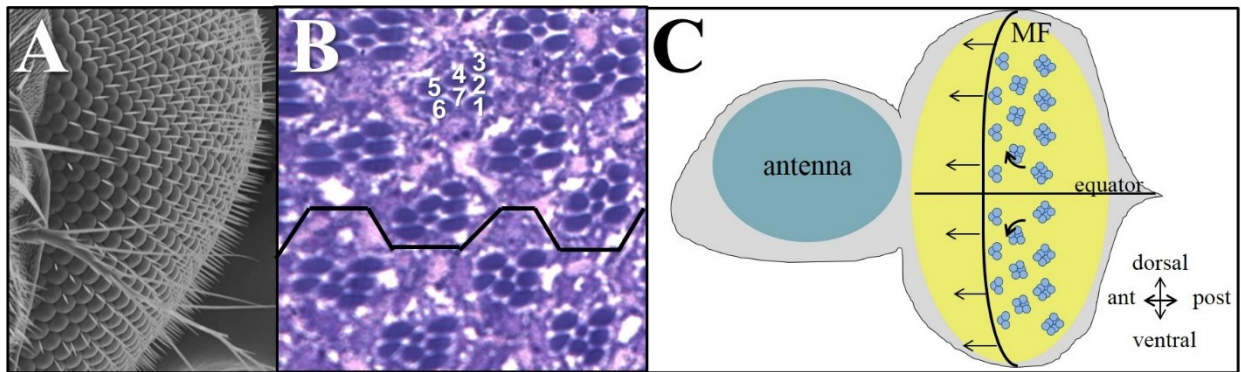


Figure 1.3 Development of the *Drosophila* eye. **A.** SEM image of the adult fly eye. Ommatidia and eye bristles are easily identified. **B.** A light microscope image of a one micron thick tangential section of a *Drosophila* eye stained with toluidine blue. Individual ommatidia are composed of 8 photoreceptor cells and arranged in a symmetrical fashion around the equator (drawn in black). **C.** The eye imaginal disc is compound and gives rise to cells of the eye (yellow) and antenna (blue). The MF progresses from posterior to anterior. Cells posterior to the MF become progressively more differentiated and begin to rotate 90° away from the equator. MF is morphogenetic furrow, ant is anterior, post is posterior. Images generated by M. Valentine. Panel C modified from [3].

II. Fly genetics

As discussed above, the quick life cycle and well-studied development of *Drosophila* make it a useful model organism. A second attribute of the fruit fly that contributes to its facility as a model organism is its genetics. *Drosophila* genetics are rather simple compared to mammals.

The fruit fly is a diploid organism and its genome includes about 14,000 genes on four chromosomes: X/Y (1), 2, 3, and 4 (very small). In most cases the fly genome carries only one copy of a gene, which eliminates problems of genetic redundancy that are often encountered in studies with mammals. Additionally, there are many useful tools and techniques that were used for the research presented here that make studying the fly particularly convenient, including balancer chromosomes, UAS-Gal4, and FLP/FRT (discussed below).

A. Balancer chromosomes

One of the advantageous tools available for *Drosophila* genetics is the balancer chromosome, which was used in nearly every fly cross performed in this research (Table 1.2). Balancer chromosomes are artificially generated chromosomes that were introduced into fly research in 1918 by H.J. Muller, who had been a student of T.H. Morgan at Columbia University [26]. Balancer chromosomes carry multiple inversions, as well as dominant marker mutations or transgenes. The multiple inversions carried by balancer chromosomes suppress recombination with wild-type homologous chromosomes during meiosis. If recombination does occur between a wild-type and a balancer chromosome, the recombinant chromosomes carry deletions, duplications and/or lose the centromere, all of which are usually lethal in the progeny. Balancer chromosomes are also homozygous lethal, so progeny receiving two copies of a balancer should not be seen in the offspring. Therefore, the advantage of balancers is that they allow for the stable maintenance of homozygous lethal mutations in a heterozygous condition as neither chromosome is homozygous viable, and the lethal mutation cannot switch to the balancer chromosome through recombination. Additionally, they carry dominant markers that allow for easy identification by phenotype and tracking of the balancer chromosome through single or multi-generation crosses (Table 1.2). There are balancer chromosomes for the first/X (first

multiple [FM]), second (second multiple [SM]), and third (third multiple [TM]) chromosomes (Table 1.2). There are also several fly lines, or balancer stocks, that carry multiple balancers and can be used to “balance” homozygous lethal mutations or transgenes.

Chromosome	Balancer	Dominant marker	Phenotype
1	<i>FM6</i>	<i>Bar (B¹)</i>	- Small eye in adult
2	<i>CyO</i>	<i>Curly (Cy)</i>	- Curly wings in adult
	<i>CyO</i>	<i>GFP</i>	- GFP expressed under actin promoter
	N/A	<i>Glazed, Black cell (GlaBc)</i>	- Glazed eye, random black cells
	N/A	<i>Irregular facets (If)</i>	- Small, rough eye
	N/A	<i>Sternopleural (wg^{Sp1})</i>	- Extra sternopleural bristles
3	<i>TM6b</i>	<i>Stubble (Sb)</i>	- Shortened bristles in adult
	<i>TM6b</i>	<i>Tubby (Tb)</i>	- Short and wide body shape in larva
	<i>TM3</i>	<i>Serrate (Ser)</i>	- Notched wing in adult
	<i>TM3b</i>	<i>Stubble (Sb)</i>	- Shortened bristles in adult
	N/A	<i>Dicheate (D¹)</i>	- Reduced or small alulae, hold wings out to sides

Table 1.2 Summary of balancer chromosomes and dominant markers used in this research. FM: first multiple, *CyO*: Curly of Oster, TM: third multiple

B. UAS-Gal4

The UAS-Gal4 system is a gene expression system that was used throughout the research presented in this dissertation [27]. This system is a standard procedure used in fly labs to control the expression of a transgene in the fly. It is a fairly simple system requiring only two components, a UAS (upstream activating sequence) enhancer and the Gal4 transcription factor (Figure 1.4). The disadvantage to the system is that it requires two transgenic fly lines. The advantage is the many combinatorial possibilities. Due to its popularity in the fly research

community, many transgenic lines have already been created and are available for immediate use.

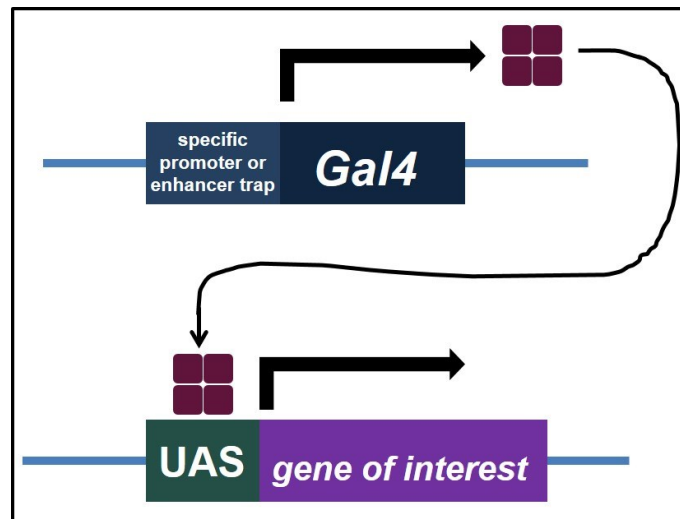


Figure 1.4 The UAS-Gal4 System. The UAS-Gal4 system requires two components: a *Gal4* transgene under the control of a specific promoter or a genomic enhancer, and the gene of interest downstream of a UAS (upstream activating sequence) enhancer. When both of these components are in a fly, Gal4 is expressed in specific cells and binds the UAS enhancer to activate expression of the gene of interest.

The UAS-Gal4 system requires that the gene of interest is under the control of a UAS enhancer (Figure 1.4). There are many plasmids available that allow for insertion of cDNA of a gene of interest downstream of the UAS enhancer, followed by insertion into the fly's genome. The UAS enhancer allows for controlled expression of the transgene, as it is only responsive to the Gal4 transcription factor (Figure 1.4). So control of expression of the transgene is dependent on control of expression of Gal4. Consequently, there are thousands of Gal4 lines, often called drivers, available from Bloomington Drosophila Stock Center at Indiana University. These lines vary in Gal4 expression, ranging from ubiquitous expression, to expression in specific tissues, to expression at specific time points during development, giving the researcher fine spatial and temporal control over transgene expression. The UAS-Gal4 system is also increasingly effective

with increasing temperature, from 18°C to 30°C. This gives control over the strength of each individual driver as well, as raising progeny at varying temperatures can provide a range of driver strengths and thus phenotype strength.

C. RNAi in flies

The UAS-Gal4 system is a useful way of controlling expression of a transgene in *Drosophila*. However, for years its main use was to study the effects of over-expression of a wild-type or mutated *Drosophila* gene, or expression of a gene from another organism. In 2007, Dietzl et al. published their work of generating a genome wide transgenic library of RNAi fly lines (Vienna *Drosophila* RNAi Center [VDRC]), which allowed for the controlled knockdown of genes in specific cells and tissues of the organism using the UAS-Gal4 system, providing an invaluable resource to the fly research community [28]. Several RNAi fly lines were used in the research presented in this dissertation, so it is appropriate to review their mechanism of action.

The RNAi fly lines were generated using short inverted DNA repeats complementary to specific mRNAs. These were inserted into a plasmid downstream of a UAS enhancer and then inserted into the genome of the fly. When transcribed, a short hairpin RNA (shRNA) is formed and cleaved by the enzyme DICER into pieces of short double stranded RNA (dsRNA), each about 21 nucleotides in length. Then, the RNAi induced silencing complex (RISC) unwinds the dsRNA into a single stranded short interfering RNA (siRNA) and uses it as a template to find the native complementary mRNA in the cell. Binding of the siRNA to its complementary mRNA induces its degradation, thus expression of the target is lowered. Since the creation of the first genome wide RNAi library, other libraries have been created, including Harvard's Transgenic RNAi Project (TRiP) [29]. Since these lines were created for use with the UAS-Gal4 system, fly

researchers now have the ability to control the intensity, tissue, and/or developmental timing of knockdown of any gene in the *Drosophila* genome.

D. FLP/FRT

Another technique available to the *Drosophila* research community is FLP/FRT, a method of targeted DNA recombination that is similar to Cre/Lox in mammals [30]. The FLP/FRT system provides a way of generating clones, or groups of cells descendant from the same parent cell, of a desired genotype within the living fly (Figure 1.5). Unlike vertebrates, cell migration and integration during development are limited in *Drosophila*. So often, daughter cells descendant from a single parent cell remain clustered together within the tissue. The FLP/FRT system can be used to cause a genomic change in the parent cell to generate, for example, clones of cells homozygous for a mutation in a heterozygous tissue, or clones of cells expressing a transgene that is not expressed in the rest of the tissue. A marker is generally used to identify the clones, making borders of clones obvious and providing a useful method for studying the effects of protein mutation and expression on cells within a developing tissue.

Like UAS-Gal4, FLP/FRT is a two-component system derived from yeast. It requires FLP recombinase (FLPase), an enzyme that mediates recombination between FLPase recombination targets (FRTs). FRTs are 34 base pair DNA sequences (GAAGTTCCTATTCTCTAGAAAGTATAGGAACTTC) and have been inserted into many places within the *Drosophila* genome. So when FLPase is expressed, it can mediate recombination between two FRT sites. Several transgenic FLPase stocks have been generated, including the commonly used *hs-FLPase* (*hs-flp*), which expresses FLPase under the control of the heat shock promoter, *hsp70*. When using *hs-flp* to generate clones in flies, an increase in

ambient temperature activates expression of FLPase. This gives the researcher temporal control over the developmental time point at which the recombination takes place.

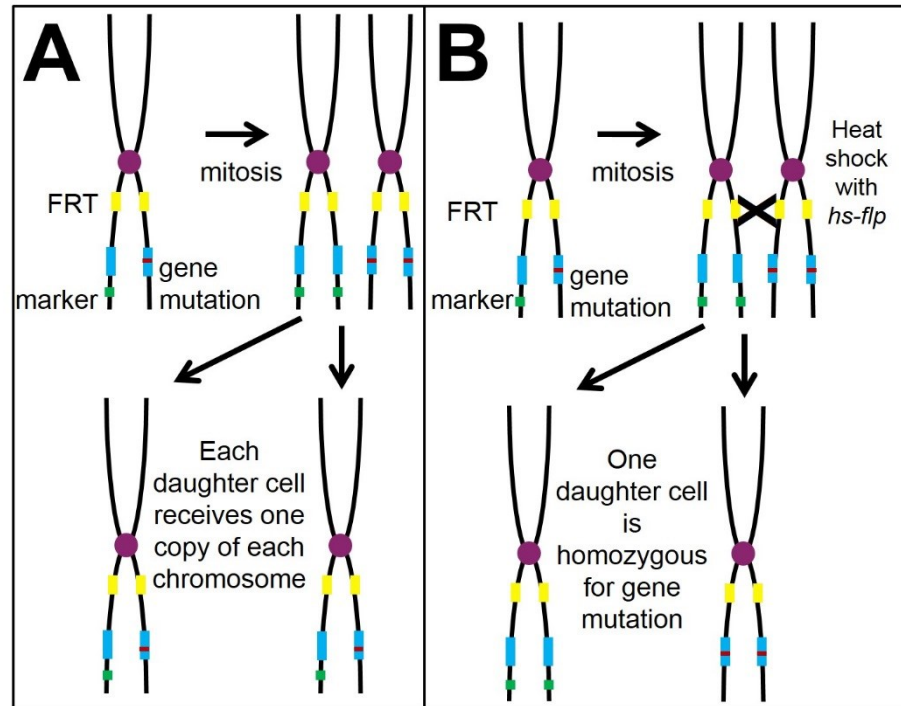


Figure 1.5 The Inducible FLP/FRT System: generate homozygous clones in heterozygous tissue. The FLP/FRT system for generating homozygous mutant clones requires two components: FRT sites on identical loci of homologous chromosomes (in yellow), and FLPase, which mediates recombination between those sites. The gene mutation of interest (in blue) must be distal to the FRT site on the chromosome, and having a visible marker such as GFP (in green) on the wild-type chromosome makes finding clones easier. **A.** During mitosis, homologous chromosomes are duplicated and the daughter cells receive one copy of each chromosome. **B.** If flies carry chromosomes with FRT sites on identical loci and *hs-flp*, heat shocking the flies during development will activate expression of FLPase, which can then mediate recombination between the two FRT sites. One of the daughter cells will receive two copies of the gene mutation of interest and no copy of the marker, while the other daughter cell receives two copies of the marker and no copy of the gene mutation of interest.

FLP/FRT recombination rates are generally quite low, so that only a few cells within a tissue experience a successful recombination event. However, the number of clones obtained can vary, depending on the induction conditions used and the position of the FRT sites. Additionally,

the recombination rate is similar for the same induction conditions, so that the size of clones generated is dependent upon the developmental time point at which FLPase was induced, i.e., clones generated at early time points will be fewer but larger, while those generated at late developmental time points will be smaller but numerous.

E. Variations of FLP/FRT

Since the development of the FLP/FRT system, variations on the system using the FLP/FRT components have been generated. When clones were generated in the research presented here, a variation which brings together the FLP/FRT and UAS-Gal4 systems was used (Figure 1.6). This merged system allowed for the generation of clones of knockdown or over-expression of the gene of interest, and allows for temporal control over the generation of those clones during development. This system required three components, two of which have already been discussed: the *hs-flp* transgene, which provided the temporal control over FLPase expression and thus clone generation, and the gene or RNAi of interest under the control of a UAS enhancer, allowing for either over-expression or knockdown. The third component was a transgene containing the Gal4 coding sequence downstream of an Actin promoter, but separated by a fragment containing a transcription stop (CD2-polyA) sequence flanked by FRT sites. This means transcription from the Actin promoter will terminate before the Gal4 coding sequence is reached. When these three transgenes are in the same fly, a heat shock activates expression of FLPase, which mediates recombination between the FRT sites, removing the CD2-polyA sequence. The Actin promoter can then activate expression of Gal4, which binds to the UAS enhancer and activates expression of the gene of interest in the clone. Again, this may be used to over-express a *Drosophila* gene, express a transgene, or knockdown expression of a gene using

an RNAi fly line. Like the traditional FLP/FRT system, the recombination is induced in only a few cells, so usually a small number of clones are generated in each fly.

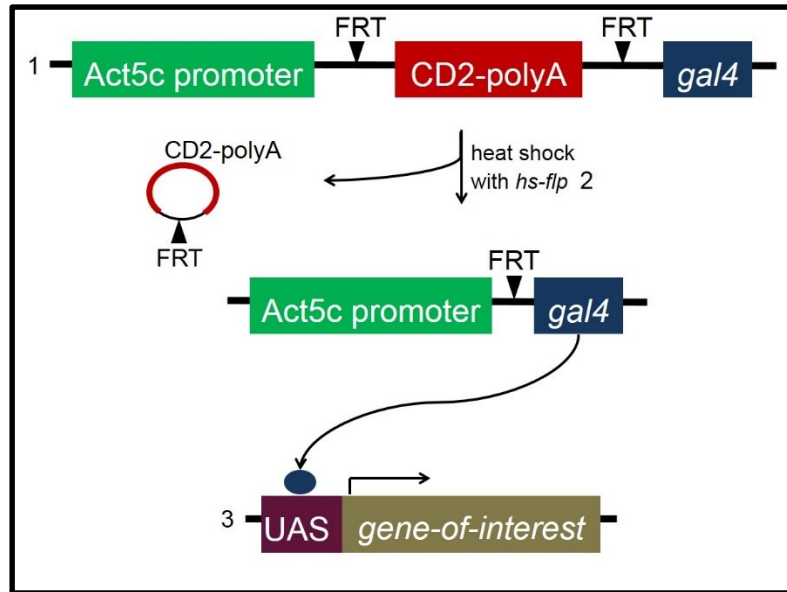


Figure 1.6 Variation of the FLP/FRT system with UAS-Gal4. This system allows for generation of clones of over-expression or knockdown of a gene of interest. It requires three transgenes, labeled 1-3. Heat shock induces production of FLPase, which mediates recombination between FRT sites and removes the CD2-polyA sequence. This removes the transcription stop signal and allows expression of Gal4 regulated by the Actin promoter. Gal4 then binds to the UAS enhancer, activating expression of the gene of interest. The gene of interest may be a copy of a cDNA for over-expression analysis, but may also be sequence to express hpRNA, to allow for knockdown analysis.

F. Fly crosses

The advantages of using *Drosophila* as a model organism culminate in the fly cross. The short life cycle and many genetic tools available make it possible to accomplish sophisticated genetics in a relatively short period of time. However, multiple generation fly crosses may be required to drive expression of a transgene or RNAi using the UAS-Gal4 system, to test for

genetic interactions between proteins and pathways, or to generate mutant clone cells within the developing tissues of the fly.

Setting up a fly cross in *Drosophila* is usually simple, and there are many features of the fly that make it convenient. In *Drosophila*, homologous recombination between chromosomes does not occur in males. This means chromosomes can be transmitted unaltered through the male line. Also, it is usually possible to generate large numbers of offspring from *Drosophila* crosses. A healthy female fly can lay up to 60 eggs per day. However, females can store males' sperm after mating, so the females used in a cross must be virgin, otherwise, the genotype of the offspring cannot be predicted. Adult flies do not mate for several hours after eclosion, so female virgins can be identified by an immature phenotype. This can include a light body color and large body indicating immature cuticle, folded wings, or a dark spot, the meconium (the remains of the last meal before pupation), on their ventral abdomen. For most crosses, it is a good idea to mate at least 10 virgin females of one genotype to a similar number of males of the second genotype. By moving the adult flies to a new containment vial with fresh food every 2 to 3 days, a large number of offspring can be collected.

There is a standard nomenclature used for denoting fly genotypes [2]. As in other organisms, wild-type chromosomes or alleles are represented as plus sign. Homologous chromosomes are separated with forward slash. So for a wild-type fly, the third chromosome would be represented as +/+. However, if a fly was heterozygous for *UAS-Chmp1*, a *Chmp1* over-expression transgene, on the third chromosome, the genotype of the fly would be written as *UAS-Chmp1*/+. Another custom is to separate two genes that are on the same chromosome with a comma. Additionally, different chromosomes are separated with a semicolon. One fly line used often in these studies is *en-Gal4, UAS-GFP*. *en-Gal4* is a driver that expresses Gal4 in the

pattern of the gene *engrailed*, and *UAS-GFP* is a transgene that allows for expression of GFP; both are located on second chromosome and so are separated with a comma. A fly with the genotype *en-Gal4, UAS-GFP/+; UAS-Chmp1/+* would represent a fly that has *en-Gal4* and *UAS-GFP* on one copy of the second chromosome, and *UAS-Chmp1* on one copy of the third chromosome, while the remaining second and third chromosomes are wild-type.

When performing crosses, Punnett Squares are useful for keeping track of chromosomes to identify progeny of the correct genotype. In an example for homozygous parents, virgin females of the genotype *ey-Gal4/ey-Gal4* (on the second chromosome, expresses Gal4 in eye) can be crossed to males of the genotype *UAS-Chmp1/UAS-Chmp1* (on the third chromosome, allows expression of Chmp1) to generate progeny over-expressing *Chmp1* in the eye (Figure 1.7A). Using a Punnett Square to track each chromosome would show that all offspring obtained from this cross will be of the genotype: *ey-Gal4/+; UAS-Chmp1/+*. Therefore, 100% of the offspring will over-express *Chmp1* in the eye.

However, there are many cases in which the flies to be crossed are not homozygous viable for the mutation or transgene of interest, and so are balanced in the heterozygous state. In an example of heterozygous parents, virgin females of the genotype *ey-Gal4/CyO* can be crossed to males of the genotype *UAS-Chmp1/TM3Ser*, again to generate flies over-expressing *Chmp1* in the eye (Figure 1.7B). However, this time the Punnett Squares would show that there are several possible genotypes in the offspring. On the second chromosome, the genotype of the progeny will be either *ey-Gal4/+* or *CyO/+*. On the third chromosome the genotype will be either *UAS-Chmp1/+* or *TM3Ser/+*. So only flies that are not *Cy* (curly wings) and not *TM3Ser* (notched wings) will be of the correct genotype. This example shows how quickly crosses can become complex, and at the same time illustrates the utility of balancer chromosomes and dominant

markers. Without balancers in this scenario, it would be much more difficult to know which offspring were of the correct genotype.

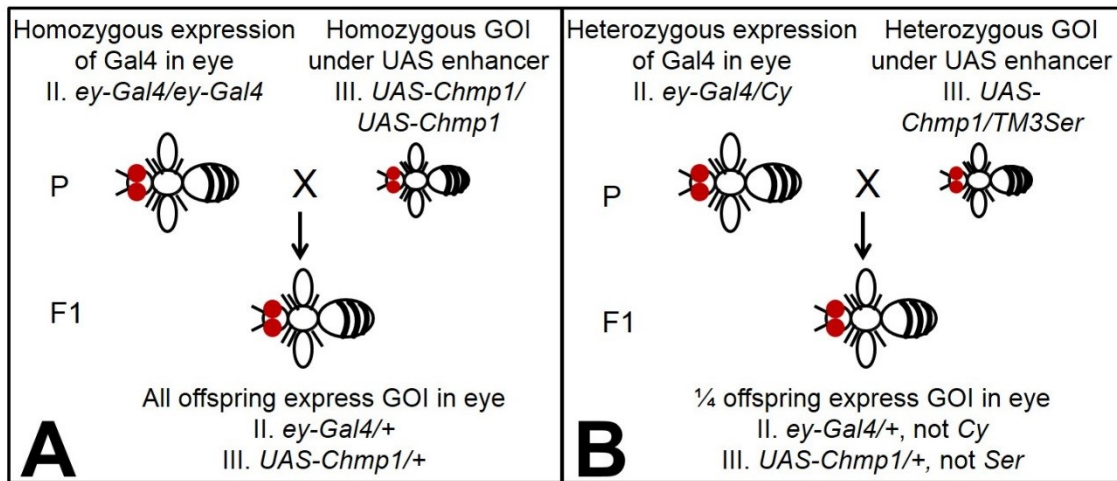


Figure 1.7 Examples of crosses in Drosophila. **A.** When crossing two homozygous stocks to drive expression of a transgene using UAS-Gal4, all offspring are of the correct genotype. **B.** Crosses are more complicated when dealing with heterozygous stocks. Only a quarter of the offspring will have the correct genotype. The dominant markers on balancer chromosomes are very useful in this situation, as they help to keep track of the chromosomes in the progeny. P is parental generation, F1 is the first filial generation. GOI = gene of interest. Roman numerals represent the chromosome on which the transgenes are located: II = second chromosome, III = third chromosome.

III. The DER pathway

The DER pathway (Figure 1.8) is involved in multiple stages of development and in multiple tissues in Drosophila, including but not limited to embryogenesis, oogenesis, and wing and eye development [31]. The DER is a traditional receptor tyrosine kinase (RTK) that signals through the Mitogen-Activated Protein Kinase (MAPK) pathway. The DER is expressed almost ubiquitously in the fly, so the patterned DER signaling that is required throughout development is specified through localized expression/activation of activators and repressors of the DER.

The DER has four activating ligands: Vein (Vn), Spitz, Gurken, and Keren. Gurken is an activator of the DER limited to the oocyte where it is required for early development in *Drosophila* [32]. Spitz is similar to the mammalian ligand, TGF α , and is the primary DER activating ligand during the development of most *Drosophila* tissues [33-35]. Spitz, Gurken, and Keren are all expressed as transmembrane proteins that must be cleaved by Rhomboid (Rho), a transmembrane protease that resides in the Golgi, in order to become active [32, 34, 36-38]. Additionally, these transmembrane activating ligands require the activity of Star, which is involved in the trafficking of these proteins from the endoplasmic reticulum to the Golgi where they are cleaved by Rho [37]. Vn is different from the other activating DER ligands in that it is secreted and constitutively active [39]. Comparatively, Vn is a weak activator of the DER, but it acts as a major ligand during wing, leg, and muscle development [40-42].

There are three inhibitors of DER signaling that were investigated in this study: Argos (Aos), Kekk-1 (Kek-1) and Sprouty (Sty). Argos is a secreted protein that binds to the activating ligand Spitz, inhibiting its ability to activate the DER [43, 44]. Kek-1 is a transmembrane protein that binds and inhibits the DER, so its inhibiting ability is limited to the cell that expresses it [45, 46]. Sty is a general intracellular inhibitor of tyrosine kinase signaling, as it inhibits Ras1 [47]. The DER is the only RTK known to signal during the development of the *Drosophila* wing.

Activation of the DER by ligand binding is followed by dimerization, phosphorylation and activation of a classical RTK signaling cascade through Ras and the MAPK pathway. In *Drosophila*, the activated receptor binds the adaptor protein Downstream of Receptor Kinase (Drk, mammalian GRB2 homologue), which then activates the guanine nucleotide exchange factor, Son of Sevenless (SOS). SOS then activates Ras1 by exchanging guanosine diphosphate

(GDP) for guanosine triphosphate (GTP). Ras1 then activates the MAPKKK, Raf1, which phosphorylates and activates the MAPKK, Downstream of Ras1 (DSOR1). DSOR1 then phosphorylates and activates the MAPK, Rolled (mammalian ERK homologue). In the nucleus, Rolled induces changes in gene expression, including the repression of Blistered (Bs) through phosphorylation of transcription factors, including Yan and Pointed [48, 49].

Proper cell signaling requires regulation of activation cellular signaling. Signaling pathways must be activated at the proper time. Additionally, it is crucial for signaling to be down-regulated when appropriate. Many receptors, including the DER, require a group of protein complexes called the Endosomal Sorting Complexes Required for Transport (ESCRT) for proper down-regulation.

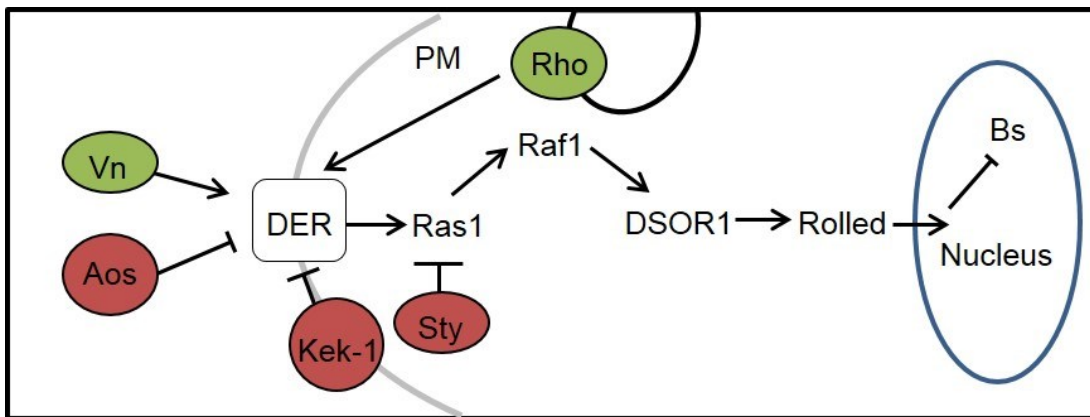


Figure 1.8 A simplified diagram of the DER pathway. Vein (Vn) is a secreted activating ligand of the Drosophila Epidermal Growth Factor Receptor (DER). Rhomboid (Rho) activates the DER from the Golgi by cleaving the transmembrane proteins Spitz, Gurken, and Keren (not shown) into DER activating ligands. When the DER is active, it activates the canonical MAPK pathway. Ras1 activates Raf1 (a MAPKKK), which phosphorylates Downstream of Ras1 (DSOR1, a MAPKK), which phosphorylates Rolled (homologue of ERK1/2, a MAPK). One effect of DER signaling is repression of Blistered (Bs) expression. Argos (Aos), Kekk-1 (Kek-1) and Sprouty (Sty) negatively regulate DER signaling. Positive regulators are in green, negative regulators are in red.

IV. The ESCRT machinery

The membrane of a cell is decorated with membrane receptor proteins that work to transmit an extracellular signal to the inside of the cell. Many of these are transmembrane receptors, such as the DER, that follow a classical signaling cascade: the signal (a ligand) binds the extracellular portion of the receptor, causing a conformational change in the receptor that relays the signal to the inside of the cell and usually results in changes in gene expression. As important as it is for a cell to be able to recognize and transmit the signal, down-regulation of the signal is also crucial for proper cellular signaling. The multivesicular body (MVB) pathway is one method of signal down-regulation of activated transmembrane receptors in the cell. MVB generation requires the ESCRT (Endosomal Sorting Complexes Required for Transport) protein complexes, which are highly conserved in eukaryotes. These complexes are involved in many cellular processes in addition to MVB generation, including HIV budding, membrane abscission during cytokinesis, autophagy, sorting lysosomal/vacuolar proteins from the Golgi, and others [50-55]. Essentially, the ESCRT complexes modify the shape of cellular membranes. All of the processes mentioned above are similar membrane modification events. They involve the deformation and budding of the membrane away from the cytoplasm to form a vesicle, followed by scission, or “pinching off” of the membrane. For example, during HIV budding, ESCRTs aid in the budding of the plasma membrane away from, i.e., out of the cell. There are four ESCRT complexes that are recruited sequentially to membranes through lipid and proteins interactions: ESCRT-0, -I, -II, and -III, as well as the Vacuolar Protein Sorting 4 (Vps4, Suppressor of K⁺ transport growth defect [SKD1] in humans) complex and several accessory proteins. However, some ESCRT-mediated processes do not require all of the ESCRT complexes. For example, ESCRT-II is not required for HIV budding or cytokinesis [56, 57].

MVB formation is the best described of all ESCRT-mediated cellular process and it requires the activity of all four ESCRT complexes. As mentioned above, the MVB pathway is important for regulation of cellular signaling pathways through down-regulation of transmembrane receptors. At the membrane, activated receptors are ubiquitinated and endocytosed into the endosome. The ESCRT machinery aids in the formation of the MVB from the endosome by mediating the invagination of the late endosomal membrane to form intraluminal vesicles (ILVs) (Figure 1.9A). This separates the receptors from the cytoplasm, thereby silencing the signals. The ILVs are then sorted to the lysosome where the receptors are degraded. Many membrane receptors have been reported to require ESCRT components for proper signaling in *Drosophila* and cultured mammalian cells, including the Epidermal Growth Factor Receptor (EGFR) and the Notch receptor [50, 58-61].

Ubiquitin acts as a sorting signal to target proteins, either activated membrane receptors or endosomal proteins from the trans-Golgi network to the endosome [62, 63]. MVB formation begins at the endosome with the ESCRT-0 complex, which organizes ubiquitinated cargo on the membrane into clusters and recruits deubiquitinating enzymes. ESCRT-I and -II assemble next on the membrane and begin the inward budding of the MVB membrane. Next, ESCRT-III is recruited and provides the scission activity of the ESCRT machinery. It still is not completely clear how this occurs and several models have been proposed [64, 65]. Studies have shown *in vivo* and *in vitro* that ESCRT-III components homo- and heteropolymerize with each other on membranes to form helical structures in circular arrays [66-69]. One model for membrane scission is that the ESCRT-III components oligomerize on the MVB membrane in a spiral and constrict the neck of the ILV (Figure 1.9B). Then the Vps4 complex binds and mediates the

disassembly of the ESCRT-III complex in an ATP-dependent process, completing MVB formation and recycling the ESCRT components back to the cytosol.

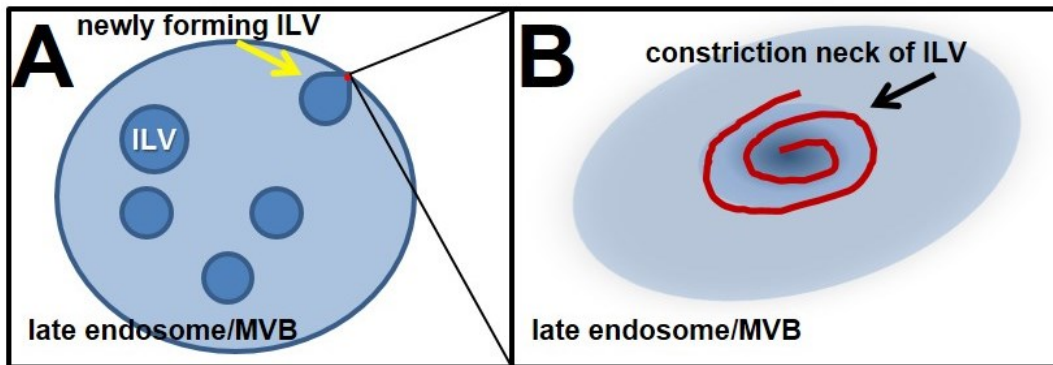


Figure 1.9 ESCRT-III function on the endosome. **A.** A multivesicular body (MVB) is formed by formation of intraluminal vesicles (ILVs) from the membrane of the late endosome. The ILVs contain activated receptor proteins (green and yellow) from the cell membrane. ESCRT-III components (red) assemble at the neck of the forming ILV (indicated by black arrow) and mediate the scission of the membrane. **B.** A view looking down onto the endosomal membrane (blue) on the constriction neck of the forming ILV. ESCRT-III components (red spiral) assemble into helical tubes and form a ring structure that closes the neck (dark blue) of the ILV.

The ESCRT-III complex is required for all ESCRT-mediated activities and provides the core function of the ESCRT machinery, which is the scission activity or “pinching off” of the membrane [70, 71]. ESCRT-III components are recruited late during ESCRT processes and are only transiently present on the membrane [72, 73]. Most of the proteins that make up the ESCRT-III complex are known as Chmps and they are highly conserved among eukaryotes. There are seven Chmps (1-7), all of which are structurally similar. Chmps have a charged five helical core, a basic helical N-terminus that targets localization to membranes, and an acidic C-terminal region that often binds regulatory factors through a MIT (microtubule interaction and transport) -interacting motif (MIM) [74-76]. The MIM allows Chmps to bind proteins that contain MIT domains [77]. The C-terminal region of Chmps can bind and autoinhibit the N-

terminal region to form a closed, or inactive conformation of the protein. This blocks membrane localization and interaction with other proteins [78, 79]. The open, or active, conformation is able to bind regulatory proteins and also allows for homo- and heterodimerization of Chmps [75, 80]. It is not known what causes the change in conformation from inactive to active protein.

V. Structure and function of Chmp1

A. Chmp1 Structure

Chmp1 (Chromatin Modifying Protein; Charged Multivesicular Protein) is a component of the ESCRT-III complex. Chmp1 is highly conserved from simple to complex eukaryotes and is known by different names in different organisms: Chmp1 (*Drosophila melanogaster*), VPS46p/Did2p (*Saccharomyces cerevisiae*), and Sal1 (*Zea mays*). To avoid confusion, I will refer to all homologues as Chmp1 from now on. Many organisms, including yeast, *Drosophila*, and some plants, express a single Chmp1 protein. Other organisms, including many insects, zebrafish, mammals and *Arabidopsis thaliana* express two Chmp1 proteins that are similar in sequence, called Chmp1A and Chmp1B. Chmp1 is a charged protein, about 200 amino acids in length. The N-terminus contains a nuclear localization sequence (NLS) and the extreme C-terminal region contains a MIM, (D/E/Q)-XX-L-XX-(Q/R)L-XX-L(K/R), where the indicated amino acids are those known to be involved in binding to an MIT domain (Figure 1.10) [81-84]. A protein BLAST identified two conserved domains in the *Drosophila* Chmp1 sequence, a Snf7 domain and a Vps24 domain (Figure 1.10). The Snf7 domain is found in the SNF multidomain family proteins that are involved in protein sorting and transport from the endosome to the vacuole/lysosome in eukaryotes. The Vps24 domain is found in a superfamily of conserved proteins involved in secretion. Additionally, an analysis of the primary amino acid sequence of *Drosophila* Chmp1 using protein structure prediction software Jpred3 (University of Dundee)

identifies 5 alpha helices, consistent with previous analyses of Chmp structures (Figure 1.10) [76].

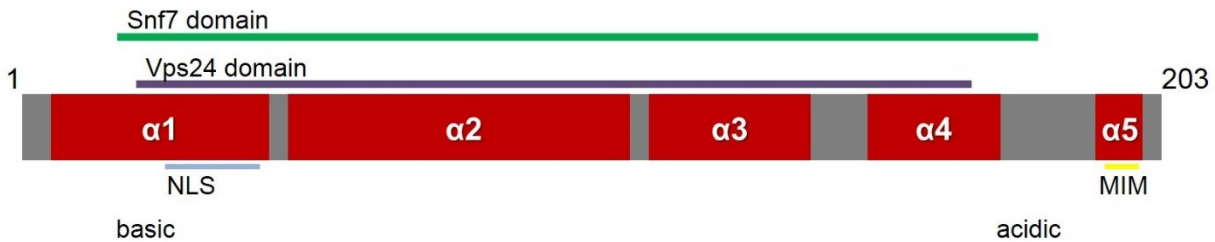


Figure 1.10 Chmp1 protein structure in Drosophila. The Drosophila Chmp1 protein is 203 amino acids in length. It contains putative Snf7 (green) and Vps24 (purple) domains, as well as 5 alpha helices (red). It has a basic N-terminus and an acidic C-terminus. The N-terminal region contains a nuclear localization sequence (NLS, blue) and the C-terminal region contains a MIT-interaction motif (MIM, yellow).

Published studies on Chmp1 have mostly been performed in either yeast or mammalian cell culture. These studies have identified roles for Chmp1 in regulating growth, protein sorting, and mitosis, and have found evidence of two seemingly distinct roles for Chmp1 in the nucleus and in the cytoplasm.

A. Chmp1 and survival

Most investigations of Chmp1 function have been performed in cell culture. However, a few studies have been performed in developing organisms and addressed the essentiality of Chmp1 for survival. In *Nicotiana benthamiana*, a close relative of the tobacco plant, loss of *Chmp1* activity had no apparent negative effect on development or viability and only caused slight changes in leaf morphology and color [85]. Additionally, in the filamentous fungus *Aspergillus nidulans*, Chmp1 was not essential for survival [86]. On the other hand, in *Arabidopsis thaliana*, *Chmp1A/1B* mutation caused lethal developmental defects in embryos [87]. The results of these studies are inconsistent, suggesting that the requirement of Chmp1 for survival is different depending upon the organism. Given the conservation of the Chmp1

sequence and ESCRT function, it is possible, and likely, that Chmp1 is involved in the same cellular processes across species. However, it seems that the overall consequences of *Chmp1* loss, i.e., the developmental defects that may be caused by mis-regulation of signaling pathways, vary between organisms.

B. Control of growth

Studies in plant and mammalian cell culture, as well as in zebrafish and plants, suggest that Chmp1 plays a role in regulation of growth. However, the results of these studies on are inconsistent. While some studies suggest that Chmp1 negatively regulates growth, others suggest that Chmp1 positively regulates growth.

Several *in vitro* studies have suggested Chmp1 has a role in controlling growth, specifically proposing that Chmp1 is a novel tumor suppressor. For example, in HEK293T (Human Embryonic Kidney, non-tumorigenic) and PanC1 (human pancreatic ductal tumor) cultured cells, knockdown of human *Chmp1A* promoted cell growth [88, 89]. On the other hand, over-expression of human *Chmp1A* halted the cell cycle in S-phase in EcR-293 cells (human embryonic kidney, stably expresses the ecdysone receptor), and also reduced cell growth in PanC1 and A498 (renal cell carcinoma) cell lines, compared to controls [81, 88, 89]. Together, these studies suggest Chmp1 negatively regulates cell growth.

A few *in vivo* studies also support a role for Chmp1 as a negative regulator of growth and even as a tumor suppressor. Similar studies from two different labs showed that HEK293T cells with reduced human *Chmp1A* activity formed tumors when injected into nude mice, while control HEK293T cells did not [88, 89]. Interestingly, when tumorous cells, either PanC1 or A498, were injected into mice and tumors formed, over-expression of human *Chmp1A*, either by Dox activation or injection of a *Chmp1* over-expression plasmid, reduced the growth of the

tumor [88, 89]. Additionally, reduction of Chmp1A activity has been linked to pancreatic and renal cancer in humans, as these tumors showed a considerable reduction of Chmp1 activity [88-90]. Taken together, these data strongly support a role for Chmp1 as a negative regulator of growth, and possibly as a tumor suppressor.

Contrary to the evidence for Chmp1 as a tumor suppressor, some studies showed that loss of Chmp1 had the opposite effect that would be expected from a tumor suppressor. For example, in the study with *Aspergillus nidulans*, loss of *Chmp1* caused conidiation (production of asexual spores) and impaired growth [86]. Additionally, in the *Arabidopsis thaliana* study, a *Chmp1A/1B* mutant caused stunted growth in seedlings [87]. Of course, this might be attributed to the requirement for *Chmp1A/1B* for survival in this species, rather than a specific effect on growth. However, in 2013 a study in humans linked homozygous *Chmp1A* mutations to pontocerebellar hypoplasia (small, underdeveloped cerebellum) and microcephaly (small head) [91]. The same study showed that cells grown in culture from the *Chmp1A*-mutant individuals had a very slow growth rate [91]. Additionally, *Chmp1A* knockdown in zebrafish reduced the size of the cerebellum and forebrain [91]. Together, these studies suggest a possible role for Chmp1 in positive regulation of growth.

There is also evidence of a role for Chmp1 in regulating cell fate decisions. In *Zea mays* (maize), loss of the Chmp1 homologue *supernumerary aleurone layers 1 (sall)* caused extra layers of aleurone cells to form in cultured endosperm [92, 93]. Though this could be an over-growth phenotype caused by over-proliferation, the authors of this study claimed that it was due to increased fate specification of aleurone cells caused by faulty endosomal trafficking [92, 93].

C. Chmp1 in the nucleus

Chmp1 was first discovered in a yeast two-hybrid screen for conserved proteins that interacted with the mammalian Polycomb-group (PcG) protein, polycomblike (mPcl1), and the *Drosophila* homolog, Pcl [81]. The PcG proteins, which were discovered in *Drosophila*, are a set of proteins that induce chromatin condensation, mediating gene silencing epigenetically during development. Chmp1 interacted with Pcl, suggesting that it may play a role in gene silencing. Additionally, a bipartite NLS was found within the Chmp1 N-terminus [81]. The NLS is a conserved feature of the Chmp1 sequence. In *Nicotiana benthamiana* the Chmp1 N-terminus (but not the whole protein) localized to the nucleus [85]. Chmp1 was also detected in the nucleus in zebrafish and human cultured cells [81, 90, 91]. So it is possible that, although the Chmp1 protein may normally localize to the cytosol, it is targeted to the nucleus upon an unknown cell signal.

On western blots, the human Chmp1 protein is detected as a doublet with bands at 32kD and 35kD, and cell fractionization studies showed that these bands corresponded to cytoplasmic and nuclear Chmp1, respectively [81]. Twelve years after the initial discovery of the two Chmp1 bands, it was reported that they are likely due to different phosphorylation states of human Chmp1, as phosphatase treatment of cellular lysates resulted in a single band [94]. This study reported the identification of three phosphorylation sites within the human Chmp1 C-terminus [94].

Interestingly, the nuclear form of human Chmp1 was only detectable by immunostaining during M phase of the cell cycle. It was closely associated with chromatin and recruited the PcG protein and transcriptional repressor, BMI1, to condensed chromatin [81]. Supporting this study, more recent investigation showed a genetic interaction between Chmp1 and BMI1 in zebrafish,

which suggested that they function together in regulating gene expression during neural development [91]. This same study showed that cultured cells from humans carrying *Chmp1A* mutations expressed high levels of the cell cycle regulator and tumor suppressor protein INK4, whose expression is normally suppressed by BMI1. The function of BMI1 was likely reduced due to the *Chmp1A* mutation, supporting a functional interaction between BMI1 and Chmp1. Although Chmp1 and BMI1 did not co-localize in zebrafish, this finding supports previous results suggesting a function for Chmp1 in negatively regulating gene expression [91].

Additional studies demonstrate interaction of Chmp1 with other nuclear proteins. In 2009, a study connected Chmp1 with All-trans Retinoic Acid (ATRA) signaling [95]. The study found that over-expression of human *Chmp1A* in PanC1 cells reduced cell growth and increased cellular levels of retinol binding protein 1 (CRBP-1) [95]. Treatment of PanC1 cells with ATRA caused an increase in total Chmp1A protein, as well as an increase in nuclear Chmp1A [95]. This increase in Chmp1A nuclear localization suggested a function for Chmp1A in the nucleus. Additionally, the same group showed that Chmp1A may regulate Ataxia Telangiectasia Mutated (ATM) through activating phosphorylation [90]. They showed that over-expression of human *Chmp1A* activated ATM and that Chmp1A colocalized with ATM in the nucleus and also increased the amount of phospho-p53 in the nucleus [89, 90]. Although ATM could be activated when the Chmp1A MIM was deleted, the increase in phospho-p53 in the nucleus required the NLS in the N-terminal region of Chmp1A, suggesting a nuclear requirement for Chmp1A [90]. p53 is a substrate for ATM, so the results of this study suggested that the ability of over-expressed *Chmp1A* to reduce cell growth might have been mediated through ATM signaling.

D. Chmp1 in the cytoplasm

Chmp1 also plays a role in the cytoplasm as a component of the ESCRT-III complex in MVB generation. Many localization studies, from yeast to plants to mammalian cell culture support this role for Chmp1, showing that it localizes in the cytoplasm to early and late endosomes [85, 86, 90, 91, 93, 96, 97]. Information from studies in yeast, fungus, and cell culture help to delineate the steps of MVB formation that require Chmp1. Late in the ESCRT pathway, Chmp1 is recruited to the endosomal membrane. Then, through the MIM, Chmp1 binds the MIT domain protein, AAA-ATPase Vps4 [82]. This binding mediates the ATP-dependent dissociation and recycling of ESCRT-III complex, completing MVB formation [96, 98]. This model for Chmp1 function is consistent with cell fractionization studies with human Chmp1, showing that most of Chmp1 in the cell is soluble, but some is peripherally associated with membranes [97]. It appears that binding of Chmp1 to Vps4 to mediate ESCRT-III disassembly is not crucial for MVB biogenesis, as MVBs are still formed when Chmp1 function is lost in yeast and *Aspergillus nidulans* [86, 96]. However, *Chmp1* mutations do cause protein trafficking defects: in Arabidopsis, *Chmp1A/1B* mutation reduced the number of ILVs detected in the MVB; in human cell culture, expression of a functionally mutant Chmp1 protein caused enlarged endosomes; and in yeast, *Chmp1* mutations caused accumulation of ESCRT-III components on endosomes [78, 87, 96, 97]. Additionally, studies show that *Chmp1* mutations in yeast, *Aspergillus nidulans*, and *Arabidopsis thaliana* cause broad protein sorting defects, i.e., protein transport from Golgi to MVB is altered [82, 86, 87, 96]. Of course, it is possible that Chmp1 has different or additional roles in different organisms. Therefore, studies in yeast and plants may not be equivalent to flies or humans.

Many of the studies discussed above suggest that Chmp1 plays a role in the nucleus, as well as the cytoplasm. In the cytoplasm, Chmp1 is required for proper ESCRT-III function during MVB generation, protein sorting, and cytokinesis. Chmp1 is also involved in chromosome stability and gene silencing, but it remains unknown how Chmp1 interacts with chromatin. There are reports of ESCRT components in the nucleus, including the tumor suppressor and ESCRT-I component, Tumor Susceptibility Gene 101 (Tsg101) [99].

E. Chmp1 and mitosis

Mutations in *Chmp1* can result in severe mitotic/cytokinetic defects. In HeLa cells knockdown of both *Chmp1A* and *Chmp1B* was associated with multiple defects during mitosis, including multinucleated cells, fragmented nuclei, unaligned metaphase chromosomes, visible midbodies (Flemming bodies, narrow intracellular bridges dense with microtubules that connect two daughter cells near the end of cell division), and multipolar spindles [69, 100]. Although human Chmp1A and Chmp1B are similar in sequence to Chmp1 in other species, they may have separate functions. Unlike human Chmp1A, human Chmp1B is involved in membrane abscission during cytokinesis in cell culture, where it recruits and binds Spastin, a microtubule-severing enzyme, at the midbody [69, 77, 101]. Indeed, in HeLa cells knockdown of both human *Chmp1A* and *Chmp1B* induced cytokinesis arrest [69]. This implies that the ESCRT-III complex may recruit a different version of the Chmp1 protein depending on the cellular process involved. Chmp1A and Chmp1B may have different binding partners (see below), giving the ESCRT machinery a way of recruiting different proteins for different jobs in the cell.

F. Conserved binding partners of Chmp1

Chmp1 has multiple known binding partners, many of which are part of the ESCRT machinery and most of which are conserved between species. For example, through its MIM

motif, Chmp1 in *Aspergillus nidulans* and yeast binds the MIT of the ATPase, Vps4/SKD1 [82, 84, 86, 96]. Chmp1-Vps4 binding was also observed in *Arabidopsis thaliana* and human cultured cells, and was required for completion of MVB biogenesis and the disassociation of ESCRT-III complexes from the MVB membrane [75, 83, 84, 87, 96, 97]. Multiple studies in human cells and yeast showed that Chmp1 also binds Increased Sodium Tolerance-1 (Ist1), a component of the Vps4 complex that inhibits Vps4 activity [69, 94, 102-104]. Studies in yeast, *Arabidopsis*, and human cultured cells showed an interaction with Chmp1 with the MIT domain protein LIP5 /Vta1p (Lyst-interacting protein 5/ Vps twenty associated 1 protein), an important component of the Vps4 complex which binds and activates Vps4 [84, 87, 98, 105-107]. Human Chmp1A and 1B also bound the endosome associated ubiquitin hydrolases, AMSH (Associated Molecule with the SH3-domain of STAM) and UBPY (Ubiquitin-specific processing Protease Y) [75, 108]. Additionally, the first study that identified Chmp1 in human cells showed that it physically interacted with both the human and *Drosophila* PcG protein, Pcl [81]. Human Chmp1 proteins also interact with each other, through both homodimerization and heterodimerization with other Chmps [75]. All of these proteins reported to bind Chmp1 are either ESCRT components (i.e. the Chmps) or recruited to the site of ESCRT activity (e.g. Vps4, AMSH).

Many organisms, including humans, express two Chmp1 proteins: Chmp1A and Chmp1B. Their sequences are similar, and they share many binding partners, they do not share the same binding affinities. For example, human Chmp1A and 1B both interacted and colocalized with Calpain-7, a calcium-dependent cysteine protease, but Chmp1B bound much more strongly than Chmp1A [109]. Additionally, Chmp1B associated with the ATPase Spastin during cytokinesis, but Chmp1A did not [77, 101].

G. Binding partners of *Drosophila* Chmp1

There have been no functional studies on Chmp1 in *Drosophila*. However, Chmp1 has been included in some large scale protein interaction studies, including the *Drosophila* Protein Interaction Map (DPiM), the goal of which is to generate a protein interaction map of the entire *Drosophila* proteome [2, 110, 111]. These have identified many binding partners for Chmp1 in *Drosophila* (Table 1.3). Interestingly, although several of these proteins are involved in protein transport and phagocytosis, both of which are known to require ESCRTs, other cellular processes are represented. Of the 27 binding partners of Chmp1, 5 play a role in translation, 6 in mRNA processing, and 2 in regulation of gene expression. This suggests that Chmp1 may play a role in regulation of gene expression, possibly at the level of translation. However, it is important to note that these interactions were identified through co-immunoprecipitation and mass spectroscopy, and so are purely physical and have not yet been confirmed through genetic studies in *Drosophila*. Interactions between Chmp1 and several of the binding partners listed, for example, CG10103, Vps4, and Chmp4B, have been observed in other organisms as well [69, 75, 82, 86, 97]. This suggests that these interactions are conserved and are therefore much more likely to be true binding partners in *Drosophila*.

Symbol	Gene name	Molecular function	Biological process
CG6259	N/A	Unknown	Protein transport*
CG6842	Vps4 (Vacuolar protein sorting 4)	ATPase activity*	Actin cytoskeleton organization, epithelial cell apical/basal polarity, regulation of growth of symbiont in host, phagocytosis, engulfment
CG10103	N/A (homologue of IST1)	unknown	unknown
CG8055	Shrb (Shrub, Chmp4A)	protein-binding	Neuron projection morphogenesis, dendrite morphogenesis, negative regulation of growth of symbiont in host
CG17492	Mib2 (Mind bomb 2)	MyosinII binding	Myoblast fusion, muscle cell homeostasis
CG4279	LSm1	Unknown	Cytoplasmic mRNA processing body assembly
CG4618	Chmp2B [†] (Charged multivesicular body protein 2b)	Unknown	Protein transport*
CG8025	Mtr3	3'-5' exoribonuclease activity *	Regulation of gene expression
CG9779	Vps24 [†] (Charged multivesicular body protein 3)	Unknown	Phagocytosis
CG14542	Vps2 [†]	Unknown	Protein transport*
CG31938	Rrp40	3'-5' exoribonuclease activity*	Regulation of gene expression
CG5317	RpL7-like (Ribosomal protein L7-like)	Structural constituent of ribosome*	Neurogenesis
CG9769	N/A	Translation initiation factor activity*	Positive regulation of Notch signaling pathway, Autophagic cell death
CG9677	Int6 (Int6 homologue)	Translation initiation factor activity*	Neuron projection morphogenesis, phagocytosis, regulation of cell cycle
CG7897	GP210 (Gp210 orthologue)	unknown	Olfactory learning, memory
CG10306	N/A	Predicted translation initiation factor activity*	Translational initiation*
CG3689	N/A	mRNA binding, hydrolase activity*	mRNA cleavage*
CG3817	N/A	Unknown	neurogenesis
CG5263	SmG (Small ribonucleoprotein particle protein SmG)	Translation repressor activity, myosin binding	Regulation of mRNA stability, negative regulation of translation, nuclear-transcribed mRNA poly(A) tail shortening, establishment of RNA localization
CG7490	RpLP0 (Ribosomal protein LP0)	Structural constituent of ribosome	Translation*
CG5655	Rsf1 (Repressor splicing factor 1)	mRNA binding*	Negative regulation of mRNA splicing via spliceosome
CG6998	Ctp (cut up)	Dynein intermediate chain binding	Reproduction, sensory organ development, etc.
CG8427	SmD3 (small ribonucleoprotein particle protein SmD3)	Unknown	Nervous system development, pole plasm oskar mRNA localization, mitosis, mitotic spindle organization, neuron differentiation, muscle organ development, lymph gland development
CG1987	Rbp1-like	Nucleotide binding*	RNA splicing
CG2099	RpL35A (ribosomal protein L35A)	Structural constituent of ribosome	Translation*
CG13608	mRpS24 (mitochondrial ribosomal protein S24)	Structural constituent of ribosome*	Translation*
CG17520	CkIIα (casein kinase IIα)	S/T kinase	Sensory organ development, macromolecule modification, locomotory behavior, cell fate commitment, etc.

Table 1.3 Protein interactions with *Drosophila* Chmp1. *Predicted function based on sequence similarity. Information retrieved from [2].

CHAPTER 2

RATIONALE, SPECIFIC AIMS AND HYPOTHESIS

I. Rationale

Many cellular signaling pathways share a common cascade structure, in which an extracellular signal is transmitted into the cell through a transmembrane receptor, ultimately causing a change in gene expression. Down-regulation of the signal is crucial for proper cellular function. One method for down-regulation of activated transmembrane receptors is the MVB pathway, which utilizes the ESCRT protein complexes, 0, I, II, and III. The ESCRT-III complex provides the core function of the ESCRT machinery, which is the scission of the neck of the ILV at the MVB. This step is crucial for MVB biogenesis, as failure to complete ILV formation impedes down-regulation of the receptor and leads to prolonged signaling to the cytoplasm.

Chmp1 is a component of the ESCRT-III complex. As an ESCRT-III component, Chmp1 binds the AAA ATPase Vps4, which completes formation of the ILV and mediates disassociation of the ESCRT-III components from the MVB membrane. There are numerous studies in yeast on Chmp1 and other ESCRT components, which focus heavily on the physical binding domains and partners of Chmp1. Other work in mammalian cell culture focuses mainly Chmp1 as a regulator of growth. Many of the results of these studies are contradictory. For example, results of over-expression and knockdown studies have linked *Chmp1* to pancreatic and renal cancers in humans, and identified Chmp1 as a putative tumor suppressor [81, 88-90, 92, 95]. On the other hand, some studies show that loss of *Chmp1* has minimal negative effects on cellular function, and others that loss of *Chmp1* impairs growth, which seems to contradict its role as a tumor suppressor [85-87, 91].

As most information on the activity of Chmp1 has been inferred from its biochemical interactions or from studies of single cells, little is known about its role in tissue development and differentiation. Indeed, few studies have investigated the mechanisms, i.e., genetic or biochemical pathways, underlying the *Chmp1* phenotypes that have been reported. Two studies from the Park lab suggest the effect of Chmp1 on growth is due to its role in the nucleus, as it appears to be involved in ATRA and ATM/p53 signaling [89, 90, 95]. Another study showed that Chmp1 may regulate expression of the BMI-INK4 locus in humans, and suggested that Chmp1 functions in the nucleus through a physical interaction with BMI [91]. Apart from these few studies, however, there is little information about the pathways by which Chmp1 has an effect on cell development and differentiation. In addition, the only studies on the role of Chmp1 in a multicellular organism have been completed in plants or fungus, rather than in an animal model [85-87, 92].

No investigation of Chmp1 function in invertebrates has been published. *Drosophila* provides an easily manipulated model system for the analysis of Chmp1 function and its importance for development. In this research, the effects of loss (knockdown) and gain (over-expression) of Chmp1 activity on tissue development were investigated with the aim of identifying the genetic or biochemical pathways Chmp1 may regulate. Because Chmp1 has not been studied in *Drosophila*, resources are limiting, i.e., no *Chmp1* mutant or antibody exists. However, with the development of the genome-wide *Drosophila* RNAi libraries, the effects of loss of *Chmp1* activity could be investigated with *Chmp1* mRNA knockdown. Additionally, transgenic fly lines that can express either wild-type or epitope-tagged Chmp1 protein were generated to investigate effects of *Chmp1* over-expression, as well as Chmp1 subcellular localization. The results of these studies should help to characterize the cellular function of

Chmp1. Additionally, the results should provide some mechanisms (e.g., regulation of cellular signaling pathways) underlying *Chmp1* phenotypes.

II. Specific Aims and Experimental Design

A. Specific Aim 1: Establish that *Drosophila* is an appropriate model to investigate Chmp1 function. Conservation of amino acid sequence, functional domains, and protein interaction domains would suggest that Chmp1 function is conserved between flies and other species. Therefore, conclusions obtained from studies on Chmp1 function in *Drosophila* would be suggestive of its function in other organisms.

1. Align *Drosophila* and human Chmp1 protein sequences to identify the degree of sequence similarity.
2. Identify conserved domains and binding partners through sequence analysis and data mining.

B. Specific Aim 2: Investigate the effects of loss of *Chmp1* in the developing fly. No *Chmp1* mutant exists, so loss of *Chmp1* was investigated using fly lines that express RNAi specific for *Chmp1* mRNA. Analysis of *Chmp1* knockdown phenotypes in the fly should provide information to address the following questions:

1. Is Chmp1 essential? No investigation of the essentiality of Chmp1 has been published in invertebrates.
 - I. Verify that RNAi is effective and specific. RNAi is likely effective and specific if similar phenotypes are observed from the expression of *Chmp1* RNAi with independently created RNAi lines.

- II. Verify whether flies survive ubiquitous *Chmp1* knockdown. Lethality associated with ubiquitous *Chmp1* knockdown during fly development would suggest that *Chmp1* is essential to development.
2. What is the phenotypic effect of *Chmp1* knockdown in specific tissues in the fly (i.e., the wing and eye)? Phenotypes obtained should give clues about which developmental pathways *Chmp1* regulates.
 - I. Knock down *Chmp1* expression in the wing and eye using specific Gal4 drivers. Analyze the phenotypes that result and hypothesize which signaling pathways are altered by *Chmp1* loss.
 3. What signaling pathways does *Chmp1* regulate?
 - I. Investigate whether the *Chmp1* knockdown phenotype is enhanced/suppressed by altered activity of the specific developmental pathways identified in B.2.I.
 - II. Investigate whether downstream targets of pathways regulated by *Chmp1* are affected when *Chmp1* is knocked down.

C. Specific Aim 3: Investigate the effects of gain of *Chmp1* in the developing fly. No fly line that allows for *Chmp1* over-expression exists, so transgenic fly lines were generated that allow for expression of wild-type or his-myc (HM)-tagged *Chmp1* protein. Analysis of *Chmp1* over-expression phenotypes in the fly should provide information to address the following questions:

1. What is the phenotypic effect of *Chmp1* over-expression in specific tissues in the fly (i.e., the wing and eye)? Phenotypes observed should give clues about which developmental pathways *Chmp1* regulates.

- I. Verify that *Chmp1* over-expression lines express functional Chmp1 protein.
Rescue of *Chmp1* knockdown by *Chmp1* over-expression would suggest that the transgenic fly lines generated express functional Chmp1 protein.
 - II. Over-express *Chmp1* in the eye and wing of the fly using specific Gal4 drivers.
Analyze the phenotypes that result and hypothesize which signaling pathways are altered by *Chmp1* over-expression.
2. What signaling pathways does Chmp1 regulate? Investigate whether the *Chmp1* over-expression phenotype is enhanced/suppressed by altered activity of specific developmental pathways identified in C.1.II.
- D. Specific Aim 4. What is the subcellular localization of Chmp1 in fly tissues? No antibody has been developed specifically against *Drosophila* Chmp1. To investigate subcellular localization of Chmp1 protein, express HM-Chmp1 in tissues of the developing fly (i.e., embryos and larval tissues).
1. How does HM-Chmp1 localize in cells of fly tissues? It is reported that Chmp1 functions in the cytoplasm and the nucleus. The subcellular localization of HM-Chmp1 should indicate where Chmp1 functions in *Drosophila* cells.
 - I. Express HM-Chmp1 in the embryo and larval tissues using specific Gal4 drivers. Detect HM-Chmp1 localization with an anti-c-Myc antibody.
 2. Does HM-Chmp1 localize to the endosome?
 - I. Express HM-Chmp1 in the embryo using specific Gal4 drivers and investigate co-localization with endosomal markers, including Rab5 and Rab9, markers for the early and late endosome, respectively.

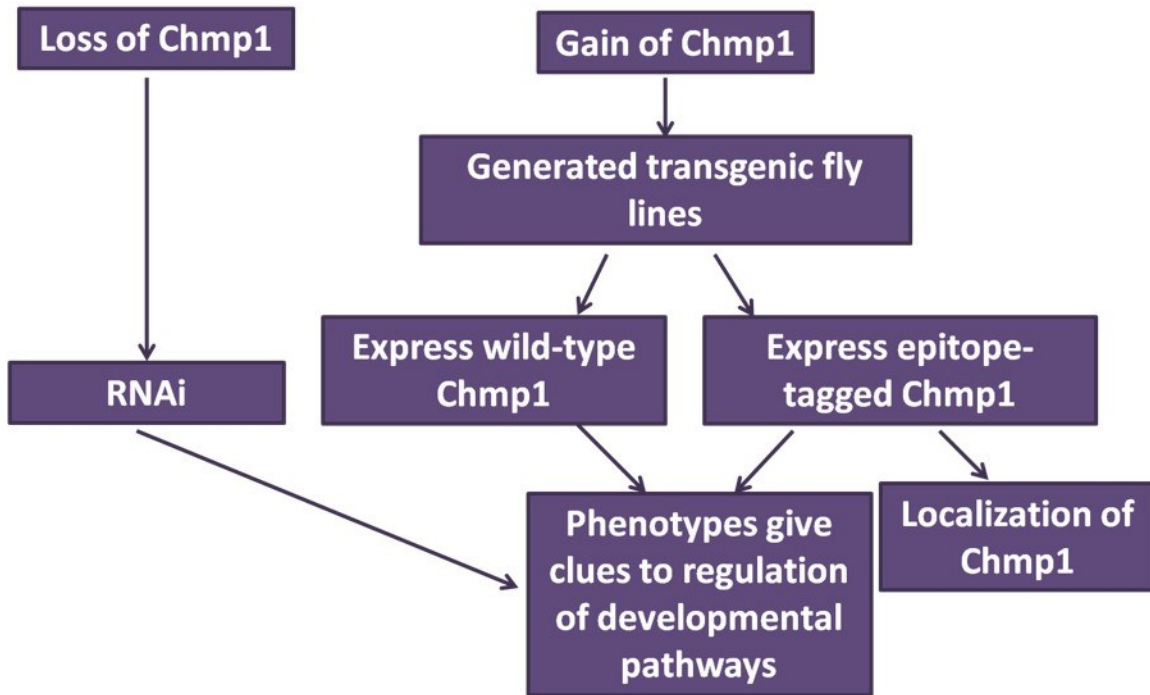


Figure 2.1. Experimental design

III. Hypotheses

A. Sequence alignments suggest that the structure of Chmp1 is conserved across species.

Hypothesis: Alignment of amino acid sequence between Chmp1 from flies and other species will likely indicate a high degree of sequence similarity. Therefore, Chmp1 function as a component of the ESCRT-III pathway and in the nucleus is likely conserved in *Drosophila*. Additionally, conclusions inferred from studies in *Drosophila* should give insight into Chmp1 function in other species.

B. & C. Chmp1 is a ubiquitously expressed protein and a component of the ESCRT-III complex, which is required for receptor down-regulation. Hypothesis: Chmp1 is essential for *Drosophila* development. Loss or gain of Chmp1 function will disrupt ESCRT-III function, including MVB biogenesis, and alter the activity of cell

signaling pathways. The resulting phenotypes will provide clues as to which specific pathways are regulated by Chmp1.

- D. Chmp1 is a component of the ESCRT-III complex, which is required for MVB biogenesis from the endosome. Numerous studies report Chmp1 localization to the early and/or late endosome. Chmp1 localization has also been observed in the nucleus. Hypothesis: *Drosophila* Chmp1 localizes to the endosome and nucleus.

CHAPTER 3

MATERIALS AND METHODS

I. Alignment of Chmp1 sequences

Chmp1 protein sequences were obtained from the National Center for Biotechnology Information (NCBI) webpage (<http://www.ncbi.nlm.nih.gov/>). Accession numbers for protein sequences used are as follows: NP_649051.3 for *Drosophila melanogaster* Chmp1, NP_065145.2 for *Homo sapiens* Chmp1B, and NP_002759.2 for *Homo sapiens* Chmp1A. Conserved domains were identified through the NCBI webpage and confirmed in the literature when possible. Alignment of the Chmp1 protein sequences was performed through the European Bioinformatics Institute (EBI) webpage (www.ebi.ac.uk/ena/) using the program ClustalX. Identical residues were labeled with an asterisk, and similar residues were labeled with one or two dots, depending on the degree of similarity.

II. Generation of transgenic fly lines

Transgenic fly lines that express *Chmp1* under the control of a Gal4 responsive UAS enhancer were generated. The clone GH26351, which contains *Chmp1* cDNA in the pOT2 vector, was obtained from the Drosophila Genomics Resource Center (DGRC). Two plasmids were used, pUAST and pUASHM, which allow for insertion into the Drosophila genome. The *Chmp1* coding sequence was amplified by PCR with the following primer pairs (Invitrogen): *UAS-HM-Chmp1* forward (GGGCCCGGATCCACGTCGCATATGTCTACGAGTTCCATGG) and *UAS-HM-Chmp1* reverse (TACCACCTCGAGTTATTCAGCCTGGCGGAGACG) for insertion into pUASHM, and *UAS-Chmp1* forward (ACGTCGGAATCCATGTCTACGGAGTTCCATGG) and *UAS-Chmp1* reverse (TACCACCTCGAGTTATTCAGCCTGGCGGAGACG) for insertion into pUAST. These

primers added *Nde1*, *Xho1*, and *EcoR1* restriction enzyme recognition sites (underlined) that allowed for insertion of the *Chmp1* cDNA into the pUAST and pUASHM plasmids. *Chmp1* cDNA was inserted downstream of a UAS enhancer into the *EcoR1/Xho1* sites of pUAST and the *Nde1/Xho1* sites of pUASHM. The pUASHM vector allows the expression of Chmp1 protein tagged with an N-terminal His-Myc (HM) tag. The amplified and cloned *Chmp1* sequence was verified by nucleotide sequencing. The *UAS-HM-Chmp1* and *UAS-Chmp1* plasmids were sent to BestGene Inc., where the transgenic flies were generated. Balanced stocks carrying the *UAS-HM-Chmp1* and *UAS-Chmp1* transgenes were produced in the Collier fly lab.

III. Fly stocks and genetics

All flies were cultured on standard cornmeal/yeast media at 25°C, unless otherwise stated. The fly stocks used in this study are listed in Table 3.1. *P[GD11219]v21788 (UAS-Chmp1-RNAi VDRC)* and *P[GD1443]v33200 (UAS-forked-RNAi)* were obtained from the Vienna Drosophila Resource Center (VDRC). *TRiP.HM05117 (UAS-Chmp1-RNAi TRiP)* was obtained from the Transgenic RNAi Project (TRiP) stocks at Harvard. *N^{55e11}/FM7Bar*, *UAS-Dx^{l7}*, and *car^l; dpp-Gal4/TM6b* were a gift from Martin Baron. All other fly lines were from Bloomington Stock Center at Indiana University. Additionally, six transgenic fly lines were generated that were used in this study (Table 3.2): the *UAS-HM-Chmp1-1* through *UAS-HM-Chmp1-4* lines can express HM-tagged Chmp1 protein; the *UAS-Chmp1-1* and *UAS-Chmp1-2* lines can express wild-type Chmp1 protein.

Name	Genotype	Chromosome
<i>Oregon R (wild-type)</i>	<i>Oregon R-C</i>	N/A
<i>UAS-Chmp1RNAi-VDRC</i>	<i>w¹¹¹⁸; P[GD11219]v21788/CyO</i>	1, 2
<i>UAS-Chmp1RNAi-TRiP</i>	<i>y¹ v¹; P[TRiP.HM05117]attP2</i>	1, 3
<i>act5c-Gal4/TM6Tb</i>	<i>y¹ w[*]; P[Act5C-GAL4]17bFO1/TM6B, Tb¹</i>	1, 3
<i>tub-Gal4/TM3Sb</i>	<i>y¹ w[*]; P[tubP-GAL4]LL7/TM3, Sb¹</i>	1, 3
<i>MS1096-Gal4</i>	<i>w¹¹¹⁸ P[w^{+mW.hs}=GawB]Bx^{MS1096}</i>	1
<i>salm-Gal4</i>	<i>w[*]; P[GawB]459.2</i>	1, 2
<i>ptc-Gal4</i>	<i>w[*]; P[GawB]ptc^{559.1}</i>	1, 2
<i>en-Gal4</i>	<i>w[*]; P[en2.4-GAL4]e16E</i>	1, 2
<i>dpp-Gal4</i>	<i>w[*]; wg^{Sp-1}/CyO; P[GAL4-dpp.blk1]40C.6/TM6B, Tb¹</i>	1, 3
<i>FRT-Gal4</i>	<i>y¹ w[*] P{GAL4-Act5C(FRT.CD2).P}D</i>	1
<i>ey-Gal4</i>	<i>y¹ w¹¹¹⁸; P{w[+mC]=ey1x-GAL4.Exel}2</i>	1, 2
<i>sev-Gal4</i>	<i>P{ry[+t7.2]=GAL4-Hsp70.sev}2/CyO; ry[*]</i>	2, 3
<i>Ij/Cy; D¹/TM3Ser</i>	<i>w[*]; Kr^{Ij-1}/CyO; D¹/TM3, Ser¹</i>	1, 2, 3
<i>Ij/Cy; D¹/TM6SbTb</i>	<i>w[*]; Kr^{Ij-1}/CyO; D¹/TM6C, Sb¹, Tb¹</i>	1, 2, 3
<i>Df(3L)BSC416/TM6Sb</i>	<i>w¹¹¹⁸; Df(3L)BSC416/TM6C, Sb¹ cu¹</i>	1, 3
<i>Df(3L)BSC832/TM6Sb</i>	<i>w¹¹¹⁸; Df(3L)BSC832, P+Pbac[XP3.RB5]BSC832/TM6C Sb¹ cu¹</i>	1, 3
<i>aos^{Δ7}/TM3Sb</i>	<i>argos^{Delta7}/TM3, Sb¹</i>	3
<i>aos^{w11}/TM3Sb</i>	<i>w⁸; P[w^{+mW.hs}=IwB]argos^{w11}/TM3, Sb¹</i>	1, 3
<i>UAS-aos on 1 & 2</i>	<i>y¹, w[*] P[w^{+mC}=UASargos.M]301021; P[w^{+mC}=UAS argos.M]30-85-1</i>	1, 2
<i>sty^{Δ5}/TM3Sb</i>	<i>w[*]; sty^{Delta5}/TM3, Sb¹ P[w^{+mC}=35UZ]2</i>	1, 3
<i>aos^{r/t}</i>	<i>argos^{r/t}</i>	3
<i>kek-1</i>	<i>y¹ wp67c23; P[y^{+t7.7} w^{+mC}=wHy]kek1^{DG23812}</i>	1, 3
<i>ve, vn</i>	<i>rho^{ve-1}, vn¹</i>	3
<i>Ij/Cy; ve¹/TM6Sb</i>	<i>w[*]; Kr^{Ij-1}/CyO; rho^{ve-1}/TM6, Sb¹</i>	2, 3
<i>vn¹</i>	<i>vn¹</i>	3
<i>UAS-GFP</i>	<i>w[*]; UAS-GFP.S65T^{T2}</i>	1, 2
<i>en-Gal4, UAS-GFP</i>	<i>w[*]; P[en2.4-GAL4]e16E,UAS-GFP.S65T^{T2}</i>	1, 2
<i>N^{55e11}/FM7Bar</i>	<i>N^{55e11} P[ry^{+t7.2}=neoFRT]19A/FM7c</i>	1
<i>car¹;dpp-Gal4/TM6b</i>	<i>w[*], car¹; P{w[+mW.hs]=GAL4-dpp.blk1}40C.6/TM6B, Tb¹</i>	1, 3
<i>UAS-Dx¹⁷</i>	<i>w[*]; P[UAS-Dx¹⁷]</i>	1, 3
<i>hsflp; Sco/Cy</i>	<i>P{hsFLP}12, y¹ w[*]; sna^{Sco}/CyO</i>	1, 2
<i>UAS-YFPRab9</i>	<i>y¹ w[*]; P[UASp-YFP.Rab9]CG3625¹³</i>	1, 2
<i>UAS-YFPRab7</i>	<i>y¹ w[*]; P[UASp-YFP.Rab7.T22N]06</i>	1, 3

Table 3.1 Fly stocks used. The *white*⁻ fly stock carries a mutation in the *white* gene, the function of which is required for the red eye color present in wild-type flies. Transgenic fly stocks or mutants are often generated in flies with white eyes (*white*⁻), which is why the first chromosome is listed as an affected chromosome in nearly all of the stocks used in this study.

Name	Chromosome
<i>UAS-Chmp1-1; D¹/TM3Ser</i>	2
<i>UASChmp1-2/Cy; D¹/TM3Ser</i>	2
<i>lf/Cy; UAS-HM-Chmp1-1/TM6SbTb</i>	3
<i>lf/Cy; UAS-HM-Chmp1-2/TM3Ser</i>	3
<i>UAS-HM-Chmp1-3; D¹/TM3Ser</i>	2
<i>lf/Cy; UAS-HM-Chmp1-4/TM3Ser</i>	3

Table 3.2 Fly lines generated in this study.

IV. Mounting fly wings

Flies were anesthetized with CO₂ and wings were dissected from flies using fine tipped forceps under a light microscope. Wings were mounted in Gary’s Magic Mountant (GMM), which is an approximately 1:1 mixture of Canada balsam and methyl salicylate.

V. Measurements and statistics

To quantify changes in vein thickness, the area of the L3 wing vein was measured from its junction with the anterior cross vein and for 200µm in the distal direction using ImageJ software [112]. At least 10 individual wings were measured for each genotype. For each wing, the L3 wing vein area was measured three times and the mean of the measurements was used for the quantification. Measurements for each genotype were represented in a box and whisker plot generated with Microsoft Excel 2007.

To determine rescue of *Chmp1* knockdown by *Chmp1* over-expression, L3 wing vein areas of less than 3400µm² were considered fully rescued. The value of 3400µm² was chosen as

the threshold of complete rescue because of the wild-type wing veins measured, wing vein areas approached but were never more than $3400\mu\text{m}^2$. An L3 wing vein area of greater than $5200\mu\text{m}^2$ was considered not rescued. The value $5200\mu\text{m}^2$ was chosen as the threshold of no rescue because of the *Chmp1* knockdown wing veins measured, wing vein areas approached but were never less than $5200\mu\text{m}^2$. Therefore, L3 wing vein areas between $3400\mu\text{m}^2$ and $5200\mu\text{m}^2$ were considered partially rescued.

All statistical analyses were performed using IBM SPSS Statistics software. First, a two-tailed student's t-test ($p < 0.05$) was used to determine whether the mean L3 wing vein area of wild-type and *Chmp1* knockdown wings were different. Then, a one-way ANOVA with a post-hoc Dunnett's t-test ($p < 0.05$) was used to determine whether the mean L3 wing vein area of *Chmp1* knockdown wings was different from wings expressing *Chmp1-RNAi* in varying genetic backgrounds (e.g., wings carrying heterozygous mutations for regulators of DER signaling, wings carrying heterozygous deletions of the *Chmp1* gene, etc.). Statistically significant differences were denoted with an asterisk on the box and whisker plot.

VI. Immunohistochemistry of embryos

Embryos were collected for 20-24 hours onto a yeasted apple juice agar plate in an embryo collection bottle at 25°C , unless otherwise stated. The embryos were washed with distilled water into a mesh basket. The *Drosophila* embryo is protected by a shell composed of an outer chorion, as well as an inner impermeable vitelline membrane. These layers must be removed to use *Drosophila* embryos for immunostaining. The embryos were first dechorionated in 50% bleach solution and then washed well with distilled water. 0.5mL of 4% formaldehyde fix and 0.5mL of heptane were added to a microcentrifuge tube. The heptane and formaldehyde formed distinct upper (heptane) and lower (formaldehyde) layers. The embryos were collected

gently from the mesh basket with a fine brush and added to the microcentrifuge tube, where they settled to the bottom of the heptane layer. To fix the embryos, the microcentrifuge tube was shaken vigorously for 10 minutes. The fixative was then removed and the embryos were devitellinized by the addition of ice cold methanol, followed by shaking. The methanol was removed and followed by a second addition of ice cold methanol. The methanol was removed and the embryos were blocked for 1 hour in 0.1% bovine serum albumin in 0.1% PBS-Triton-X (BSA-PBST) with rotating. A fresh solution containing the primary antibody diluted in BSA-PBST was added to the embryos in the microcentrifuge tube, and they were incubated for 1 hour to overnight (at 4°C if overnight) with rotating. After incubation with the primary antibody, the embryos were washed two times in BSA-PBST for 10 minutes each with rotating. A fluorescently-tagged secondary antibody diluted in BSA-PBST was added to the microcentrifuge tube containing the embryos, and they were incubated for 1 to 3 hours with rotating. The tube was wrapped in foil during this step and for the remainder of the protocol to shield the fluorescently tagged secondary antibody from light. After incubation with the secondary antibody, the embryos were washed two times in BSA-PBST for 10 minutes each with rotating. They were then mounted onto a glass slide in Vectashield mounting media with DAPI, sealed with nail polish, and stored at 4°C protected from light until the time of imaging. Embryos were imaged on a Leica confocal microscope. All steps were carried out at room temperature, unless otherwise stated.

VII. Immunohistochemistry of imaginal discs

Imaginal discs were dissected from crawling 3rd instar larvae in 1X PBS. Using forceps, the larva, with its dorsal side up, was held about a third or half way from its posterior end. Using a second pair of forceps, the anterior end of the larva was pinched and pulled anteriorly. If pulled

slowly, the wing discs are usually easily identified. To prevent damage to the discs by handling, they were left attached to either a portion of the head or the trachea of the larva, if possible. The discs were collected into a small mesh basket filled with 1X PBS contained in a well of a 24 well plate. The basket was moved to a new well for each solution used in the following protocol. The discs were fixed in 4% formaldehyde fix for 20 minutes to 1 hour with rocking. They were washed twice for 30 minutes each in 1mL of 0.1% bovine serum albumin in 0.1% PBS-Triton-X (BSA-PBST) with rocking. The discs were blocked in 1mL BSA-PBST for 1 hour with rocking. They were then incubated in 1mL primary antibody diluted in BSA-PBST and incubated for 1 hour to overnight (at 4°C if overnight) with rocking. Then, the discs were incubated with the fluorescently-tagged secondary antibody and incubated for 1 to 3 hours with rocking. During this incubation and the remaining steps of the protocol, the discs were protected from light. The discs were then washed twice in 1mL of BSA-PBST for 30 minutes each with rocking. Under a dissecting microscope, the wing discs were dissected away from the head/trachea in 80% glycerol on a glass microscope slide. The discs were mounted in Vectashield mounting media with DAPI onto a microscope slide and imaged using a Leica confocal microscope. All steps were carried out at room temperature, unless otherwise stated.

VIII. Antibodies used for immunostaining

1 ^o or 2 ^o	Antibody	Developed in	From	Concentration
1 ^o	Anti-DRSF	Mouse	Active Motif	1:250
1 ^o	Anti-Rab5	Rabbit	AbCam	1:500
1 ^o	Anti-Vps4	Rabbit	from Harold Stenmark (The Norwegian Radium Hospital)	1:500
1 ^o	Anti-c-myc	Mouse	Sigma	1:500
2 ^o	Alexafluor 647	Chicken	Molecular probes	1:500
2 ^o	Alexafluor 555	Goat	Molecular probes	1:500

Table 3.3 Antibodies used in these studies for immunostaining of embryos and imaginal wing discs.

IX. Eye preparation and sectioning

Flies were anesthetized on a CO₂ pad, the heads were cut off using a scalpel, and very carefully a part of one eye was cut off to allow for penetration of the fixative. The heads were transferred to 200µL of 2% gluteraldehyde in 0.1M sodium phosphate buffer pH 7.2 in a microcentrifuge tube on ice. The heads were fixed for 10 minutes and spun in a microcentrifuge for 1 minute at 10,000 rpm. Then 200µL of 2% OsO₄ in 0.1M sodium phosphate buffer pH 7.2 (osmium solution) was added and the eyes were fixed for 1 hour on ice. The gluteraldehyde/osmium solution was replaced with 200µL of osmium solution and the eyes were incubated on ice for 1-6 hours. The fixative was removed and the eyes were dehydrated in 10 minute steps with an ethanol (EtOH) series on ice: 30%, 50%, 70%, 90%, and then twice with 100% EtOH at room temperature. The eyes were then washed in propylene oxide (Fisher, reagent grade) twice for 10 minutes each at room temperature. The propylene oxide was replaced with a 1:1 propylene oxide:Durcupan resin mixture and rotated slowly overnight at room temperature. The following mixture of components created a suitable soft resin of Durcupan for mounting and sectioning the eyes: 13.5g resin A, 11.125g hardener B, 0.625g accelerator C, and

2.5g plasticizer D. The 1:1 mixture of propylene oxide:Durcupan was replaced with a 100% Durcupan mixture and incubated for 3 hours at room temperature. The heads were then transferred to 100% Durcupan resin and arranged within a mold (Figure 3.1A). They were baked overnight at 70°C. The sectioning surface of the resin containing the fly heads was then trimmed with a razor blade into an asymmetric trapezoid (Figure 3.1B). This minimized the area of the block for better sectioning, and provided a way to identify the orientation of the eye tissue within the sections. The embedded eyes were sectioned with a newly cut glass knife on a Sorvall MT5000 into 0.5 to 1.0µm thick sections, which were transferred with a small wooden spatula to drops of water on a glass slide. The water was dried on an 80°C hot plate and cooled to adhere the sections to the slide. Drops of 0.1% Toluidine blue (w/v) were applied to the sections, and the microscope slide was set on an 80°C hot plate for 20 seconds (just until the Toluidine dye began to bubble). The slides were rinsed thoroughly with distilled water and air dried. A drop of DPX mounting medium was added on top of the sections. A cover slip was laid onto the DPX and weighted with two pennies. The DPX was allowed to dry overnight. The sections were imaged on a compound light microscope with a 60X oil immersion lens.

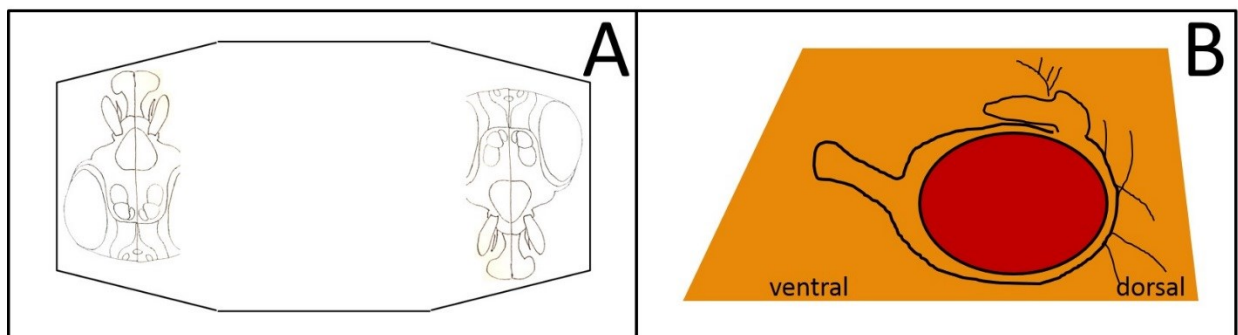


Figure 3.1 Orientation of fly heads in resin block for eye sectioning. A. The uncut eye of the fly head was positioned anterior side up near the edge of the mold. B. The sectioning surface of the resin block was trimmed into an uneven trapezoid shape so that the dorsal and ventral eye could be identified in the sections.

CHAPTER 4

RESULTS

I. Chmp1 is conserved and essential

The *Drosophila* Chmp1 protein (Flybase ID: FBgn0036805) is encoded by the *Chmp1* gene (*CG4108*), which is located in the region 75D6 on the left arm of the third chromosome (Figure 4.1A). The *Drosophila* genome carries a single *Chmp1* gene. The genomes of many model organisms, including mammals, contain two *Chmp1* genes, *Chmp1A* and *Chmp1B*, both of which are highly homologous to *Drosophila* *Chmp1*. This makes *Drosophila* an ideal model to study Chmp1 function as there is not the complication of genetic redundancy caused by the activity of closely related genes. Alignment of the *Drosophila* Chmp1 protein sequence with human Chmp1A and Chmp1B reveals that they share a conserved NLS, as well as an MIM (Figure 4.1B). *Drosophila* and human Chmp1 proteins also share Snf-7 and Vps24 domains. In amino acid sequence, *Drosophila* Chmp1 is most like human Chmp1B; they are 74% identical and 90% similar (Figure 4.1B). Through co-immunoprecipitation assays and mass spectroscopy, *Drosophila* Chmp1 has been shown to bind many proteins, including Vps4 and the *Drosophila* homologue of Ist1, CG10103 (Table 1.3) [111]. Reports show that Chmp1 binds these proteins in yeast and human cultured cells, suggesting that the function of Chmp1 is well conserved between yeast, humans, and *Drosophila* [82, 104]. Interestingly, other Chmp1 binding partners include quite a few proteins involved in translation and mRNA processing, as well as phagocytosis (Table 1.3). To summarize, as *Drosophila* expresses only one Chmp1 protein that shares binding partners and sequence features of mammalian Chmp1 proteins, it provides a good model to study the function of Chmp1.

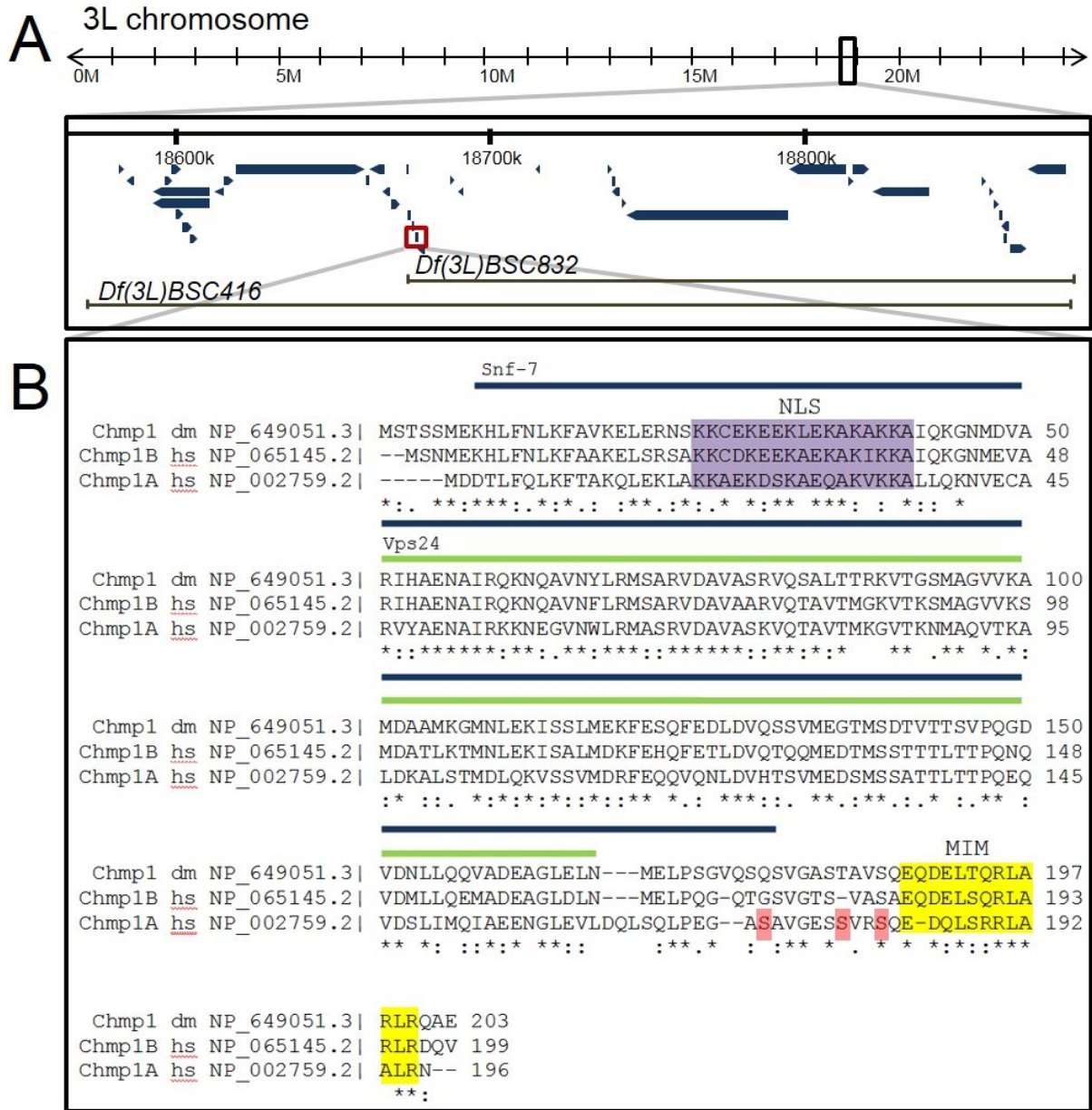


Figure 4.1 Chmp1 is conserved. **A.** Genomic region surrounding the *Chmp1* gene (boxed in red). The genomic regions removed by the chromosomal deletions *Df(3L)BSC832* and *Df(3L)BSC416* are indicated. The positions of genes located near *Chmp1* are indicated by blue arrows. **B.** ClustalX alignment of the human and Drosophila *Chmp1* protein sequences. The *Chmp1* protein contains a nuclear localization sequence (NLS, purple), an MIT-interacting motif (MIM, yellow), and Snf-7 (blue) and Vps24 (green) domains as predicted by sequence analysis. Phosphorylation sites identified for human *Chmp1A* are highlighted in pink. Residues that are similar in all three sequences are indicated by one or two dots (depending upon the degree of similarity) below the alignment, and identical residues are indicated by an asterisk.

Most information on the activity of Chmp1 has been inferred from biochemical or cell culture studies, so little is known about its role in tissue development and differentiation. Expression analysis has revealed that *Drosophila* Chmp1 is expressed throughout development in all larval and adult tissues assayed, which suggests that Chmp1 activity can be studied in a range of tissues [2, 113]. Observing the phenotypic effects of loss of Chmp1 activity should give novel insights into Chmp1 function, i.e., what proteins it interacts with or which signaling pathways it regulates. The effect of loss of Chmp1 was assessed using two independent *Drosophila* RNAi lines, one from the VDRC (*UAS-Chmp1RNAi-VDRC*) and one from the TRiP stocks (*UAS-Chmp1RNAi-TRiP*) that allowed for targeted *Chmp1* knockdown (*UAS-Chmp1RNAi*) [28]. These fly lines express hpRNAs under the control of a Gal4-responsive UAS enhancer that target different regions of the *Chmp1* mRNA. To test whether Chmp1 was essential for viability, *Chmp1* was knocked down ubiquitously throughout development. *tub-Gal4/TM3Sb* and *act5c-Gal4/TM6Tb* males were crossed to *UAS-Chmp1RNAi-TRiP* and *UAS-Chmp1RNAi-VDRC/Cy* virgin females in four separate crosses (Figure 4.2). Because the UAS-Gal4 system is temperature dependent, the F1 generation from each cross was raised at 25°C, 28°C, and 30°C to compare phenotypes at different temperatures.

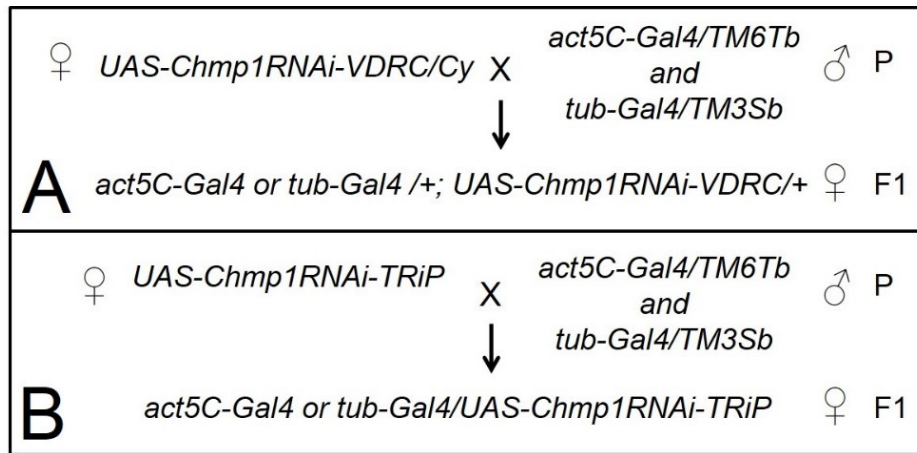


Figure 4.2 Cross design to test ubiquitous *Chmp1* knockdown. **A.** Cross design for ubiquitous *Chmp1* knockdown using the VDRC RNAi insert, located on the second chromosome. **B.** Cross design for ubiquitous *Chmp1* knockdown using the TRiP RNAi insert, located on the third chromosome. P is parental generation, F1 is filial generation. Only F1 progeny of the desired genotype are shown.

When *Chmp1* was knocked down ubiquitously during fly development at 30°C and 28°C, the only progeny that eclosed were *Sb*, *Tb*, or *Cy*, indicating that they either did not carry the Gal4 driver or did not carry the UAS transgene (i.e. they were not *Chmp1* knockdown flies). At 25°C, no flies survived ubiquitous knockdown using the TRiP RNAi line. Additionally, no flies survived when *Chmp1* was knocked down ubiquitously using the VDRC RNAi line with *tub-Gal4*. In these crosses, expression of *Chmp1* RNAi was lethal at or before the pupal stage of development. However, occasional escapers, all of which were female, survived ubiquitous *Chmp1* knockdown using the VDRC RNAi line with *act5c-Gal4*. The surviving flies had thickened wing veins, mildly rough eyes, and a general failure to thrive. This is possibly indicative of degree of *Chmp1* knockdown, i.e., the RNAi line from the TRiP stocks may have provided a more effective knockdown than the VDRC line. It is also possible that the *tub-Gal4/TM3Sb* fly line drives Gal4 expression stronger than the *act5C-Gal4/TM6Tb* fly line.

It is possible that the lethality observed with *Chmp1* RNAi expression was caused by off target RNAi effects. In fact, according to the VDRC website, the *UAS-Chmp1RNAi-VDRC* line has a potential off-target of the gene *natalisin* (*CG34388*), which is involved in male mating behavior [114]. Additionally, knockdown of *natalisin* using a VDRC RNAi fly line is lethal before the pupal stage, similarly to *Chmp1* knockdown [115]. The fact that only female survivors were observed could also support the possibility of the off-target effects causing lethality. However, *Chmp1* knockdown was lethal using two independent RNAi lines that target different portions of the *Chmp1* mRNA. Therefore, *Chmp1* may be essential for proper development in *Drosophila*.

II. *Chmp1* knockdown produces a cell fate change in the wing

Because ubiquitous *Chmp1* knockdown was lethal, the UAS Gal4 system was used to limit knockdown to the wing, a well-characterized tissue that is not essential for *Drosophila* development. *MS1096-Gal4*, *salm-Gal4*, *ptc-Gal4*, or *en-Gal4* drivers were used to drive *Chmp1* knockdown. Each driver expresses Gal4 in the pattern of a developmental gene in the wing (Figure 4.3).

The *MS1096-Gal4* driver expresses Gal4 protein relatively strongly in the dorsal compartment of the wing. This is a useful driver for several reasons. First, as sometimes over-expression or knockdown of a gene has weak phenotypic effects, the *MS1096-Gal4* driver allows for stronger over-expression or knockdown of the gene-of-interest to generate stronger phenotypes. Second, the *MS1096-Gal4* driver only expresses Gal4 on the dorsal wing, so it only affects the dorsal wing veins: L3, L5 and distal L4 (Figure 4.3). When studying genes involved in wing vein patterning, the ventral wing veins remain unaffected and can provide an in-tissue

negative control. Third, the *MS1096-Gal4* transgene is inserted on the X chromosome, which can increase the ease with which genetic crosses can be performed.

The *salm-Gal4*, *ptc-Gal4*, and *en-Gal4* driver transgenes are each located on the second chromosome and drive Gal4 expression on both dorsal and ventral wing surfaces. *salm-Gal4* and *ptc-Gal4* are moderate drivers. *salm-Gal4* drives Gal4 expression from the posterior of the L2 wing vein to midway between the L4 and L5 wing veins (Figure 4.3). *ptc-Gal4* has a similar but narrower region of expression between the L3 and L4 wing veins (Figure 4.3). *en-Gal4* is a stronger driver and has a very precise boundary of expression. *en-Gal4* expresses Gal4 in the pattern of the *engrailed* gene, in the anterior cells of each parasegment of the developing fly. In the wing, this corresponds to the posterior compartment. The anterioposterior (AP) compartment boundary in the wing is located a few cells anterior of the L4 wing vein. The expression of *engrailed* begins a few cells anterior to the AP compartment boundary (Figure 4.3).

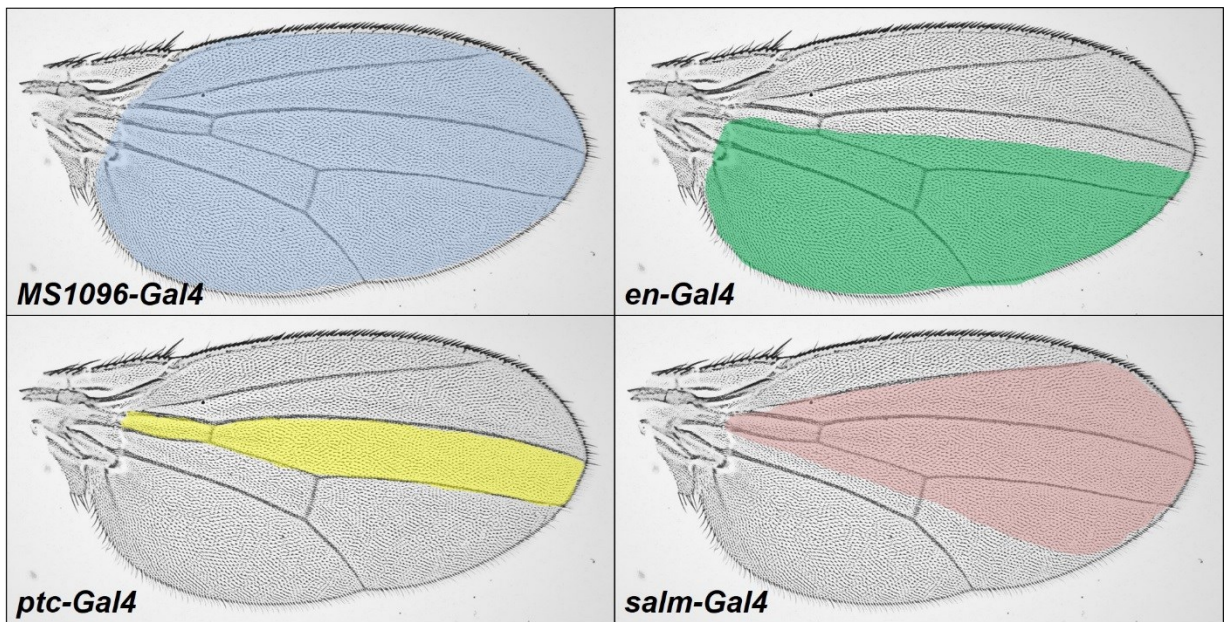


Figure 4.3 Expression patterns of wing drivers. Diagrams of the *Drosophila* wing showing expression of Gal4 in color by different drivers. Distal is right, anterior is uppermost.

To achieve *Chmp1* knockdown in the wing, *UAS-Chmp1RNAi-TRiP* homozygous and *UAS-Chmp1RNAi-VDRC/Cy* virgin females were crossed to *MS1096-Gal4*, *salm-Gal4*, *ptc-Gal4*, or *en-Gal4* homozygous males and the progeny was grown at 25°C, 28°C, and 30°C (Figure 4.4). Straight winged (not *Cy*) flies were of the correct genotype. Wings from females were dissected and mounted onto a microscope slide in GMM.

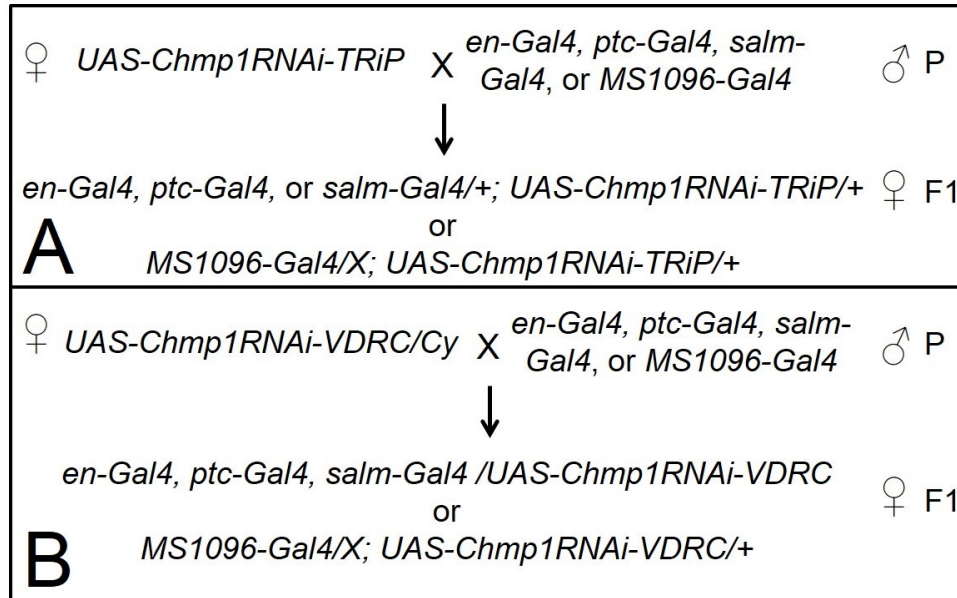


Figure 4.4 *Chmp1* knockdown cross design. **A.** Cross design for *Chmp1* knockdown in the wing using the TRiP RNAi insert, located on the third chromosome. **B.** Cross design for *Chmp1* knockdown in the wing using the VDRC RNAi insert, located on the second chromosome. P is parental generation, F1 is filial generation. Only F1 progeny of the desired genotype are shown.

Knockdown of *Chmp1* primarily on the dorsal side of the wing (*MS1096-Gal4/X; UAS-Chmp1RNAi-VDRC/+*) resulted in thickening of the dorsal wing veins, L3, L5, and distal L4 (Figure 4.7B). Thickening of the wing veins was observed with *Chmp1* knockdown using several Gal4 drivers, and the phenotype was only observed in the pattern of the driver (i.e., *en-Gal4* expresses Gal4 in the posterior wing, and only posterior wing veins were thickened), suggesting that the vein phenotype was specifically due to expression of *Chmp1* RNAi, rather than due to other genetic interactions (Figures 4.7E and G).

Similar thick vein phenotypes were observed using the independently created TRiP RNAi fly line that targeted a different portion of the *Chmp1* mRNA, showing that the vein thickening was likely due to *Chmp1* knockdown rather than off target effects, in which the hpRNA causes degradation of other mRNAs (Figure 4.7D, F, and H). *Chmp1* knockdown with the TRiP line resulted in a stronger wing vein phenotype (i.e., thicker wing veins) than was observed with the VDRC line, suggesting that the TRiP line produced more effective knockdown than the VDRC line, which is consistent with the findings with ubiquitous *Chmp1* knockdown.

In order to produce the thick veins phenotype, it seemed that *Chmp1* expression had to be reduced rather strongly. That is, strong drivers (*MS1096-Gal4* and *en-Gal4*) and higher temperatures (28°C and 30°C) were required to observe a phenotype that differed much from wild-type. At 25°C, the wing vein thickening was discernible, at 28°C it was moderate, and at 30°C it was severe. In fact, at 30°C the wing veins became so thick that they could not easily be distinguished from the intervein tissue (Figure 4.5). Therefore, 28°C was used to analyze the effects of *Chmp1* knockdown on wing vein development, as this would allow identification of both enhancement and suppression of the vein phenotype. Although the Chmp1 protein levels were not measured to quantify the level of *Chmp1* knockdown, the mildness of the vein thickening phenotype may suggest that, at least during wing development, a relatively small amount of functional Chmp1 was sufficient for cellular function and tissue development. However, it could also indicate that the RNAi fly lines are not particularly effective, or that Chmp1 is highly expressed and therefore difficult to reduce significantly, or that the Chmp1 protein perdures though mRNA levels are reduced.

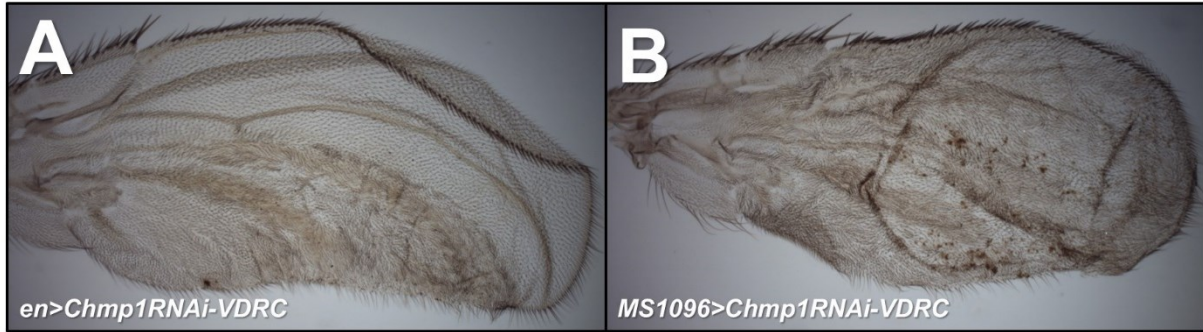


Figure 4.5 *Chmp1* knockdown at 30°C. Light micrographs of wings from female *Drosophila* raised at 30°C. Distal is right, anterior is uppermost. **A.** *en-Gal4/UAS-Chmp1RNAi-VDRC*. **B.** *MS1096-Gal4/X; UAS-Chmp1RNAi-VDRC/+*.

The change in wing vein thickness between wild-type and *Chmp1* knockdown wings was statistically significant. To quantify the change in wing vein thickness between genotypes, the area of the L3 wing vein was measured for 200 microns past the anterior cross vein (acv) in at least 10 individual flies. The measured values were plotted in a box and whisker plot (Figure 4.8). A student's t-test ($p < 0.05$) was used to compare the area of the L3 wing vein between *Chmp1* knockdown and wild-type flies.

To provide further evidence that the observed phenotype was due to *Chmp1* knockdown, *Chmp1* was knocked down in flies heterozygous for loss of the *Chmp1* gene. No *Chmp1* mutant currently exists, so two chromosomal deletions, *Df(3L)BSC416* and *Df(3L)BSC832* that remove the *Chmp1* gene were used (Figures 4.1 and 4.6). *MS1096-Gal4; GlaBc/Cy* virgin females were crossed to *UAS-Chmp1RNAi-VDRC/Cy* males. From the F1 generation, males that were *MS1096-Gal4/Y; Gla/UAS-Chmp1RNAi-VDRC* were collected and crossed to virgin females that were either *Df(3L)BSC832/TM6Sb* or *Df(3L)BSC419/TM6Sb*. From this cross, flies that were female, not *Gla*, and not *Sb* were of the correct genotype (*MS1096-Gal4/X; UAS-Chmp1RNAi-VDRC/+; Df(3L)BSC832/+* and *MS1096-Gal4/X; UAS-Chmp1RNAi-VDRC/+; Df(3L)BSC419/+*).

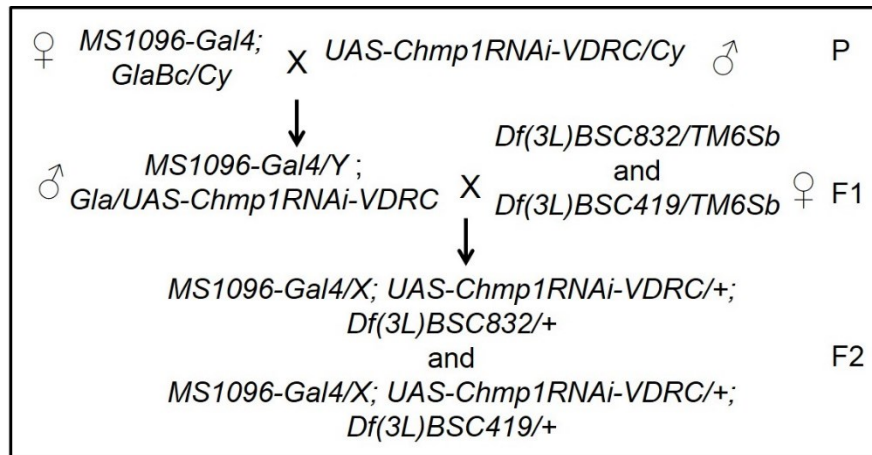


Figure 4.6 Cross design for *Chmp1* knockdown in *Chmp1* heterozygous background. P is parental generation, F1 is first filial generation, F2 is second filial generation. Only F1 and F2 progeny of the desired genotypes are shown.

When *Chmp1* was knocked down in the wings of flies carrying heterozygous chromosomal deletions that removed the *Chmp1* gene, the *Chmp1* knockdown phenotype was enhanced (Figures 4.7I and J). To quantify the changes in wing vein thickness, the area of the L3 wing vein was measured for 200 microns past the anterior cross vein (acv) in at least 10 individual flies and the values were represented in a box and whisker plot (Figure 4.8). A one-way ANOVA with a post-hoc Dunnett's t-test ($p < 0.05$) compared the area of the L3 wing vein of flies with *Chmp1* knockdown in a *Chmp1* heterozygous background to flies with *Chmp1* knockdown alone and showed that they were not significantly different (Figure 4.8). However, the general enhancement of the *Chmp1* knockdown phenotype observed in a *Chmp1* heterozygous background supports the finding that the thick vein phenotype is due to loss of *Chmp1*.

As reduced *Chmp1* activity results in thickened wing veins, it appears that one role of *Chmp1* is to negatively regulate wing vein size. Thickened wing veins are classically associated with a cell fate change from intervein to vein cell in the wing [14]. So it is important to note that,

although it appears that *Chmp1* knockdown causes wing veins to overgrow, the wing vein thickening was not due to extra growth, but a change in cell fate. In wild-type wings, veins are only a few cells in width. However, when *Chmp1* was knocked down, cells that would normally border the wing vein as intervein cells adopted a vein fate instead, causing a thickened wing vein in the adult. This caused the number of cells between veins to appear reduced, and was especially obvious when *Chmp1* was knocked down with *ptc-Gal4* (Figure 4.7H). So, as *Chmp1* knockdown results in thickened wing veins, *Chmp1* appears to be a negative regulator of wing vein differentiation, favoring an intervein cell fate over a vein fate.

Driving *Chmp1* knockdown on the dorsal wing with *MS1096-Gal4* produced an upward curving of the wing at the margin, resulting in a concave wing. This phenotype was likely caused by a reduction in the area of the dorsal wing surface, perhaps due to smaller cell size. During wing development, each wing cell produces one hair. This means that hair density on the wing surface gives an indication of the apical surface size of wing cells [116, 117]. When *Chmp1* knockdown was driven by *MS1096-Gal4* or *en-Gal4*, intervein regions had increased wing hair density, suggesting a smaller cell size than wild-type cells (compare Figure 4.7K with 4.7L).

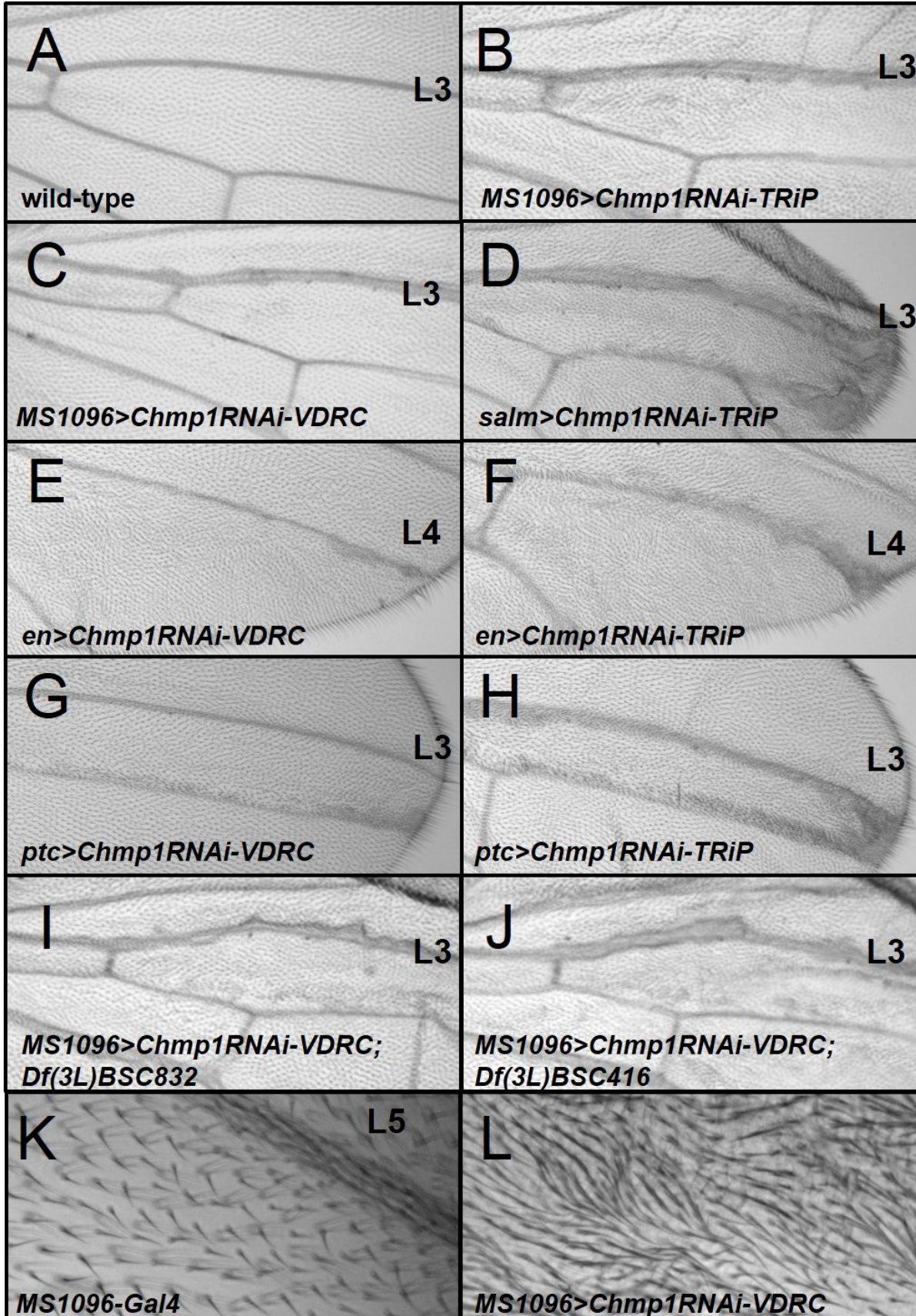


Figure 4.7 *Chmp1* knockdown results in thickened wing veins. Light micrographs of adult female wings raised at 28°C. The L3 or L4 wing vein is indicated, distal is right, anterior is uppermost. **A.** *Oregon R*. **B, D, F, and H.** *Chmp1* knockdown in the wing with the TRiP line caused thickened wing veins. **B.** *MS1096-Gal4/X; UAS-Chmp1RNAi-TRiP/+*. **D.** *salm-Gal4/+; UAS-Chmp1RNAi-TRiP/+*. **F.** *en-Gal4/+; UAS-Chmp1RNAi-TRiP/+*. **H.** *ptc-Gal4/+; UAS-Chmp1RNAi-TRiP/+*. **C, E, and G.** *Chmp1* knockdown using the VDRC line causes thick veins. **C.** *MS1096-Gal4/X; UAS-Chmp1RNAi-TRiP/+*. **E.** *en-Gal4/UAS-Chmp1RNAi-VDRC*. **G.** *en-Gal4/UAS-Chmp1RNAi-VDRC*. **I and J.** Heterozygosity for two chromosomal deletions (Figure 4.1) containing the gene encoding *Chmp1* enhances the *Chmp1* knockdown phenotype. **I.** *MS1096-Gal4/X; UAS-Chmp1RNAi-VDRC/+; Df(3L)BSC832/+*. **J.** *MS1096-Gal4/X; UAS-Chmp1RNAi-VDRC/+; Df(3L)BSC416/+*. **K.** Wing hairs are spaced evenly in *MS1096-Gal4* wings. **L.** *Chmp1* knockdown results in a higher density of wing hairs. Region shown is posterior to the L5 wing vein. *MS1096-Gal4/X; UAS-Chmp1RNAi-VDRC*. Images A-J taken at the same magnification. Images K and L taken at the same magnification.

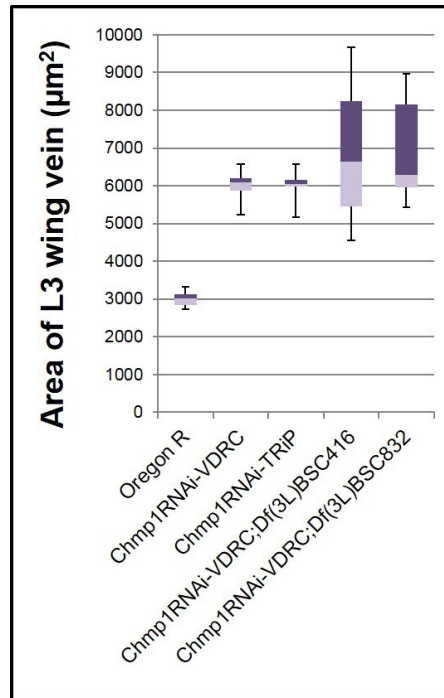


Figure 4.8 *Chmp1* knockdown in wings heterozygous for the *Chmp1* gene: wing vein measurements. A box and whisker plot depicting the area of the measured L3 wing vein in square microns. The upper and lower brackets represent the maximum and minimum measurements, respectively. Heterozygosity for the *Chmp1* gene enhances the *Chmp1* knockdown phenotype, though not statistically significantly. All genotypes shown had wing veins that were significantly thicker than wild-type. Statistical differences were determined by a one-way ANOVA with post-hoc Dunnett's, $p < 0.05$.

To further evaluate *Chmp1* function in *Drosophila*, two transgenic fly lines were generated that allowed for over-expression of either the wild-type *Chmp1* protein or an N-terminal His-Myc (HM) tagged *Chmp1* [118]. Two vectors, pUAST and pUASHM were used to generate these fly lines (see Chapter 3 Section I for method). The vectors contained a *white*⁺ marker and a multiple cloning site downstream of a UAS enhancer, all flanked by p-element ends that mediated insertion into the genome of the fly. The *Chmp1* cDNA was inserted into the multiple cloning site of each vector. The pUASHM vector added an HM tag to *Chmp1*. The pUAST and pUASHM vectors containing the *Chmp1* cDNA were sent to BestGene Inc., where the transgenic flies (*UAS-Chmp1* and *UAS-HM-Chmp1*, respectively) were generated. Transgenic flies were crossed to a fly stock containing multiple balancer chromosomes to determine the chromosomal location of each insertion, and to generate a balanced stock. Twenty independent lines were generated that carried a random insertions of one of the constructs within their genome, usually on the second and/or third chromosomes. Transgenes in different chromosomal locations may show different levels of expression, so having a selection of different insertions is useful. Also, having insertions on different chromosomes provides more flexibility when generating specific genetic combinations.

As the insertions were marked with *white*⁺, dark red eyes in transgenic fly lines usually indicate that the insertion can be expressed at higher levels than flies with lighter orange or yellow eyes. Varying eye colors were likely due to the site of insertion, i.e., if the insertion was located within a highly expressed portion of the fly genome, then a darker eye resulted. On the other hand, if the insertion was located within a portion of the genome that is not highly expressed, a lighter eye resulted. Dark red eyes can also indicate the presence of multiple insertions. So of the twenty fly lines received, those with the darkest eyes were chosen first for

balancing in an attempt to select for highly expressing lines. When balancing the fly lines, the chromosome carrying the insertion was determined through crossing to a fly stock carrying multiple balancers and dominant markers. All insertions were on either the second or the third chromosome, and only fly lines with a single insertion chromosome were used in the study.

If the *Chmp1* transgenes can produce functional Chmp1 protein, then they should rescue the *Chmp1* knockdown phenotype. To test this, *UAS-Chmp1* or *UAS-HM-Chmp1*, *UAS-Chmp1RNAi*, and a driver had to be present in the same fly. Different crosses were required for lines carrying *UAS-Chmp1* or *UAS-HM-Chmp1* on the second chromosome (*UAS-Chmp1-1* and *-2*, *UAS-HM-Chmp1-3*) or the third chromosome (*UAS-HM-Chmp1-1*, *-2*, and *-4*) (Figure 4.9A and B). For lines carrying *UAS-Chmp1* or *UAS-HM-Chmp1* on the second chromosome (Figure 4.9A), *UAS-Chmp1* or *UAS-HM-Chmp1/Cy; D¹/TM3Ser* virgin females were crossed to *If/Cy; UAS-Chmp1RNAi-TRiP/TM3Sb* males. From the progeny of that cross, *Cy*, *D¹* males (*UAS-Chmp1* or *UAS-HM-Chmp1/Cy; UAS-Chmp1RNAi-TRiP/D¹*) were collected and crossed to *MS1096-Gal4* virgin females. From this cross, females that were not *Cy* and not *D¹* were of the correct genotype (*MS1096-Gal4/X; UAS-Chmp1* or *UAS-HM-Chmp1/+; UAS-Chmp1RNAi-TRiP/+*). For lines carrying *UAS-Chmp1* or *UAS-HM-Chmp1* on the third chromosome (Figure 4.9B), *If/Cy; UAS-HM-Chmp1/TM6Sb* or *TM3Ser* virgin females were crossed to *UAS-Chmp1RNAi-VDRC/Cy; D¹/TM3Ser* males. From the progeny, *Cy*, *D¹* males (*UAS-Chmp1RNAi-VDRC/Cy; UAS-HM-Chmp1/D¹*) were collected and crossed to *MS1096-Gal4* virgin females. From this cross, females that were not *Cy* and not *D¹* were of the correct genotype (*MS1096-Gal4/X; UAS-Chmp1RNAi-VDRC/+; UAS-HM-Chmp1/+*). Wings were dissected and mounted in GMM on a microscope slide.

As a control, a fly line that allows for expression of GFP under Gal4 control, *UAS-GFP* was used in place of the *Chmp1* over-expression transgene. In this case, the *UAS-GFP* and *UAS-Chmp1RNAi* transgenes had to be present in the same fly, along with a driver (Figure 4.9C). *UAS-GFP* males were crossed to *MS1096-Gal4; GlaBc/Cy* virgin females. From the progeny, males that were *Gla* and not *Cy* (*MS1096-Gal4/Y; UAS-GFP/Gla*) were collected and crossed to *UAS-Chmp1RNAi-VDRC/Cy* virgin females. From this cross, females that were not *Cy* and not *Gla* were of the correct genotype (*MS1096-Gal4/X; UAS-GFP/UAS-Chmp1RNAi-VDRC*).

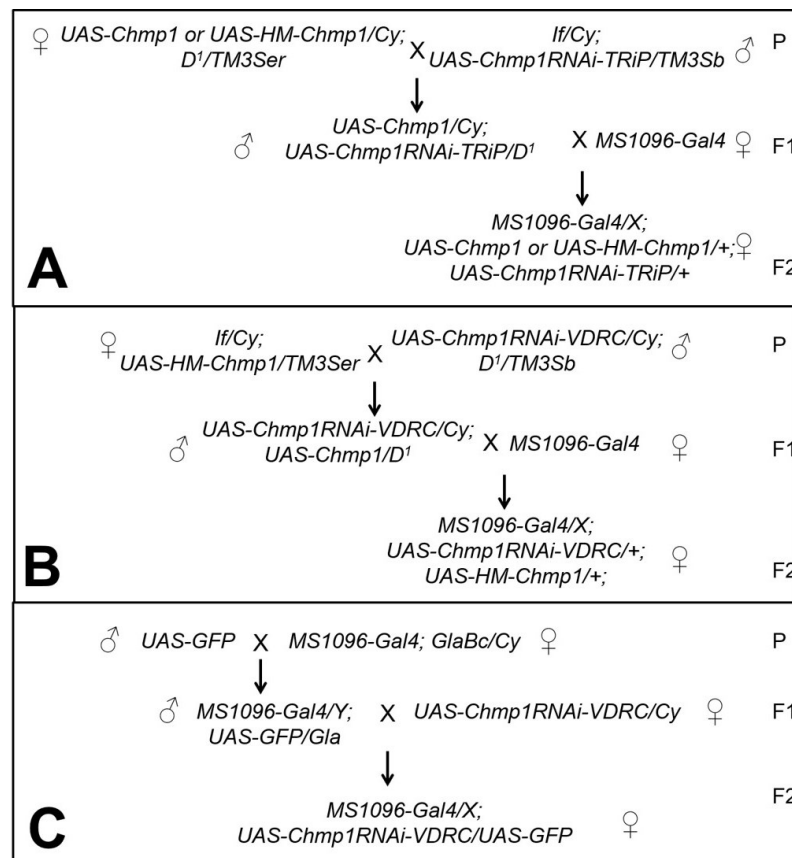


Figure 4.9 Cross design for rescue of *Chmp1* knockdown with *Chmp1* over-expression. A. Cross design for lines in which *UAS-Chmp1* or *UAS-HM-Chmp1* was located on the second chromosome. **B.** Cross design for lines in which *UAS-Chmp1* or *UAS-HM-Chmp1* was located on the third chromosome. **C.** Cross design for control cross, using *UAS-GFP*. P is parental generation, F1 is first filial generation, F2 is second filial generation. Only F1 and F2 progeny of the desired genotypes are shown.

To quantify the changes in wing vein thickness, the area of the L3 wing vein was measured for 200 microns past the anterior cross vein (acv) in at least 10 individual flies and the values were represented in a box and whisker plot (Figure 4.11). A one-way ANOVA with a post-hoc Dunnett's t-test ($p < 0.05$) compared the area of the L3 wing vein of flies expressing *Chmp1RNAi*, concomitant with *UAS-Chmp1*, *UAS-HM-Chmp1*, or *UAS-GFP* to flies expressing *Chmp1RNAi* alone (Figure 4.11). Expression of *UAS-Chmp1* or *UAS-HM-Chmp1* concomitant with *Chmp1RNAi* under *MS1096-Gal4* control significantly decreased the thick vein phenotype in all lines tested. In fact, expression of *UAS-Chmp1* completely rescued the thick vein phenotype in over 60% of wings (Figure 4.10E and F, 4.11, and Table 4.1), while partial rescue was observed in 34% of wings (Figure 4.10E' and F', 4.11, and Table 4.1). Only 3% of wings showed no rescue of the *Chmp1* knockdown phenotype by *Chmp1* over-expression (Figure 4.10E'', 4.11, and Table 4.1). Expression of the HM-*Chmp1* partially rescued the *Chmp1* knockdown phenotype in over 80% of wings analyzed (Figure 4.10A' - 4.10D', 4.11, and Table 4.1), while full rescue was observed in about 13% of wings (Figure 4.10A - 4.10D, 4.11, and Table 4.1), and no rescue in 5% of wings (Figure 4.10A'' - 4.10B'', 4.11, and Table 4.1). The rescue observed in these experiments was not simply the result of reduced Gal4 binding to the *Chmp1RNAi* promoter due to the presence of a second UAS promoter, as wings with over-expression of a gratuitous protein (*UAS-GFP*) concomitant with *Chmp1RNAi* were not significantly different from wings with *Chmp1* knockdown alone. Additionally, expression of *UAS-GFP* concomitant with *Chmp1RNAi* never fully rescued the wing vein phenotype and only provided partial rescue in approximately 30% of wings (Table 4.1, Figure 4.11).

These results suggest that the *Chmp1* over-expression transgenes can produce a functional *Chmp1* protein. The low frequency of failure to rescue might be explained by the

activity of *Chmp1* RNAi, which inevitably targets both *Chmp1* mRNA from both the endogenous *Chmp1* gene and the *Chmp1* over-expression transgenes. The ability of wild-type *Chmp1* to provide better rescue than HM-*Chmp1* suggests that HM-*Chmp1* may be less active or less stable than the wild-type *Chmp1*. This could be due to the epitope tag that either caused HM-*Chmp1* to be degraded more quickly than the wild-type *Chmp1*, or inhibited some of the function of *Chmp1*. It could also be due to the insertion site of the transgenes; perhaps by chance the HM-*Chmp1* transgenes tested were in regions of chromatin that are less accessible to transcription compared to the wild-type *Chmp1* transgenes. The finding that over-expressed *Chmp1* can rescue the thick vein phenotype further supports the conclusion that this phenotype results specifically from *Chmp1* knockdown, rather than off-target effects. It also supports the proposal that *Chmp1* negatively regulates wing vein differentiation and promotes intervein cell fate. Additionally, it confirms that the *Chmp1* over-expression lines are functional and may be used for further studies.

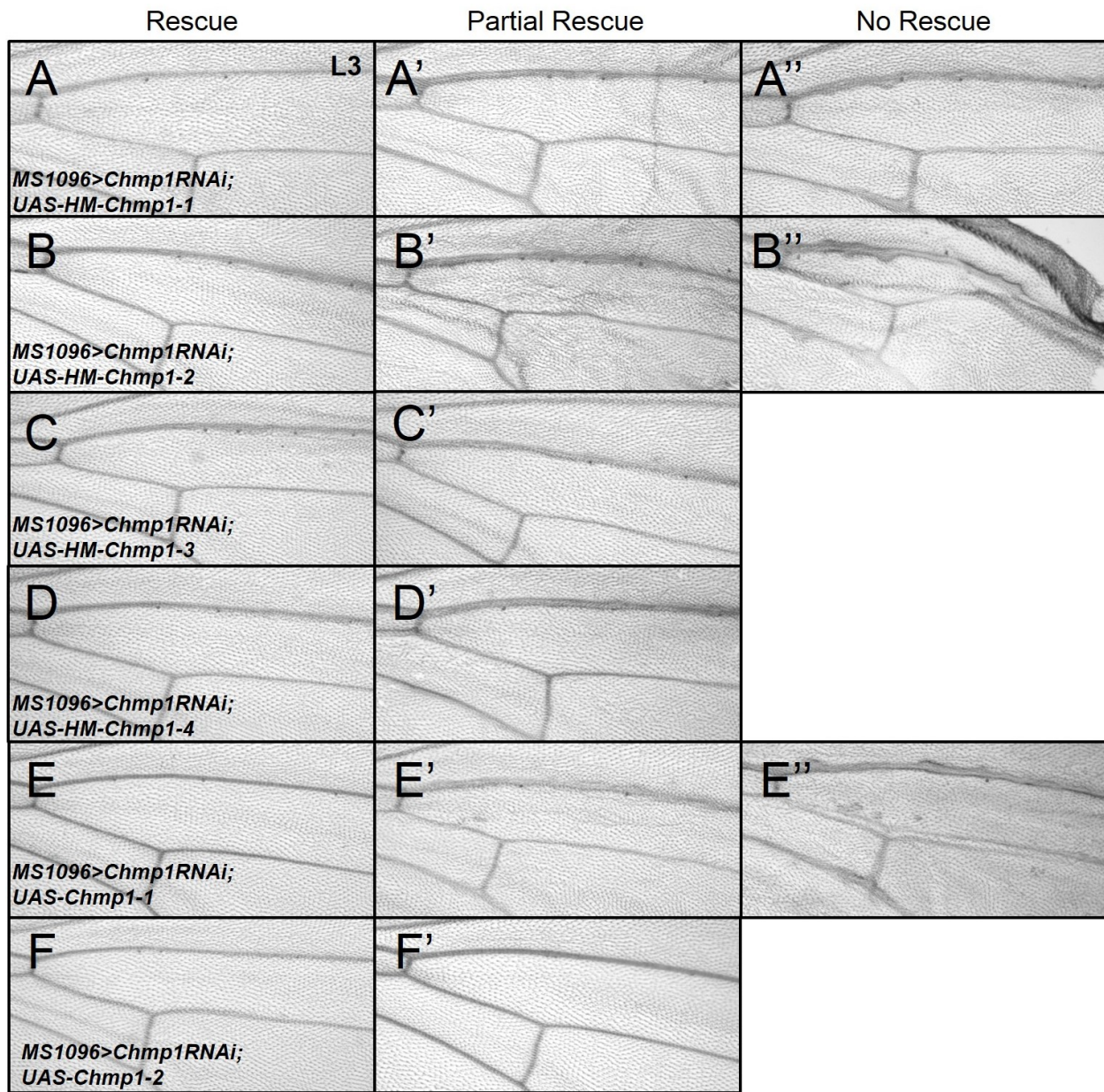


Figure 4.10 *Chmp1* over-expression rescues the *Chmp1* knockdown phenotype. Light micrographs of adult female wings raised at 28°C. L3 vein is indicated, distal is right, anterior is uppermost. **A-F**. Complete rescue of *Chmp1* knockdown with *Chmp1* over-expression. Area of L3 wing vein less than 3400µm². **A'-F'**. Partial rescue of the *Chmp1* knockdown phenotype with *Chmp1* over-expression. Area of L3 wing vein between 3400 and 5200µm². **A''-E''**. No rescue of the *Chmp1* knockdown phenotype with *Chmp1* over-expression. Area of L3 wing vein larger than 5200µm². A-A''. *MS1096-Gal4/X; UAS-Chmp1RNAi-VDRC/+; UAS-HM-Chmp1-1/+*. B-B''. *MS1096-Gal4/X; UAS-Chmp1RNAi-VDRC/+; UAS-HM-Chmp1-2/+*. C-C''. *MS1096-Gal4/X; UAS-Chmp1RNAi-VDRC/UAS-HM-Chmp1-3*. All wings of this genotype displayed at least partial rescue. D-D''. *MS1096-Gal4/X; UAS-Chmp1RNAi-VDRC/+; UAS-HM-Chmp1-4/+*. All wings of this genotype displayed at least partial rescue. E-E''. *MS1096-Gal4/X; UAS-Chmp1RNAi-VDRC/UAS-Chmp1-1*. F-F''. *MS1096-Gal4/X; UAS-Chmp1RNAi-VDRC/UAS-HM-Chmp1-2*. All wings of this genotype displayed at least partial rescue.

Genotype:	MS1096> Chmp1RNAi, UAS-HM-Chmp1- 1	MS1096> Chmp1RNAi, UAS-HM-Chmp1- 2	MS1096> Chmp1RNAi, UAS-HM-Chmp1- 3	MS1096> Chmp1RNAi, UAS-HM-Chmp1- 4	MS1096> Chmp1RNAi, UAS-Chmp1- 1	MS1096> Chmp1RNAi, UAS-Chmp1- 2	MS1096> Chmp1RNAi, UAS-GFP
Full rescue (<3400µm ²)	0	2 (7%)	8 (27%)	6 (19%)	18 (58%)	20 (67%)	0
Partial rescue (3400-5200µm ²)	24 (83%)	27 (90%)	22 (73%)	25 (81%)	11 (35%)	10 (33%)	5 (33%)
No rescue (>5200µm ²)	5 (17%)	1 (3%)	0	0	2 (7%)	0	10 (67%)
Total wings	29	30	30	31	31	30	15

Table 4.1 *Chmp1* over-expression can rescue the *Chmp1* knockdown phenotype.

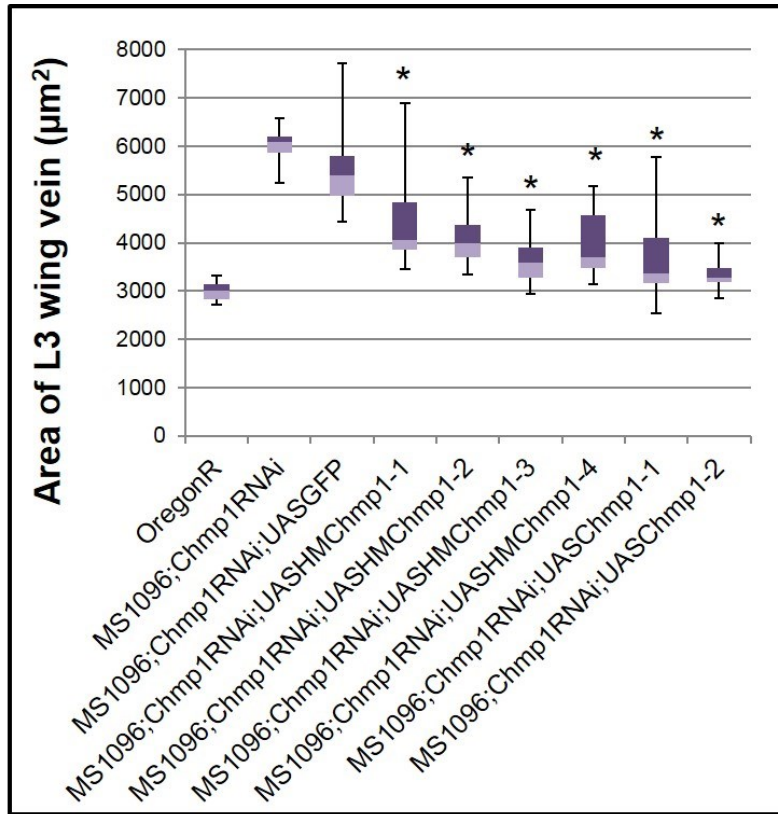


Figure 4.11 *Chmp1* over-expression rescues *Chmp1* knockdown: wing vein measurements.

A box and whisker plot depicting the area of the measured L3 wing vein in square microns. The upper and lower brackets represent the maximum and minimum measurements, respectively. All genotypes shown had wing veins that were significantly thicker than wild-type. Asterisks mark genotypes with wing veins that were significantly thinner than *Chmp1* knockdown. Significant differences were determined by a one-way ANOVA with post-hoc Dunnett's, $p < 0.05$.

III. *Chmp1* interacts with regulators of DER signaling

Studies suggest that ESCRT machinery negatively regulates EGFR signaling. For example, in mammalian cells over-expression of the ESCRT-0 component hepatocyte growth factor receptor substrate (Hrs) or loss of the ESCRT-I component Tsg101 [58, 119] caused impaired EGFR degradation. Additionally, losing activity of Hrs in *Drosophila* impaired degradation of the DER, causing enhanced EGFR signaling indicated by increased phospho-ERK [59, 120]. In *Drosophila*, the DER signaling pathway promotes the development of wing veins.

When the activity of two positive regulators of DER, Rhomboid (Rho) and Vein (Vn), is lost (a *rho^{ve-1}, vn^l* homozygous mutant wing), veins are lost as well (Figure 4.13C). On the other hand, enhanced DER signaling, e.g., by over-expression of *rho*, causes thickened and extra wing veins [36]. So the thick wing veins observed with *Chmp1* knockdown might have been caused by over-active DER signaling, due to a failure of ESCRT machinery to down-regulate the DER. If *Chmp1* negative regulates the DER signal, then reducing DER signaling in a *Chmp1* knockdown wing should suppress the thick vein phenotype. On the other hand, increasing DER signaling should enhance the *Chmp1* knockdown phenotype.

To test this, *Chmp1* was knocked down in wings heterozygous for loss of function alleles of either positive or negative regulators of DER signaling. To achieve this, the *Chmp1* RNAi transgene, a driver, and one loss of function allele for regulators of the DER had to be present in the same fly (Figure 4.12). Positive regulators of the DER tested were Rho and Vn, and negative regulators tested were Kekk-1 (Kek1), Sprouty (Sty) or Argos (Aos). *MS1096-Gal4; Cy/Sco* virgin females were crossed to *UAS-Chmp1RNAi-VDRC/Cy* males. From this cross, *Sco* males (*MS1096-Gal4/Y; UAS-Chmp1RNAi-VDRC/Sco*) were crossed to virgin females carrying loss of function alleles for regulators of DER signaling that were either homozygous viable or balanced with *TM3Sb*. From the progeny, females that were not *Sco* and not *Sb* were of the desired genotype. Wings were dissected off and mounted in GMM on a microscope slide.

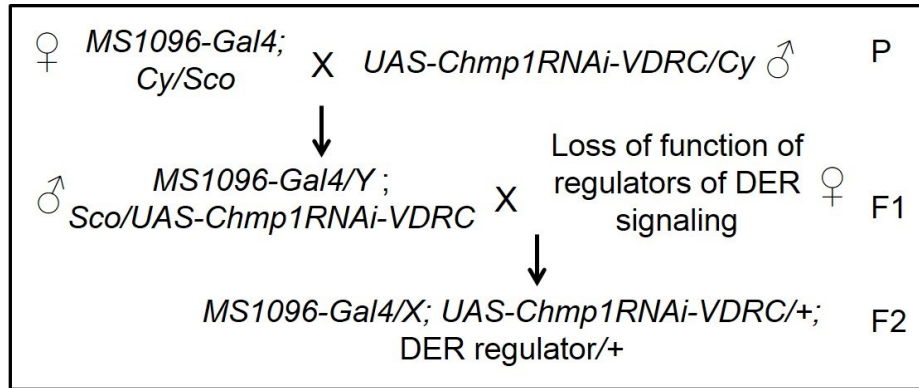


Figure 4.12 Cross design testing for interaction between *Chmp1* and DER regulators. All loss of function alleles for regulators of DER signaling used were on the third chromosome, as was the *aos* over-expression transgene (*UAS-aos*). The loss of function alleles used were *rho^{ve-1}*, *vn¹*, *kek1*, *sty^{A5}*, *aos^{A7}*, *aos^{rlt}*, and *aos^{w11}*. *sty^{A5}*, *aos^{A7}*, and *aos^{w11}* were balanced with *TM3Sb*, the others alleles and *UAS-aos* were homozygous. P is parental generation, F1 is first filial generation, F2 is second filial generation. Only F1 and F2 progeny of the desired genotypes are shown

To quantify the changes in wing vein thickness, the area of the L3 wing vein was measured for 200 microns past the anterior cross vein (acv) in at least 10 individual flies and the values were represented in a box and whisker plot (Figure 4.14). A one-way ANOVA with a post-hoc Dunnett's t-test ($p < 0.05$) compared the area of the L3 wing vein of flies expressing *Chmp1RNAi* in backgrounds heterozygous for mutations in DER regulators to flies expressing *Chmp1RNAi* alone (Figure 4.11).

In *Chmp1* knockdown wings that were also heterozygous for loss of function alleles of two positive regulators of the DER pathway, *rho^{ve-1}* and *vn¹* (*MS1096-Gal4/X; UAS-Chmp1RNAi-VDRC/+; rho^{ve-1}, vn¹/+*), the wing vein phenotype was partially suppressed (Figure 4.13D). This genetic interaction was a first indication that *Chmp1* may regulate DER signaling in the *Drosophila* wing. Wings that were just heterozygous for *rho^{ve-1} vn¹* appeared wild-type, which means that the suppression of the vein thickening phenotype was not simply an additive effect. No suppression was observed when *Chmp1* was knocked down in *rho^{ve-1}* heterozygous

wings, although partial suppression was observed in *vn*^l heterozygous wings (Figure 4.13E and F). This suggests that the suppression observed in *rho*^{ve-1}, *vn*^l heterozygous wings was due to loss of *vn*, rather than loss of *rho*. An interaction with Vn rather than Rho, is interesting, especially as these two proteins are reported to have a synergistic role in the wing [121, 122]. This result could be due to the relatively strong ability of Rho to activate the DER, while Vn is considered a relatively weak activator. Thus, a single copy of the *rho* gene might still enhance DER signaling significantly, but a single copy of the *vn* gene may provide little activity.

Reduced activity of positive regulators of the DER pathway suppressed the *Chmp1* knockdown phenotype in the wing, suggesting that Chmp1 negatively regulates DER signaling. If Chmp1 negatively regulates the DER signal, then reduced activity of negative regulators of DER signaling should enhance the *Chmp1* knockdown phenotype. When *Chmp1* was knocked down in wings heterozygous for loss of function alleles for negative regulators of DER signaling, Kek-1 (*MS1096-Gal4/X; UAS-Chmp1RNAi-VDRC/+; kek1*^{DG23812/+}), Sty (*MS1096-Gal4/X; UAS-Chmp1RNAi-VDRC/+; sty*^{A5/+}), Aos (*MS1096-Gal4/X; UAS-Chmp1RNAi-VDRC/+; aos*^{A7/+}, *MS1096-Gal4/X; UAS-Chmp1RNAi-VDRC/+; aos*^{r/t/+}, and *MS1096-Gal4/X; UAS-Chmp1RNAi-VDRC/+; aos*^{w11/+}), wing veins were thicker than those observed with *Chmp1* knockdown alone (Figure 4.13F-J). However, wings that were heterozygous for just *kek1*^{DG23812}, *sty*^{A5}, *aos*^{r/t}, *aos*^{w11}, or *aos*^{A7} appeared wild-type, suggesting that the enhancement of the vein phenotype is not simply an additive effect. The opposite effects of the loss of positive and negative DER regulators on the *Chmp1* knockdown phenotype are consistent with a role for Chmp1 in negative regulation of the DER signaling pathway.

Argos negatively regulates DER signaling by binding to and suppressing the function of Spitz and Keren, which are DER activating ligands. Over-expression of *aos* with *MS1096-Gal4*

causes loss of portions of the dorsal wing veins. Interestingly, when *MS1096-Gal4* drove both *Chmp1* RNAi and *aos* over-expression, the portions of the wing vein normally lost with *aos* over-expression are absent, but the remaining veins are thickened (Figure 4.13L). The inability of *Chmp1* knockdown to restore wing vein differentiation suggests that loss of Chmp1 cannot restore the DER signaling lost when *aos* is over-expressed. This is consistent with a role for Chmp1 downstream of Aos.

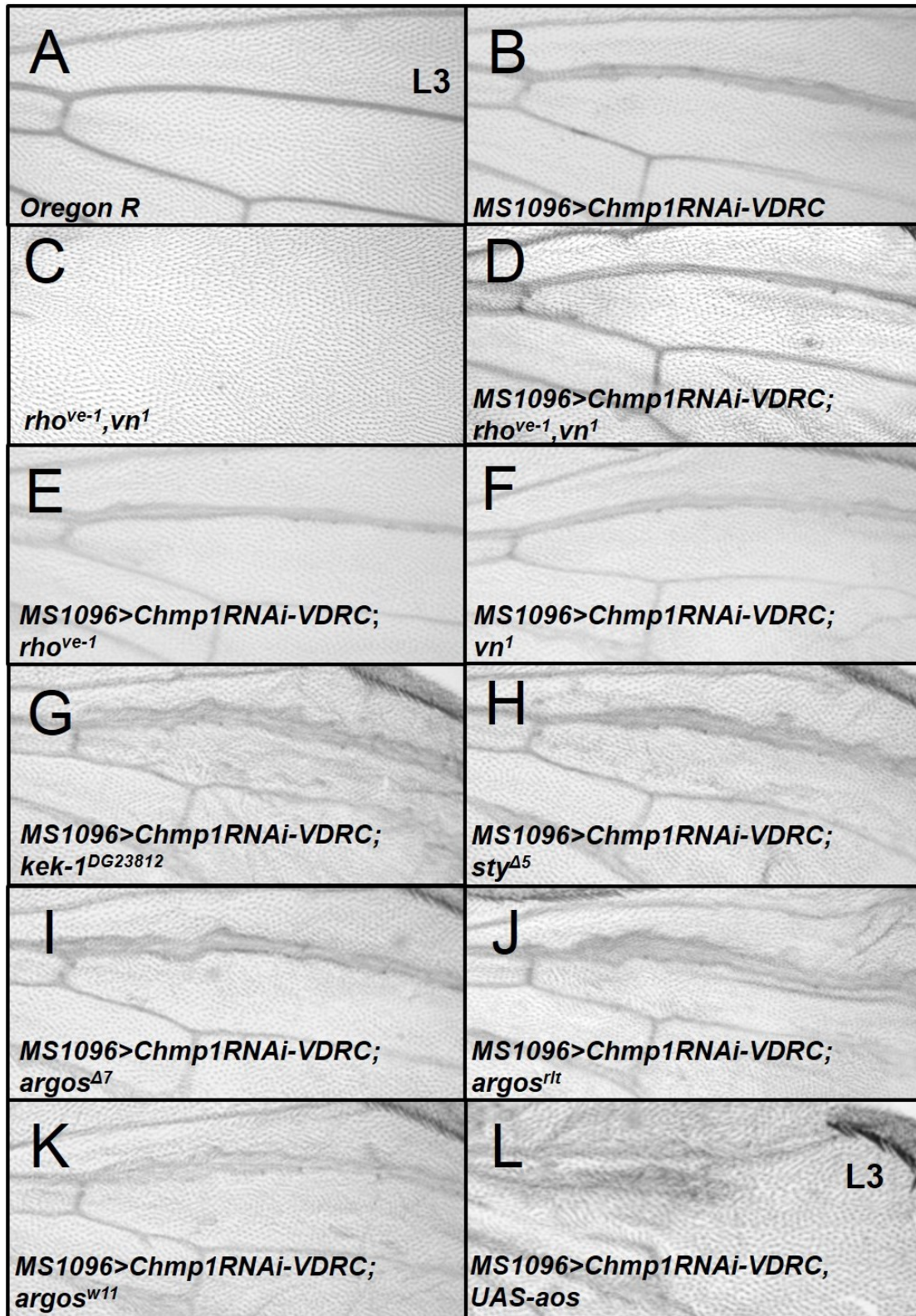


Figure 4.13 Chmp1 interacts with regulators of DER signaling in Drosophila. Light micrographs of adult female wings raised at 28°C. Distal is right, anterior is uppermost. **A.** Oregon R. **B.** *MS1096-Gal4/X; UAS-Chmp1RNAi-VDRC/+*. *Chmp1* knockdown caused thick wing veins. **C.** *rho^{ve-1}, vn¹*. Wings homozygous for loss of function alleles of positive regulators of DER signaling, *rho^{ve-1}, vn¹* have lost most wing veins. **D.** *MS1096-Gal4/X; UAS-Chmp1RNAi-VDRC/+; rho^{ve-1}, vn¹/+*. A heterozygous *rho^{ve-1}, vn¹* background partially suppressed the *Chmp1* knockdown phenotype. **E.** *MS1096-Gal4/X; UAS-Chmp1RNAi-VDRC/+; rho^{ve-1}/+*. Heterozygous *rho^{ve-1}* did not suppress the *Chmp1* knockdown. **F.** *MS1096-Gal4/X; UAS-Chmp1RNAi-VDRC/+; vn¹/+*. Heterozygous *vn¹* suppressed the *Chmp1* knockdown phenotype. **G-K.** Wings heterozygous for loss of function alleles for negative regulators of DER enhanced the *Chmp1* knockdown phenotype. **G.** *MS1096-Gal4/X; UAS-Chmp1RNAi-VDRC/+; kek1^{DG23812}/+*. **H.** *MS1096-Gal4/X; UAS-Chmp1RNAi-VDRC/+; sty⁴⁵/+*. **I.** *MS1096-Gal4/X; UAS-Chmp1RNAi-VDRC/+; aos⁴⁷/+*. **J.** *MS1096-Gal4/X; UAS-Chmp1RNAi-VDRC/+; aos^{rt}*. **K.** *MS1096-Gal4/X; UAS-Chmp1RNAi-VDRC/+; aos^{w11}*. **L.** *MS1096-Gal4/UAS-aos; UAS-Chmp1RNAi-VDRC/UAS-aos*. Wing veins that are not lost through over-expressing *aos* are thickened due to *Chmp1* knockdown. The wings shown for each genotype are representative of the means of all the wings analyzed. For quantification see Figure 4.9.

When the mean of L3 wing vein area of each genotype was plotted in a box and whisker plot, it became apparent that wild-type wings and *Chmp1* knockdown wings had a narrower range of wing vein areas than *Chmp1* knockdown wings that were heterozygous for loss of function alleles of DER signaling regulators (Figure 4.14). As *Chmp1* knockdown driven with Gal4 is sensitive to temperature, this could reflect an increased sensitivity of the *Chmp1* knockdown phenotype to changes in ambient temperature in different genetic backgrounds. However, though *Chmp1* did not genetically interact with Rho, the mean for the other *Chmp1*-DER regulator interaction genotypes was consistent with the proposal that *Chmp1* negatively regulates DER signaling. First, loss of function alleles for all the negative regulators of DER signaling tested increased the wing vein area in *Chmp1* knockdown wings. Three different negative regulators of DER signaling were investigated, each with a different mechanism of

action on DER signaling. Second, positive and negative regulators of DER had opposite effects on the thickened wing veins caused by *Chmp1* knockdown.

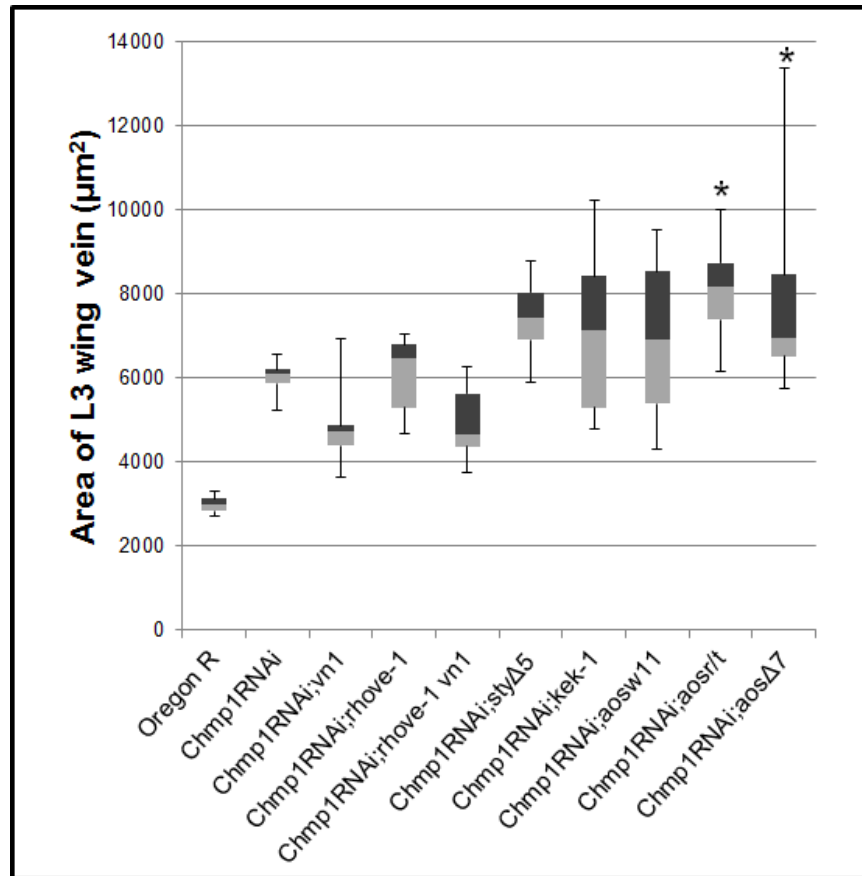


Figure 4.14 Wing vein measurements for *Chmp1* knockdown flies with altered DER signaling. A box and whisker plot depicting the area of the measured L3 wing vein in square microns. The upper and lower brackets represent the maximum and minimum measurements, respectively. Heterozygosity for loss of Vn activity, a positive regulator of DER signaling, partially suppressed the *Chmp1* knockdown phenotype. Heterozygosity for loss of activity of Sty, Kek, or Aos, negative regulators of DER signaling, show an enhanced *Chmp1* knockdown phenotype. All genotypes shown had significantly thicker wing veins than wild-type. Asterisks represent a statistically significant difference from *Chmp1* knockdown. Significant differences were determined by a one-way ANOVA with post-hoc Dunnett's, $p < 0.05$.

IV. *Chmp1* negatively regulates DER signaling

The results presented in the previous section suggest that *Chmp1* negatively regulates DER signaling, as reduced activity of positive and negative regulators of DER signaling had

opposite effects on the thick wing vein phenotype caused by *Chmp1* knockdown. If *Chmp1* regulates DER signaling, then the expression of genes regulated by the DER signaling pathway should be altered under *Chmp1* knockdown conditions. Blistered (Bs, also called Drosophila Serum Response Factor [DSRF]) is a transcription factor whose expression is negatively regulated by DER signaling. So if *Chmp1* knockdown causes an over-active DER signaling pathway, Bs expression should decrease in *Chmp1* knockdown cells. To test this, *Chmp1* was knocked down in third instar wing discs under the control of *en-Gal4* (Figure 4.15). *UAS-Chmp1RNAi-TRiP* homozygous males were crossed to *en-Gal4, UAS-GFP* homozygous virgin females and progeny were grown at 30°C. Crawling third instar larvae wing discs were dissected, immunostained for Bs, and imaged on a confocal microscope. *en-Gal4* drove *Chmp1* knockdown in the posterior of the wing disc (marked by GFP fluorescence from *UAS-GFP*), so that Bs staining intensity could be compared between the anterior and posterior of the disc. Unexpectedly, there was no striking difference in the intensity of fluorescence between the halves of the disc.

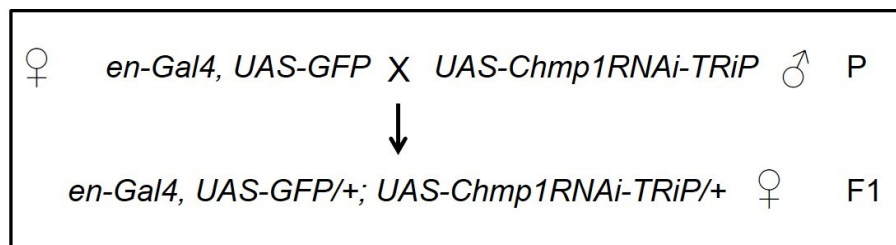


Figure 4.15 Cross design for *Chmp1* knockdown marked with GFP in the posterior wing disc. P is parental generation, F1 is first filial generation, F2 is second filial generation.

As an alternative approach, clones of *Chmp1* knockdown marked by GFP expression were generated in the wing disc. To achieve this, *hs-flp; UAS-Chmp1RNAi-TRiP* virgin females were crossed to *FRT-Gal4; UAS-GFP* males (Figure 4.16). The progeny were developed at 25°C, heat shocked at 37°C for 1 hour between 48-72 hours into development to induce *Chmp1*

knockdown clones (see Chapter 1, Section II.E.). To induce maximal *Chmp1* knockdown in clones, larvae were grown for the remaining developmental time at 30°C, as the UAS-Gal4 system is more active at higher temperatures. Female crawling third instar larvae (*hs-flp/FRT-Gal4; UAS-GFP/+; UAS-Chmp1RNAi-TRiP/+*) were of the correct genotype and so were selected, and wing discs were dissected and immunostained for Bs.

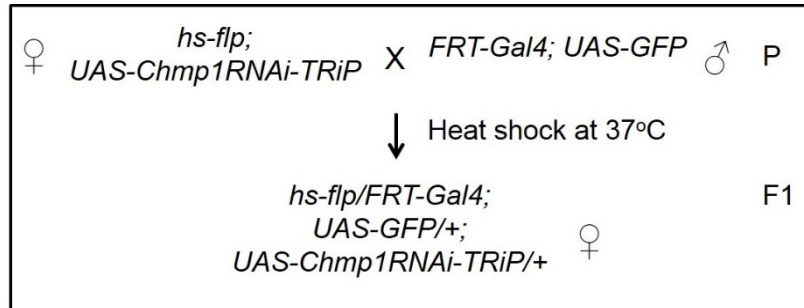


Figure 4.16 Cross design for generating *Chmp1* knockdown clones marked with GFP in wing discs. Developing flies of the F1 generation were heat shocked for 1 hour between 48-72 hours of development. All F1 females were of the correct genotype. P is parental generation, F1 is first filial generation. Only the desired F1 progeny is shown.

Some flies from this cross were allowed to develop to the adult stage to ensure that clones were being generated. The GFP marker was not visible in adult wings, but areas of thickened wing veins were present, suggesting that clones of *Chmp1* knockdown were being generated (Figure 4.17D and E). Bs is normally expressed in the intervein regions of the wing disc and repressed in provein regions (Figure 4.17A and A'). Large clones (>120 cells) of *Chmp1* knockdown that spanned vein and intervein regions reduced Bs expression within the clone (Figures 4.17B, B' and C, C'). However, smaller clones of *Chmp1* knockdown did not have an observable effect on Bs expression even though similar sized clones could induce vein formation (shown below, Figure 4.19C). This was possibly because Bs levels were observed in imaginal disc clones, but the final fate decision between vein and intervein cell does not occur until well into the pupal stage, by which time Bs levels may be altered [15, 21]. Therefore, it is possible

that it takes more time to see an effect of *Chmp1* knockdown on Bs expression than had elapsed since the induction of these small imaginal disc clones. Alternatively, Chmp1 protein may perdure through clone formation, so it may still be present in small clones even though the *Chmp1* mRNA levels are reduced.

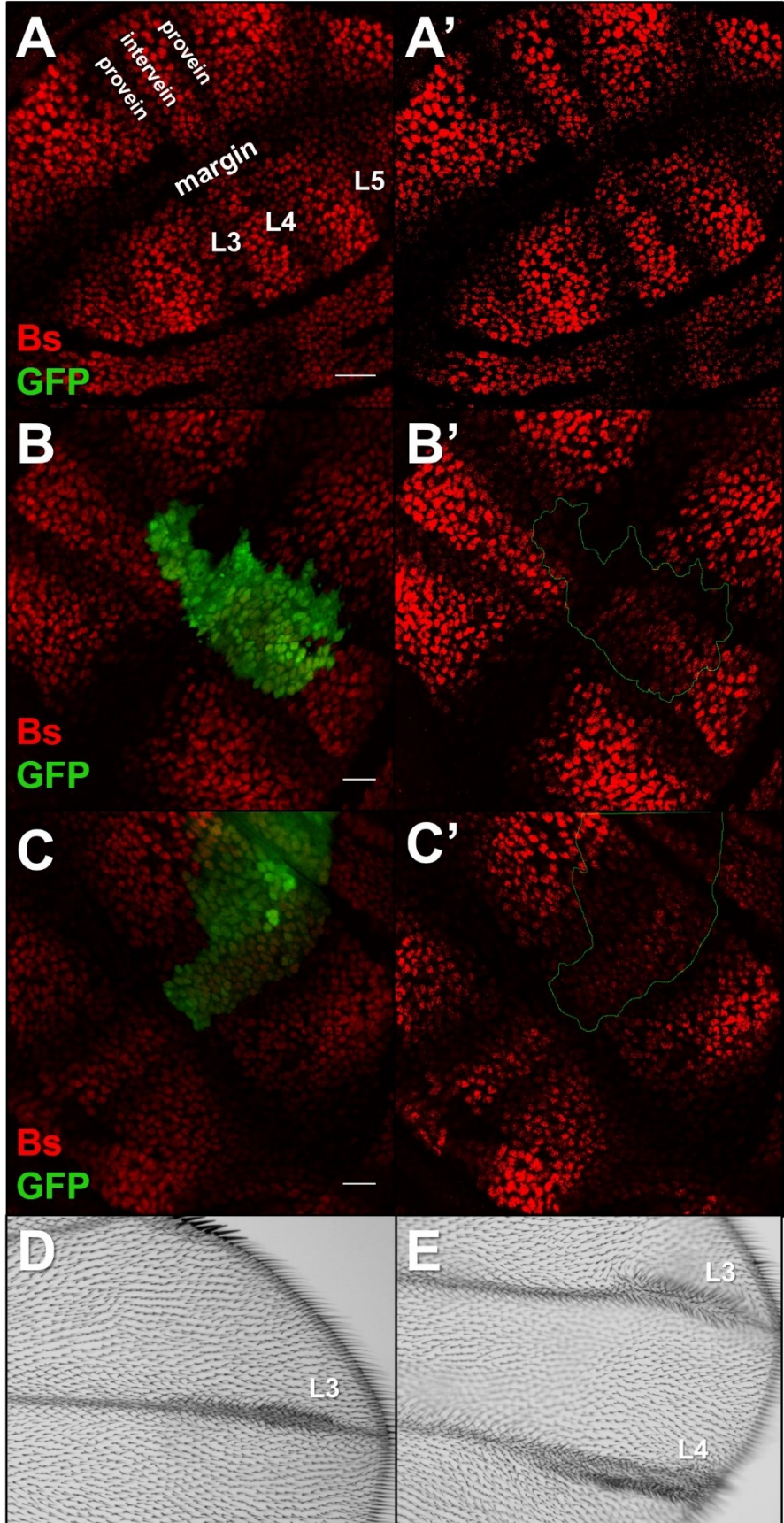


Figure 4.17 *Chmp1* knockdown reduced Bs staining in imaginal discs. A-C’. Confocal images showing clones of *Chmp1* knockdown marked with GFP (green) in the third instar wing disc from larvae raised at 30°C. All wings shown were of the genotype *hs-flp/FRT-Gal4; UAS-Chmp1RNAi-TRiP/+; UAS-GFP/+*. Discs were immunostained for Blistered (Bs). Scale bar is 20µm. **A.** Bs (red) is expressed in the intervein regions of the wing disc and is repressed in the provein territories. Longitudinal proveins, L3, L4, and L5, and wing margin are labeled. **A’.** The same disc as A, but thresholded. **B and C.** Large clones (>120 cells) of *Chmp1* knockdown marked by GFP expression (green). **B’ and C’.** Same clones as B and C respectively, but thresholded with the GFP fluorescence removed and clones outlined in green. **D and E.** Light micrographs of adult female wings showing clones of *Chmp1* knockdown indicated by regions of wing vein thickening. Distal is right, anterior is uppermost.

To investigate the effect of *Chmp1* knockdown in the wing further, clones of both *Chmp1* and *forked* knockdown were generated in the adult wing. *forked* knockdown caused a wing hair phenotype in the clones, giving a way to distinguish the clone cells from the rest of the wing cells. To achieve this, *FRT-Gal4/FM6B¹; Cy/UAS-forkedRNAi* virgin females were crossed to *hs-flp/Y; UAS-Chmp1RNAi-VDRC/Cy* males (Figure 4.18). The progeny were allowed to grow for 120-144 hours at 25°C, and then heat shocked for 1 hour at 37°C, and grown at 28°C for the remaining development. Adult females that were not *Cy* and not *B¹* were of the correct genotype (*FRT-Gal4/hs-flp; UAS-forkedRNAi/UAS-Chmp1RNAi-VDRC*).

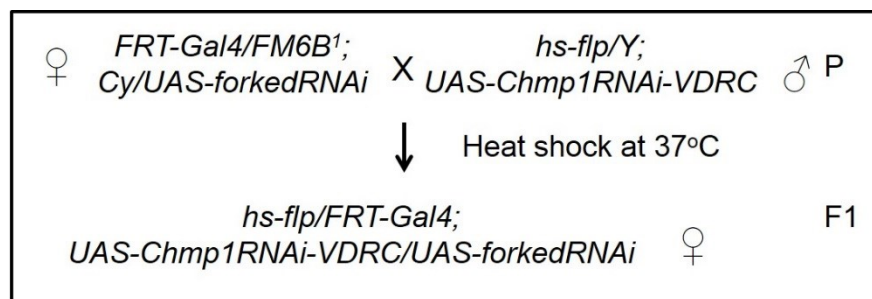


Figure 4.18 Cross design for *Chmp1* and *forked* knockdown clones in the adult wing. The developing F1 generation was heat shocked for 1 hour at 37°C 120-144 hours into development. Adult F1 females that were not *Cy* and not *B¹* were of the correct genotype and are the only F1 progeny shown. P is parental generation, F1 is first filial generation.

Clones of *Chmp1* knockdown in adult wings that overlapped veins caused a cell fate change from intervein to vein, resulting in widening of the wing vein (Figure 4.19B). In these clones, only cells adjacent to the wing vein were converted to vein cells (i.e., the number of cells making up the thickness of the wing vein increased), even when the clone extended well into intervein tissue. The cell fate change was also restricted to clone cells, implying that the effect of *Chmp1* knockdown is cell autonomous. Most of the *Chmp1* knockdown clones had smooth edges, in contrast to the usual irregular edges observed in clonal analyses. Smooth edges were also characteristic of *bs⁻* clones, which is compatible with the finding that *Bs* expression was reduced in *Chmp1* knockdown clones [123]. Interestingly, some of the *Chmp1* knockdown clones that were located entirely within intervein tissue did not induce vein cell differentiation (Figure 4.19A), while other intervein clones did (Figure 4.19C). Therefore, it seems that the effect of *Chmp1* on wing vein differentiation is spatially dependent, suggesting that *Chmp1* does not directly determine whether a cell differentiates into a vein or intervein cell. Rather, *Chmp1* knockdown altered the balance of signaling within these cells and pushed towards adopting a vein fate, rather than an intervein fate. In fact, clones of *Chmp1* knockdown typically caused intervein to vein cell fate changes in regions adjacent to normal veins, where the DER pathway should be most active. These results are consistent with a role for *Chmp1* in negatively regulating the DER signaling pathway.

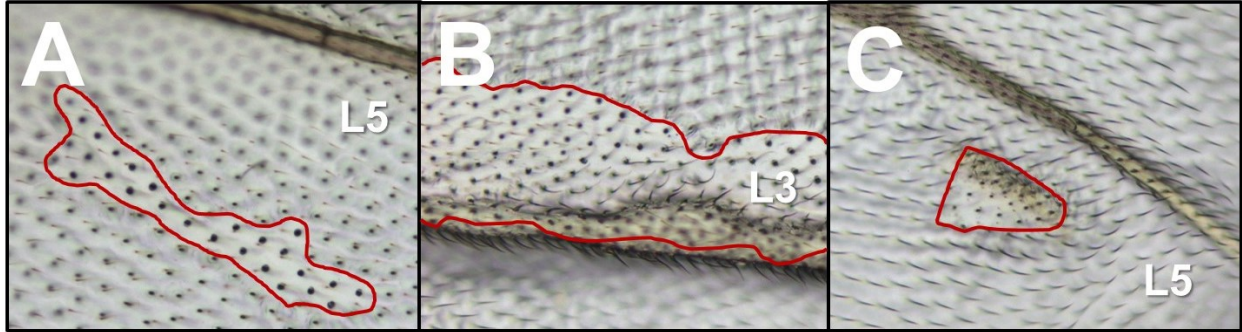


Figure 4.19 Clones of *Chmp1* and *forked* knockdown in the adult wing. Light microscope images of adult female wings. Distal is right, anterior is uppermost **A.** *Chmp1* knockdown clone located entirely within intervein tissue, posterior to the L5 wing vein showing no vein differentiation. **B.** *Chmp1* knockdown clone that overlapped the L3 wing vein caused wing vein thickening. **C.** *Chmp1* knockdown clone located within intervein tissue induced wing vein formation.

V. Over-expression of *Chmp1*

Transgenic lines were created to investigate the effects of *Chmp1* over-expression in the fly. If *Chmp1* knockdown caused thick wing veins due to over-active DER signaling, then over-expression may cause narrowing or loss of wing veins due to inhibited DER signaling. *Chmp1* knockdown and over-expression had opposite effects on growth in the mammalian cell culture studies, so the same antagonistic effects might be expected in *Drosophila*.

To investigate the effect of *Chmp1* over-expression, *Chmp1* was over-expressed in the dorsal wing using *MS1096-Gal4*. Males carrying *UAS-Chmp1* and *UAS-HM-Chmp1* balanced with *Cy*, *TM3Ser*, or *TM6SbTb* were crossed to *MS1096-Gal4* virgin females and progeny were grown at 25°C, 28°C, or 30°C (Figure 4.20A and B). Adult female and male flies that were not *Cy*, *Ser*, or *Sb* were of the correct genotype (*MS1096-Gal4/+; UAS-Chmp1* or *UAS-HM-Chmp1/+*), and their wings were mounted on a microscope slide in GMM.

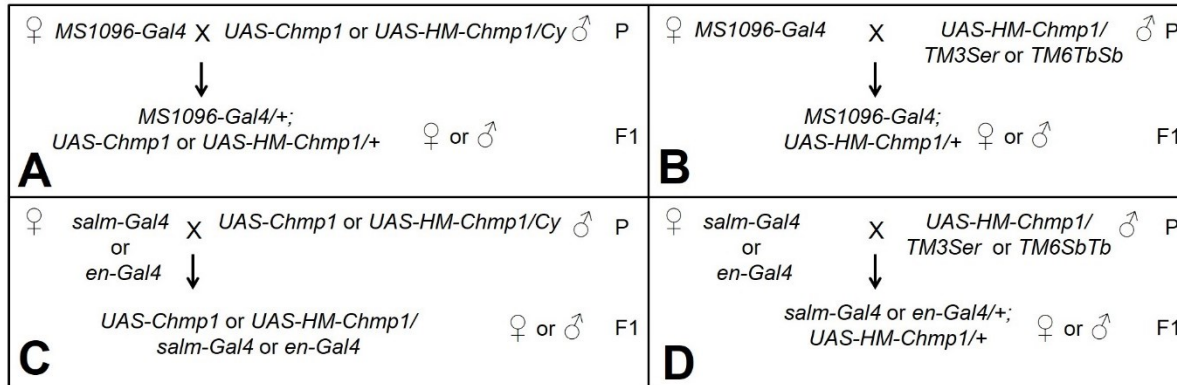


Figure 4.20 Cross design for achieving *Chmp1* over-expression in the *Drosophila* wing. A. Cross for over-expressing wild-type or HM-tagged *Chmp1* protein from a second chromosome insertion with *MS1096-Gal4*. **B.** Cross for over-expressing HM-tagged *Chmp1* protein from a third chromosome insertion with *MS1096-Gal4*. **C.** Cross for over-expressing wild-type or HM-tagged *Chmp1* protein from a second chromosome insertion with *salM-Gal4* or *en-Gal4*. **D.** Cross for over-expressing wild-type or HM-tagged *Chmp1* protein from a third chromosome insertion with *salM-Gal4* or *en-Gal4*. *UAS-Chmp1-1* and *-2*, and *UAS-HM-Chmp1-3* insertions are on the second chromosome and balanced with *Cy*. *UAS-HM-Chmp1-2* and *-4* insertions are on the third chromosome balanced with *TM3Ser*. The *UAS-HM-Chmp1-1* insertion is on the third chromosome and balanced with *TM6SbTb*. P is parental generation, F1 is first filial generation. Only F1 progeny of the desired genotype are shown.

Chmp1 over-expression in the dorsal wing most commonly resulted in deltas, or widening of the distal tips of the dorsal wing veins (Figure 4.21A-F). Additionally, some wings showed ectopic wing vein formation (Figure 4.21A, C and D, white arrows). The over-expression phenotype only increased slightly in penetrance and severity with the increasing culture temperature, which is expected to increase the activity of the UAS-Gal4 system. These over-expression phenotypes were mainly observed in male wings, while most female wings appeared wild-type. The *MS1096-Gal4* transgene is located on the X chromosome and normally shows higher activity in males than females. Additionally, the *MS1096-Gal4* transgene is inserted near the *beadex* gene and can increase *beadex* expression [2]. *Beadex* negatively regulates expression of *Apterous*, which in turn negatively regulates *Serrate* and *Fringe*, both of which are activating ligands of the Notch receptor [124-126]. Therefore, *MS1096-Gal4*

occasionally interacts with certain genetic backgrounds to cause a phenotype in the wing, including the formation of deltas. So, it was possible the delta formation observed was an artifact. In fact, this idea is supported by the observation that there is little increase in phenotype with temperature.

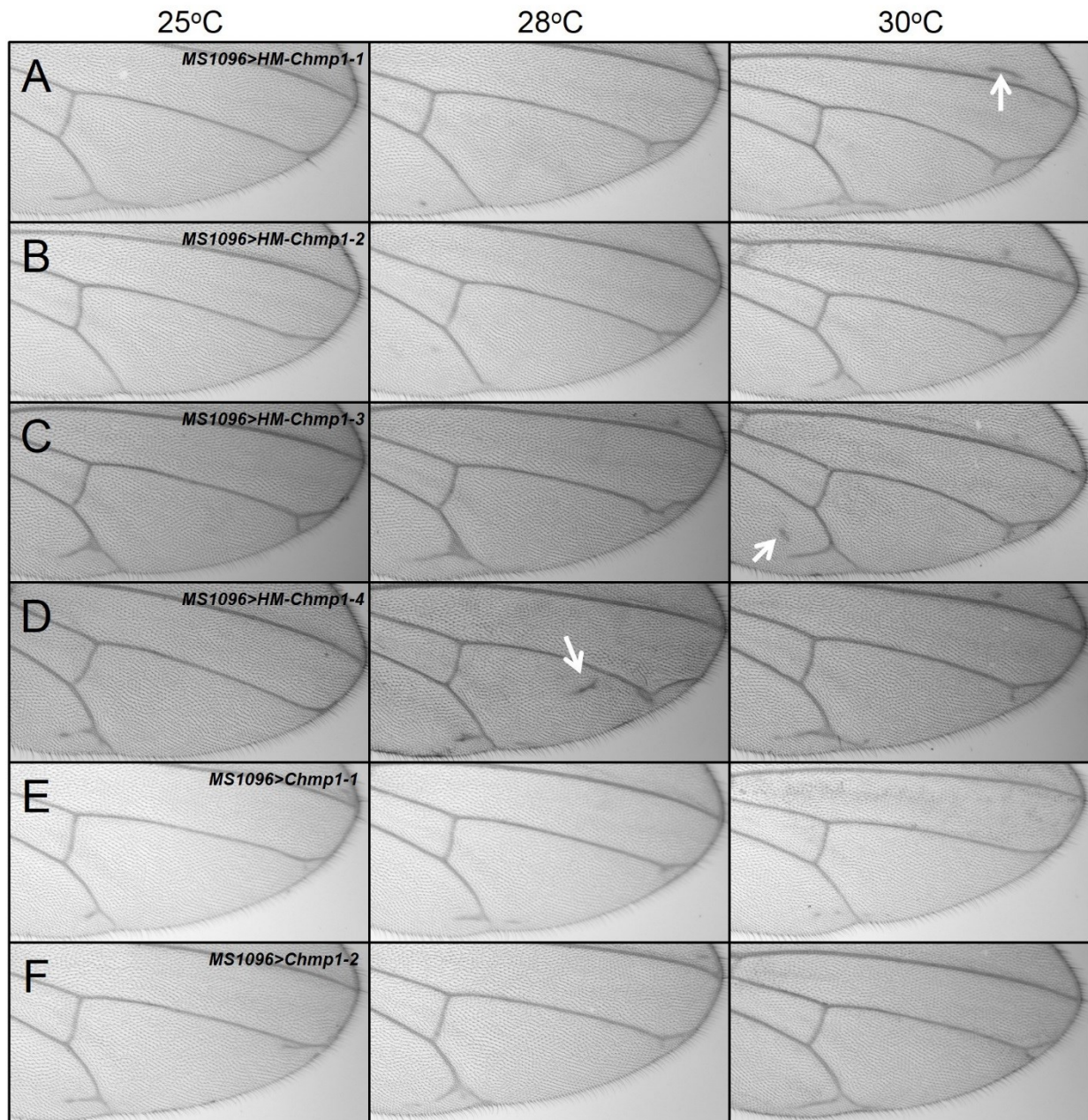


Figure 4.21 *Chmp1* over-expression with *MS1096-Gal4* in the *Drosophila* wing causes vein deltas. Light micrographs of wings from adult males at 25, 28, and 30°C. Distal is right, anterior is uppermost. **A-D**. Over-expression of *HM-Chmp1* under the control of *MS1096-Gal4* causes wing vein deltas that do not become more prominent with increasing cultivation temperature (i.e., increasing levels of *Chmp1* expression). Ectopic vein formation indicated by white arrows. **E and F**. Over-expression of wild-type *Chmp1* under the control of *MS1096-Gal4* also causes wing vein deltas that do not become more prominent with increasing temperature.

To test whether the deltas observed were a genuine result of *Chmp1* over-expression rather than an artifact of an interaction with *MS1096-Gal4*, *Chmp1* was over-expressed in the wing with two other drivers, *salm-Gal4* and *en-Gal4* (see Figure 4.4 for expression pattern). *UAS-Chmp1* or *UAS-HM-Chmp1* males were crossed to *salm-Gal4* and *en-Gal4* females and the progeny were grown at 25°C, 28°C, and 30°C (Figure 4.20). Male and female flies that were not *Cy*, *Ser*, or *Sb* were of the correct genotype.

When *Chmp1* was over-expressed with these different drivers, there were no deltas formed at 25°C or 28°C. However, at 30°C occasional deltas were observed, though the effect was much weaker than with *MS1096-Gal4*, and they were only present in a small number of wings (Figure 4.22). This may suggest that the delta phenotype observed was caused by *Chmp1* over-expression and was not due to a genetic interaction with the *MS1096-Gal4* driver, though it was enhanced by the presence of the *MS1096-Gal4* insert. The levels of over-expression of *Chmp1* were not tested as there is no antibody against *Drosophila* Chmp1. However, the detection of HM-Chmp1 in *Drosophila* tissues (shown in Chapter 4, Section IX) and the ability of *Chmp1* over-expression to rescue the *Chmp1* knockdown wing vein phenotype suggest that functional Chmp1 protein is expressed from these transgenes. So the minor wing defects observed under presumably strong *Chmp1* over-expression suggest that the development of this tissue is not especially sensitive to increased levels of Chmp1 protein.

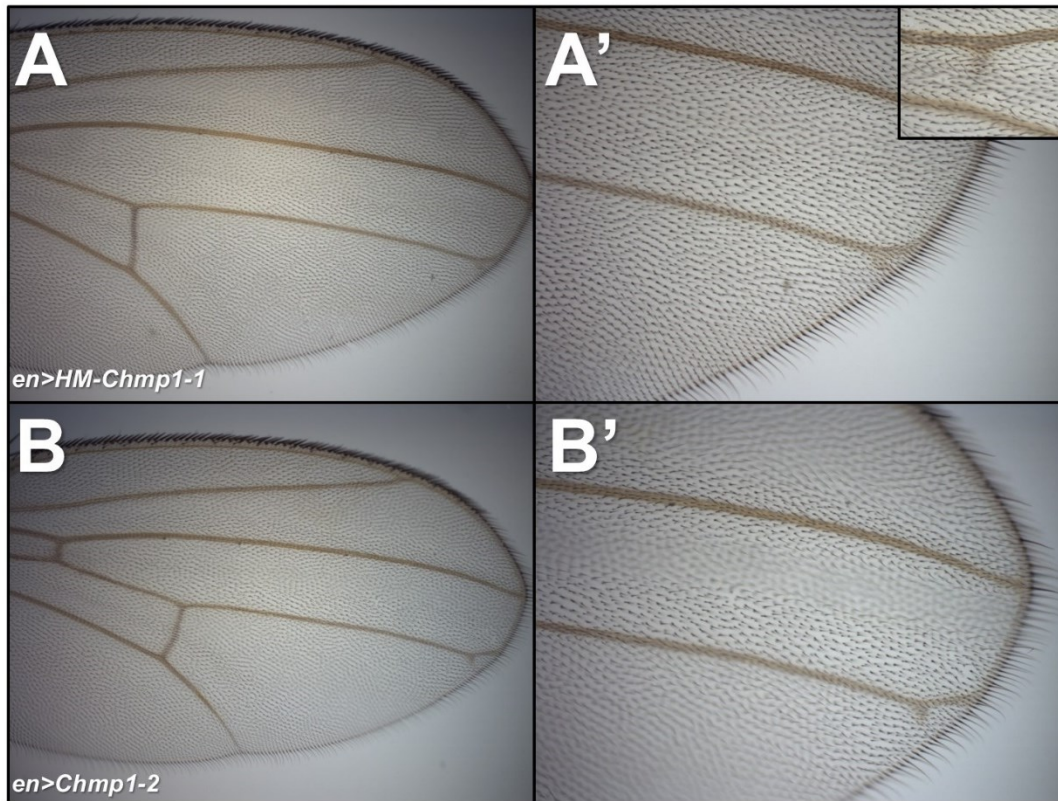


Figure 4.22 *Chmp1* over-expression in the *Drosophila* wing causes deltas. Light micrographs of wings from adult females at 30°C. Distal is right, anterior is uppermost. **A and A'**. *en-Gal4/+; UAS-HM-Chmp1-1/+*. A' is an enlarged from A. Over-expression of *HM-Chmp1* caused loss of anterior cross vein (indicated in upper right box) and wing vein deltas. **B and B'**. *en-Gal4/UAS-Chmp1-2*. B' is enlarged from B. *Chmp1* over-expression caused occasional wing vein deltas.

In addition to the phenotypes discussed above, a second phenotype was observed occasionally in *Chmp1* over-expression wings. Although it was only present in flies over-expressing wild-type *Chmp1* protein, this phenotype was observed with both the *MS1096-Gal4* and *en-Gal4* drivers. In addition to vein defects (Figure 4.23B), wings from these flies also had disorganized hairs (discussed in Chapter 6). Often, the veins on these wings had ill-defined borders compared to wild-type (Figure 4.23). In some cases the wing vein appeared thickened (compare the L3 veins in Figure 4.23B and A), and in other cases small portions of wing veins were missing (Figure 4.23A). Some wings also had opaque regions, indicating a failure of

imaginal disc cells to clear out of the wing at maturation, as well as wing vein deltas (Figure 4.23B). The same phenotype appeared in both male and female flies and at all temperatures, though it was strongest at 30°C.

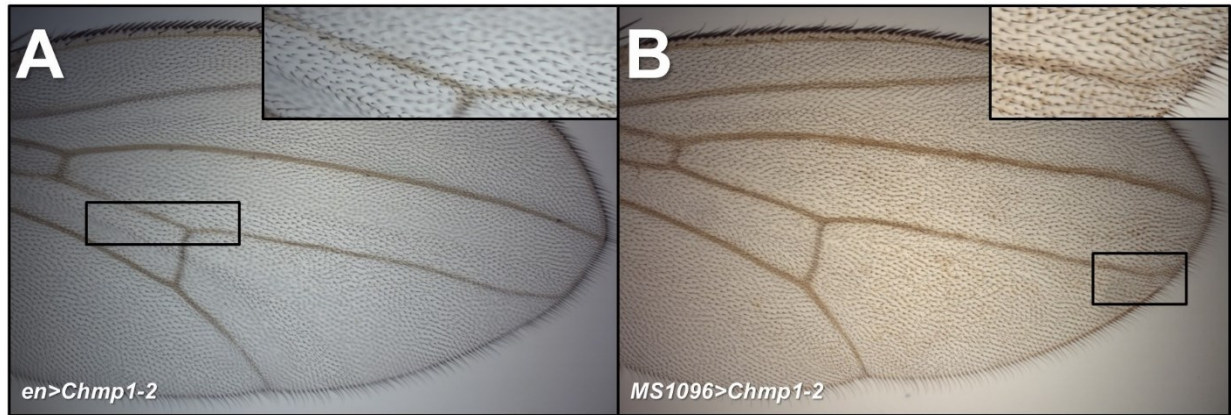


Figure 4.23 Rare phenotypes caused by *Chmp1* over-expression in the *Drosophila* wing. Light micrographs of wings from adult male cultivated at 30°C. Distal is right, anterior is uppermost. **A and B.** Over-expression of wild-type *Chmp1* causes slightly thicker wing veins, deltas, disorganized hairs, and failure of clearing of imaginal cells out of the wing. **A.** *en-Gal4/UAS-Chmp1-2*. **B.** *MS1096-Gal4/Y; UAS-Chmp1-2/+*.

VI. Investigation into *Chmp1* regulation of Notch-Delta signaling

Reduced activity of Delta, a Notch receptor ligand, causes the formation of ‘deltas,’ or distal widening of wing veins, in the *Drosophila* wing. Like the DER signaling pathway, Notch-Delta signaling is involved in wing vein development. In fact, the DER and Notch signaling pathways interact antagonistically during wing vein specification. While the DER pathway promotes wing vein formation/fate, Notch signaling restricts wing vein formation/fate. So a gain of DER signaling can cause thickened wing veins, and a loss of Notch signaling can produce the same phenotype. Signaling through Notch is also important for formation of the wing margin and bristles; loss of Notch signaling can cause notching, or loss of the wing margin and loss of bristles (e.g. Figure 4.26A).

In *Drosophila*, loss of the ESCRT-II component Vps25 caused an increase in Notch signaling, suggesting a requirement for ESCRT machinery for negative regulation of Notch-Delta signaling [61]. Loss of other *Drosophila* ESCRT components, including Hrs, Tsg101, and Vps20, have been shown to cause mis-regulation of Notch signaling in *Drosophila* as well [59, 61]. Thus, it is possible Chmp1 regulates Notch signaling. Although no classic Notch phenotypes, such as ectopic wing margin or notching of the wing margin, were observed under *Chmp1* knockdown or over-expression conditions, the widened wing veins and deltas observed through *Chmp1* over-expression may indicate that Chmp1 regulates Notch signaling. A hypomorphic Notch allele, N^{55el} , was used to investigate the possibility of Chmp1 regulating Notch signaling in the wing. Heterozygous $N^{55el}/+$ flies lose some Notch receptor function. Wings from these flies have slightly thicker wing veins, deltas, and show mild notching of the wing margin in approximately 20% of wings (Figure 4.26A). To test whether Chmp1 regulates Notch signaling, *Chmp1* was knocked down under the control of the *MS1096-Gal4* driver in a heterozygous N^{55el} background (Figure 4.24). If Chmp1 negatively regulated Notch signaling, the concomitant loss of Notch and Chmp1 activity should cause the frequency and/or size of notches to decrease. On the other hand, if Chmp1 positively regulated Notch signaling, loss of both Notch and Chmp1 activity should cause the frequency and/or size of notches to increase.

In order to test whether Chmp1 regulates Notch signaling, the *Chmp1RNAi* transgene, a driver, and the N^{55el} allele had to be combined into the same fly. *w; GlaBc/Cy* virgin females were crossed to *MS1096-Gal4* males (Figure 4.24A). From the progeny of that cross, *Gla* straight winged virgin females were collected (*MS1096-Gal4/X; GlaBc/+*) and crossed to *UAS-Chmp1RNAi-VDRC/Cy* males. From the progeny of this cross, *Gla* (not *Cy*) males with the *Chmp1* knockdown phenotype (*MS1096-Gal4/Y; UAS-Chmp1RNAi-VDRC/GlaBc*) were

collected. These males were crossed to $N^{55e11}/FM7Bar$ virgin females. Progeny from this cross were grown at 28°C to maintain consistency with previous *Chmp1* knockdown crosses. Females among these progeny that were not *Bar* and not *Gla* were of the correct genotype ($MS1096-Gal4/N^{55e11}; UAS-Chmp1RNAi-VDRC/+$). Wings were dissected and mounted onto a glass slide in GMM. For a negative control cross, $N^{55e11}/FM7Bar$ virgin females were crossed to $MS1096-Gal4/Y$ males (Figure 4.24B). These flies carry the same *Notch* mutation and *Gal4* transgene as the experimental flies, but do not carry the *Chmp1-RNAi* transgene, and so do not experience *Chmp1* knockdown. The progeny were grown at 28°C to maintain consistency with the experimental cross. Females from the progeny of this cross that were not *Bar* were of the correct genotype ($MS1096-Gal4/N^{55e11}$) and wings were mounted on a glass slide in GMM.

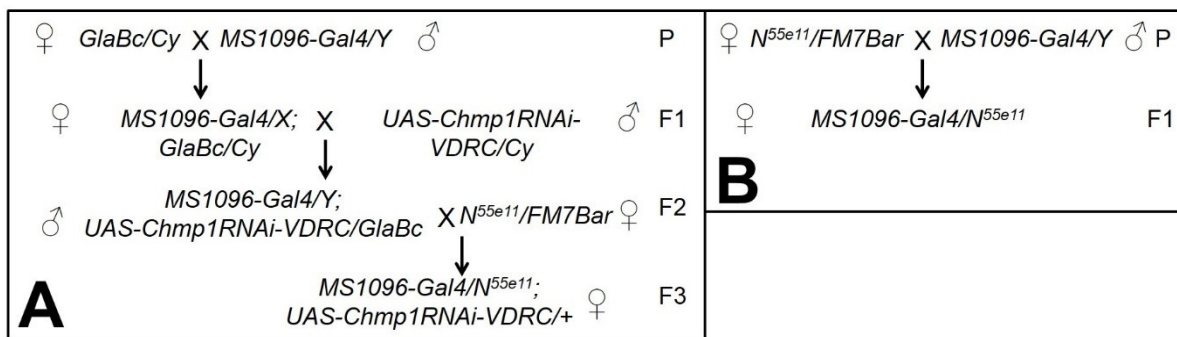


Figure 4.24 Cross design to test for an interaction between *Chmp1* and *Notch* using the *MS1096-Gal4* driver. **A. Achieving *Chmp1* knockdown under *MS1096-Gal4* control in a heterozygous N^{55e11} background. The F3 generation was grown at 28°C. **B.** Control cross. F1 generation was grown at 28°C. P is parental generation, F1 is first filial generation, F2 is second filial generation, F3 is third filial generation. Only progeny of interest are shown in each generation.**

When *Chmp1* knockdown was driven with *MS1096-Gal4* in the N^{55e11} heterozygous wing, the notches associated with N^{55e11} were completely suppressed (Figure 4.26D). Out of 31 wings, none experienced notching. This result suggested that *Chmp1* negatively regulated *Notch* signaling, and was consistent with expectations based on the established role of the ESCRT

complexes in negatively regulating signaling pathways. However, notching was completely suppressed in the control wings (*MS1096-Gal4/N^{55el1}*) as well, with zero out of 48 wings showing notching (Figure 4.26B). This suggested that the presence of the *MS1096-Gal4* transgene, rather than *Chmp1* knockdown, suppressed the wing notches associated with the *N^{55el1}* allele. To test whether the *MS1096-Gal4* insertion suppressed wing notching in general, the ability of *MS1096-Gal4* to suppress the wing notching associated with the dominant *Serrate* (*Ser*) mutation was tested. *MS1096-Gal4* virgin females were crossed to *If/Cy; D¹/TM3Ser* males and progeny were grown at 28°C to maintain consistency with previous crosses. Flies from the offspring that were not *D¹* and therefore should carry the *Ser* mutation were analyzed (*MS1096-Gal4/X or Y; TM3Ser/+*). These flies showed a complete suppression of notching, suggesting that the *MS1096-Gal4* insertion indeed suppressed wing notching. Because *Serrate* is a Notch ligand, this result suggests that the *MS1096-Gal4* insertion increases Notch signaling. This could occur through increased expression of *Beadex*, since the *MS1096-Gal4* transgene is inserted near the *beadex* gene. As *Beadex* negatively regulates Notch ligands, increased *Beadex* activity might cause a decrease in Notch signaling.

Because *MS1096-Gal4* was unsuitable for driving *Chmp1* knockdown in the *N^{55el1}/X* background, the experiment was repeated with a different driver, *dpp-Gal4*, which is located on the third chromosome (Figure 4.25A). *UAS-Chmp1RNAi-VDRC/Cy; D¹/TM3Ser* virgin females were crossed to *wg^{Sp1}/Cy; dpp-Gal4/TM6Tb* males. Larvae that were not *Tb* were collected, and *Cy* and *D¹* males that emerged from these larvae were of the genotype needed (*UAS-Chmp1RNAi-VDRC/Cy; dpp-Gal4/D¹*). These males were crossed to *N^{55el1}/FM7Bar* virgin females and progeny were grown at 28°C to maintain consistency with previous *Chmp1* knockdown crosses. From these progeny, wings from females that were not *Cy*, not *D¹*, and not

Bar (N^{55e11}/X ; *UAS-Chmp1RNAi-VDRC/+*; *dpp-Gal4/+*) were dissected and mounted in GMM on a microscope slide. Several control crosses were completed to verify that any changes in notching frequency observed were in fact due to *Chmp1* knockdown (Figure 4.25B-D). The first control cross generated flies that were N^{55e11}/X to ensure that the *FM7Bar* balancer did not affect notching frequency. *Oregon R* males were crossed to $N^{55e11}/FM7Bar$ virgin females. From the progeny, wings from females that were not *Bar* were of the correct genotype (N^{55e11}/X) and were mounted. In previous experiments, the presence of the *MS1096-Gal4* transgene altered the notching frequency typically observed in N^{55e11} flies. To ensure this was not the case for the *dpp-Gal4* driver, a second control cross was performed that generated flies carrying the N^{55e11} allele and the *dpp-Gal4*. *wg^{Sp1}/Cy*; *dpp-Gal4/TM6Tb* males were crossed to $N^{55e11}/FM7Bar$ virgin females. From the progeny, wings from females that were not *Tb* and not *Bar* were of the correct genotype (N^{55e11}/X ; *dpp-Gal4/+*) and were mounted. To test the sensitivity of the N^{55e11} allele to genetic background, flies were generated that carried the N^{55e11} allele, as well as the *Chmp1RNAi* transgene. For the third control cross, *UAS-Chmp1RNAi-VDRC/Cy* males were crossed to $N^{55e11}/FM7Bar$ virgin females. From the progeny, wings from females that were not *Cy* and not *Bar* were of the correct genotype (N^{55e11}/X ; *UAS-Chmp1RNAi-VDRC/+*) and were mounted.

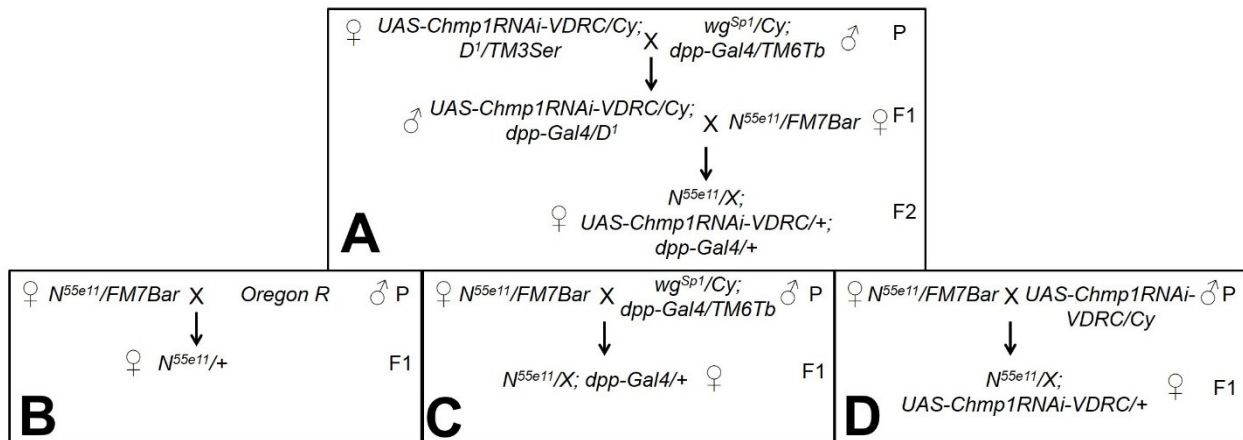


Figure 4.25 Cross design to test for an interaction between Chmp1 and Notch using the *dpp-Gal4* driver. **A.** Experimental cross to achieve *Chmp1* knockdown with *dpp-Gal4* in a heterozygous *N^{55e11}* background. The F2 generation was raised at 28°C. **B-D.** Control crosses. F1 generations were raised at 28°C. P is parental generation, F1 is first filial generation, F2 is second filial generation. Only genotypes of interest are shown.

When *Chmp1* was knocked down under the control of the *dpp-Gal4* driver in a *N^{55e11}* heterozygous background, both the thickened vein phenotype and the frequency of notches associated with *N^{55e11}* were slightly increased, which would seem to suggest that Chmp1 positively regulates Notch signaling (Table 4.2). Although this was unexpected because other studies show that ESCRTs negatively regulate Notch signaling [61], it was a possible interaction and it would fit with the *Chmp1* knockdown wing phenotype. It is known that Notch negatively regulates wing vein thickness. Thus, if Chmp1 positively regulated Notch signaling, then loss of Chmp1 activity would reduce Notch signaling and cause the thick wing veins associated with *Chmp1* knockdown. However, notching frequency was highly variable depending upon the genetic background (Table 4.2). For example, in flies that carried the *N^{55e11}* allele alone, notching occurred in about 20% of wings. Flies carrying the *N^{55e11}* allele and just the *dpp-Gal4* or the *UAS-Chmp1RNAi-VDRC* transgene had an increased notching frequency to about 40%. When the *N^{55e11}* allele was balanced with the *FM7Bar* balancer, the notching frequency increased to

over 60%. Notching was more frequent at higher temperatures, consistent with the temperature sensitivity of the N^{55el1} allele. The variability of the notching phenotype in different genetic backgrounds makes the data gained from these crosses difficult to interpret.

Knockdown of *Chmp1* caused a thickened wing vein when driven with either *MS1096-Gal4* or *dpp-Gal4* (Figure 4.26C and F). A weaker but consistent wing vein phenotype, a slight thickening in the distal L3 wing vein, was observed when *dpp-Gal4* was used to drive *Chmp1* knockdown as it drives Gal4 expression relatively weaker than *MS1096-Gal4*. Similarly, wings heterozygous for the N^{55el1} allele had a thicker wing vein (Figure 4.26A and A'). When *Chmp1* knockdown was driven with either *MS1096-Gal4* or *dpp-Gal4* in an N^{55el1} heterozygous wing, the wing vein was thicker than observed with *Chmp1* knockdown or in an N^{55el1} heterozygote (Figure 4.26D and G). This is probably an additive effect, presumably due to a combination of over-active DER signaling caused by loss of Chmp1 activity and the partial loss of Notch activity associated with the N^{55el1} allele.

The results showing the sensitivity of the N^{55el1} associated wing phenotype to genetic background are concerning, especially because testing suppression/enhancement of this phenotype is an established method used for analyzing interactions with the Notch signaling pathway. For example, the N^{55el1} allele was used in a similar experiment to provide evidence that the *Drosophila* phosphocholine cytidyltransferase (CCT, the rate-limiting enzyme in phosphatidylcholine synthesis) positively regulates Notch signaling [127]. This single test was not the only evidence provided to support the finding. However, the validity of results obtained with this specific approach is questionable in light of the data presented here.

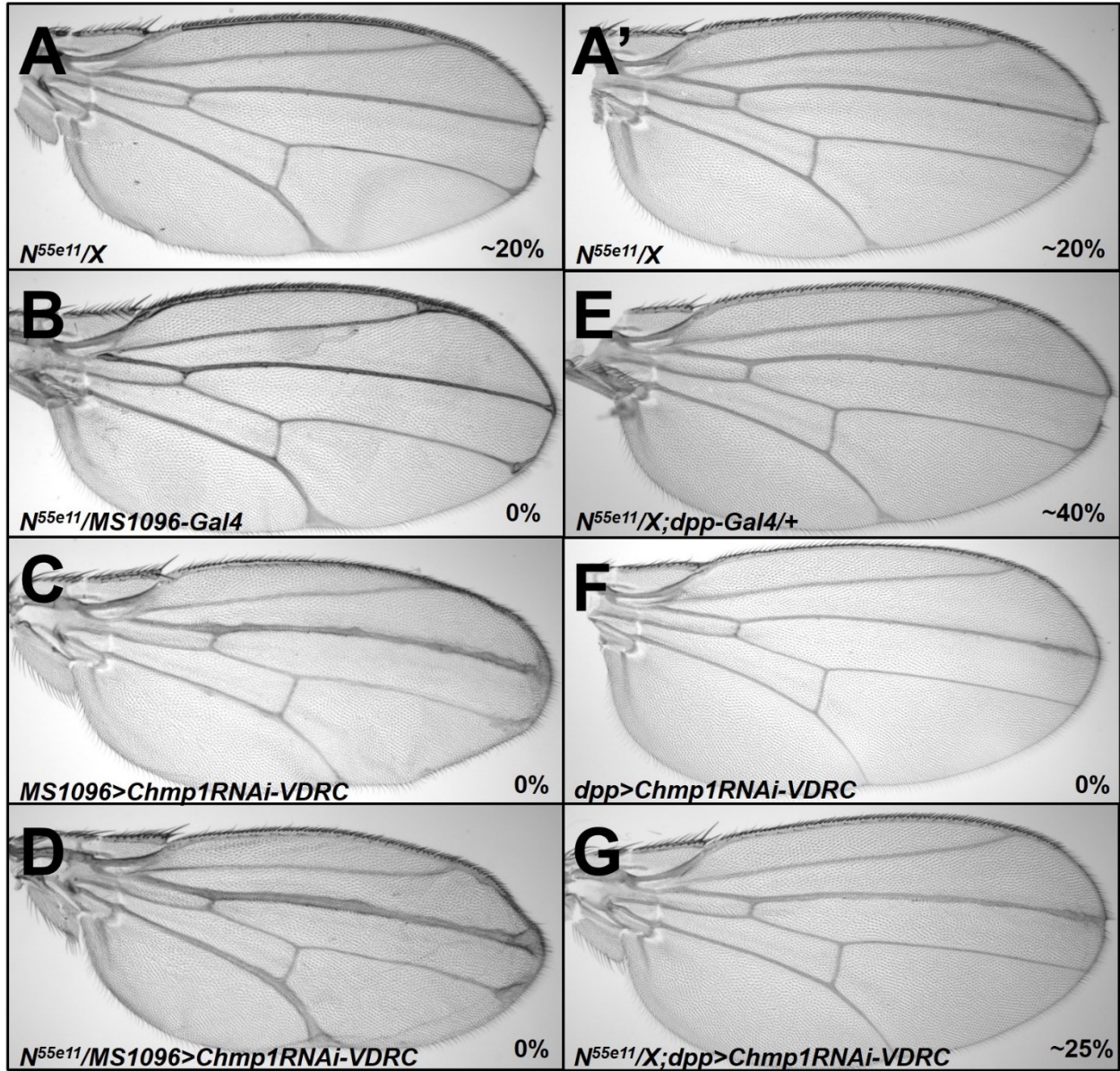


Figure 4.26 Variable notching phenotypes associated with various genotypes. Light micrographs of adult wings raised at 28°C. Distal is right, anterior is uppermost **A.** *N^{55ell}* heterozygous wing with a moderate wing phenotype (notching, deltas, and thick veins). **A'.** *N^{55ell}* heterozygous wing with a milder wing phenotype (notching, delta, and thick veins). **B.** Presence of *MS1096-Gal4* in a *N^{55ell}* heterozygous wing completely suppressed notching. **C and F.** Driving *Chmp1* knockdown under the control of *MS1096-Gal4* or *dpp-Gal4* caused thick wing veins. **D.** Driving *Chmp1* knockdown under the control of *MS1096-Gal4* in a heterozygous *N^{55ell}* background suppressed notching and enhanced the wide veins and delta phenotypes. **E.** The presence of *dpp-Gal4* in a *N^{55ell}* heterozygous wing enhanced notching frequency. **G.** Driving *Chmp1* knockdown under the control of *dpp-Gal4* in a *N^{55ell}* heterozygous wing slightly enhanced notching frequency, and enhanced the wide veins phenotype. Percentage of wings of each genotype showing notching is indicated at the bottom right of each panel.

genotype	number of notched wings	percentage
<i>N^{55ell}/FM7Bar</i>	97/157	62%
<i>N^{55ell}/X</i>	10/49	20%
<i>N^{55ell}/X;dpp-Gal4</i>	38/92	41%
<i>N^{55ell}/X;UAS-Chmp1RNAi</i>	19/50	38%
<i>N^{55ell}/X;dpp>Chmp1RNAi</i>	20/75	27%

Table 4.2 Notching frequencies of individual genotypes. Wings were counted from flies that were raised at 28°C.

Notch signaling can be activated in a ligand-independent as well as a ligand-dependent manner. Ligand-independent activation of Notch requires Deltex (Dx), an E3 ubiquitin ligase and a positive regulator of Notch signaling. Dx promotes Notch monoubiquitination and induces Notch endocytosis and incorporation onto the late endosomal membrane. At the late endosome, γ -secretase mediates the cleavage of the intracellular domain (NICD), which propagates the Notch signal [128, 129]. Dx also suppresses the incorporation of Notch into MVBs. This causes retention of Notch in the endosomal membrane, increasing the number of Notch molecules cleaved by γ -secretase and thereby increasing the Notch signal. The cleaved NICD can then enter the nucleus and activate transcription factors that enhance or suppress expression of target

genes. In *Dx*-induced ligand-independent activation of Notch, the location of the Notch receptor is key; Notch must reach the late endosome to be activated, but must be kept out of the ILVs of the late endosome/MVB, as this would remove the NICD from the cytoplasm and prevent it being cleaved thus inhibiting the Notch signal [130]. Since *Chmp1* is a component of the ESCRT machinery, which is involved in MVB formation, it is possible that *Chmp1* is involved in the regulation of ligand-independent Notch signaling. If this is the case, faulty MVB formation caused by *Chmp1* knockdown could prevent the normal degradation/silencing of the Notch receptor. This would allow more opportunity for Notch receptor cleavage, and could lead to increased Notch signaling, which would be evident as ectopic wing margin and bristles (i.e., margin and bristles extend into the wing blade).

To test for involvement of *Chmp1* in the ligand-independent activation of Notch, the hypomorphic *carnation* mutation *car^l*, and the *UAS-dx* transgene were used. When *dx* is over-expressed, the Notch receptor is driven into the endocytic pathway and becomes over-activated. In the wing, *dx* over-expression causes ectopic wing margin and bristles due to increased Notch activation (Figure 4.29B). *Carnation* (Vps33p homologue) is a component of the homotypic fusion and vacuole protein sorting (HOPS) protein complex that is involved in trafficking from the early to the late endosome, and from the late endosome to the lysosome [129, 131, 132]. Mutation of *Carnation*, such as in the *car^l* mutant, can block progression of proteins, including Notch, from the early endosome to the lysosome where Notch would become activated. This causes loss of the Notch signal and therefore notching of the wing margin. Thus, the *car^l* allele was used in combination with *dx* over-expression as a control to show the phenotypic consequences of driving Notch into the endocytic pathway, and then blocking its activation (i.e., the opposite result of what was expected with *Chmp1* knockdown and *Dx* over-expression). To

generate the control, *car^l; dpp-Gal4/TM6Tb* males were crossed to *UAS-dx¹⁷* virgin females and the progeny that were not *Tb* (*car^l/+; dpp-Gal4/UAS-dx¹⁷*) were collected and wings mounted (Figure 4.27).

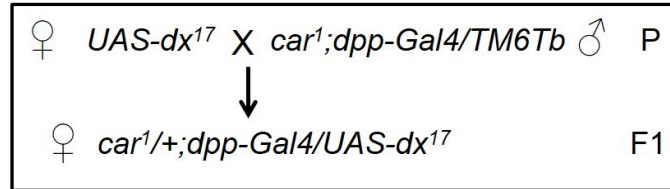


Figure 4.27 Control cross design to show interaction between Car and Deltex. Females that were not *Tb* were of the correct genotype. P is parental generation, F1 is first filial generation. Only the desired genotype in the filial generation is shown.

When *dx* is over-expressed in a background heterozygous for *car^l*, the ectopic wing margin phenotype caused by *dx* over-expression is transformed into a notch phenotype (Figure 4.29C). Presumably, this is due to removal of Notch from the membrane by *dx* over-expression in combination with interference of the early endosome/lysosome pathway due to the *car^l* mutation. This leads to a loss of Notch signaling indicated by wing notching. If loss of *Chmp1* disrupts endocytic trafficking and blocks Notch progressing to the lysosome as the *car^l* mutation does, then notching should occur when *dx* is over-expressed concomitantly with *Chmp1* knockdown. Another possibility is that loss of *Chmp1* stalls MVB formation and increases the time Notch spends in the limiting membrane of the late endosome, so in this case, an increase in Notch signaling could be expected, resulting in ectopic margin.

To test for a genetic interaction between *Chmp1* and *Dx*, i.e., ligand-independent Notch signaling, *Chmp1* knockdown and *dx* over-expression were driven in the same wing under the control of the *dpp-Gal4* driver (Figure 4.28). *UAS-Chmp1RNAi-VDRC/Cy* virgin females were crossed to *Cy/If; D^l/TM6Sb* males and from the progeny, virgin females that were *Cy* and *Sb*, but not *If*, were collected (*UAS-Chmp1RNAi-VDRC/Cy; TM6Sb/+*). In a separate cross, *dpp-*

Gal4/TM6Tb males were crossed to *Cy/If; D¹/TM3Ser* virgin females, and from the progeny males that were *If* and *Ser*, but not *Cy* (*If/+; dpp-Gal4/TM3Ser*) were collected. The *UAS-Chmp1RNAi-VDRC/Cy; TM6Sb/+* virgin females were then mated to the *If/+; dpp-Gal4/TM3Ser* males, and males that were *If* and *Sb*, but not *Cy* or *Ser* (*UAS-Chmp1RNAi-VDRC/If; dpp-Gal4/TM6Sb*) were collected from the progeny. These males were crossed to *UAS-Dx¹⁷* virgin females. Progeny from this cross that were not *If* and not *Sb* were of the correct genotype (*UAS-Chmp1RNAi-VDRC/+; dpp-Gal4/UAS-Dx¹⁷*).

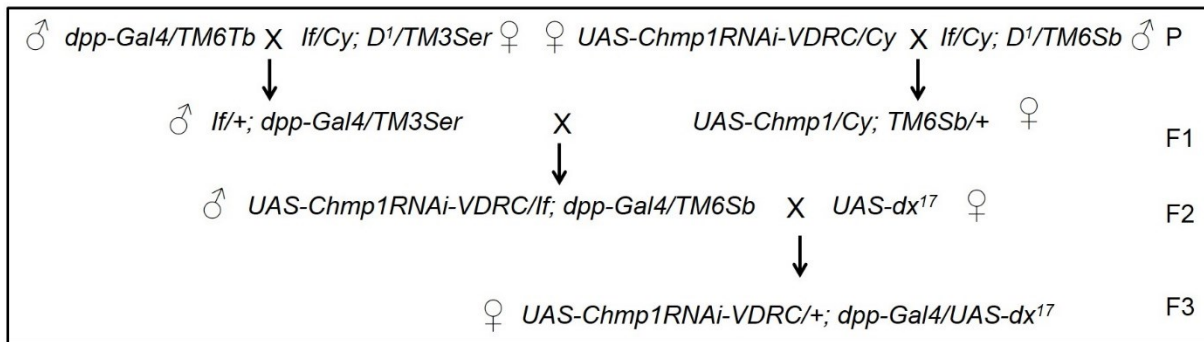


Figure 4.28 Cross design to test for an interaction between *Chmp1* and *Deltex*. Females that were not *If* and not *Sb* were of the correct genotype. P is parental generation, F1 is first filial generation, F2 is second filial generation, F3 is third filial generation. Only the desired genotype from each filial generation is shown.

As shown before, knockdown of *Chmp1* with *dpp-Gal4* causes thickening of the L3 wing vein (Figure 4.29A). Interestingly, when *Chmp1* was knocked down in a wing over-expressing *dx*, the result was ectopic bristles within the wing blade, as well as a loss of marginal bristles, which could be considered a weak notching phenotype (Figure 4.29D). Additionally, the distal portion of the L3 wing vein was lost.

These phenotypes are puzzling, because loss of wing vein and ectopic bristles are normally associated with gain of Notch function, while notching indicates a loss of Notch function. The loss of the distal wing vein was never observed when *dx* was over-expressed under

the control of *dpp-Gal4*, even though increased Dx activity is known to increase Notch signaling. In fact, the opposite was observed; *dx* over-expression generated slightly thicker wing veins. Likewise, wing vein loss was never observed under *Chmp1* knockdown conditions alone. This suggests that the vein loss is a specific result of loss of Chmp1 activity in combination with gain of Dx activity. Over-expression of *dx* drives Notch into the endocytic pathway and prevents its incorporation into the MVB. If *Chmp1* knockdown inhibits normal MVB formation then the combined effect of *dx* over-expression and *Chmp1* knockdown might cause increased Notch signaling, which could explain the loss of distal wing vein and the ectopic bristles. However, this does not account for the minor notches observed, which may suggest that in some wing cells Notch was blocked from progressing to the late endosome where it would be activated. This seems unlikely as the literature reports that the role of Chmp1 and other ESCRT components is not the trafficking of Notch to the late endosome, but rather moving Notch from the limiting membrane of the late endosome into the ILVs of the MVB. Additionally, it does not seem likely that the same combination of factors might increase Notch activation in some cells and decrease it in other cells within the same tissue. The contradictory nature of these observed phenotypes make the results of this experiment difficult to interpret. However, the phenotypes indicative of activated Notch signaling, i.e., loss of the L3 wing vein and extra bristles within the wing blade, were more obvious and consistent than the notching phenotype, which would indicate loss of the Notch signal.

It is also interesting that over-expression of *dx* causes a slightly thickened wing vein, especially considering that *dx* mutants also have thickened wing veins as well. This may suggest that driving Notch into the endocytic pathway has different effects in different parts of the wing, i.e., activating Notch at the wing margin, but inactivating it in the wing veins. An alternative is

that the effect of a certain dose of Dx is different in different parts of the wing. Possibly, the same amount of *dx* over-expression activates Notch at the wing margin, but has a dominant-negative effect in vein tissue that reduces Notch signaling.

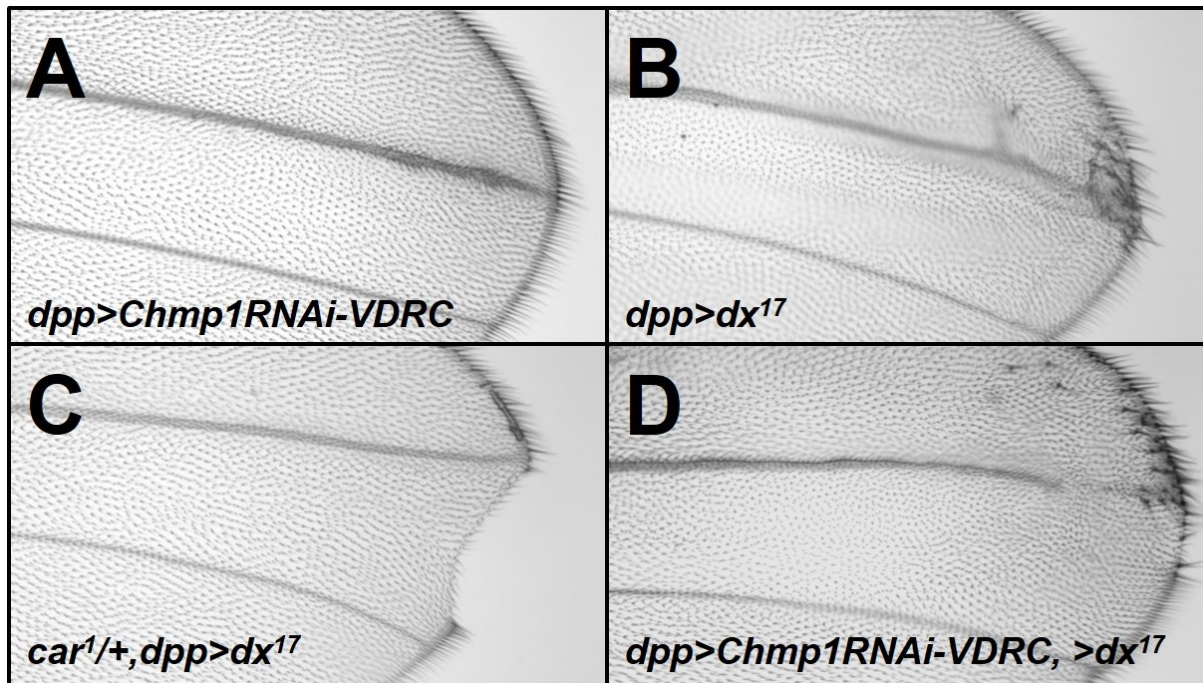


Figure 4.29 Interaction between Chmp1 and Deltex. Light micrographs of adult female wings grown at 25°C. Distal is right, anterior is uppermost. **A.** *Chmp1* knockdown driven with *dpp-Gal4* causes a slightly larger wing vein. **B.** Driving over-expression of *dx* with *dpp-Gal4* causes slightly wider wing vein, as well as ectopic wing margin. **C.** Driving *dx* over-expression with *dpp-Gal4* in a background heterozygous for *car¹* causes wing notching. **D.** *dx* over-expression and *Chmp1* knockdown with *dpp-Gal4* causes a wider wing vein, ectopic margin, and a mild notching phenotype (loss of distal marginal bristles).

VII. Testing for interactions between *Chmp1* and regulators of the DER using *Chmp1* over-expression lines

Heterozygosity for loss of function alleles of positive or negative regulators of the DER suppressed and enhanced the *Chmp1* knockdown phenotype, respectively. This result suggested that *Chmp1* negatively regulates DER signaling in the *Drosophila* wing. If *Chmp1* over-expression leads to an increase in *Chmp1* activity and thus decreased DER signaling, then, for

example, heterozygosity for loss of function alleles of positive regulators of the DER concomitant with *Chmp1* over-expression might cause thinning or loss of wing veins.

To test for an interaction between *Chmp1* and regulators of DER signaling, the *en-Gal4* driver, the *UAS-Chmp1* or *UAS-HM-Chmp1* transgene, and a loss of function allele for either positive or negative regulators of the DER had to be combined into the same fly (Figure 4.30). *en-Gal4; D¹/TM3Sb* virgin females were crossed to female virgins carrying loss of function alleles for the DER regulators Sty (*If/Cy;sty^{Δ5}/TM3Sb*), Aos (*If/Cy;argos^{w11}/TM3Sb*), or Rho and Vn (*If/Cy;ve,vn*). From this cross, males that were *If* and *D¹* (not *Sb*) were collected (*en-Gal4/If; sty^{Δ5}, argos^{w11}, or ve,vn/D¹*). These males were crossed to *UAS-HM-Chmp1-3* or *UAS-Chmp1-2/Cy* virgin females. Wings from females from this cross that were not *If*, *Cy*, or *D¹* were of the correct genotype (*en-Gal4/UAS-HM-Chmp1-3* or *UAS-Chmp1-2; rho^{ve-1}, vn¹/+, en-Gal4/UAS-HM-Chmp1-3* or *UAS-Chmp1-2; sty^{Δ5}/+, en-Gal4/UAS-HM-Chmp1-3* or *UAS-Chmp1-2; aos^{w11}/+*) and mounted onto a microscope slide in GMM.

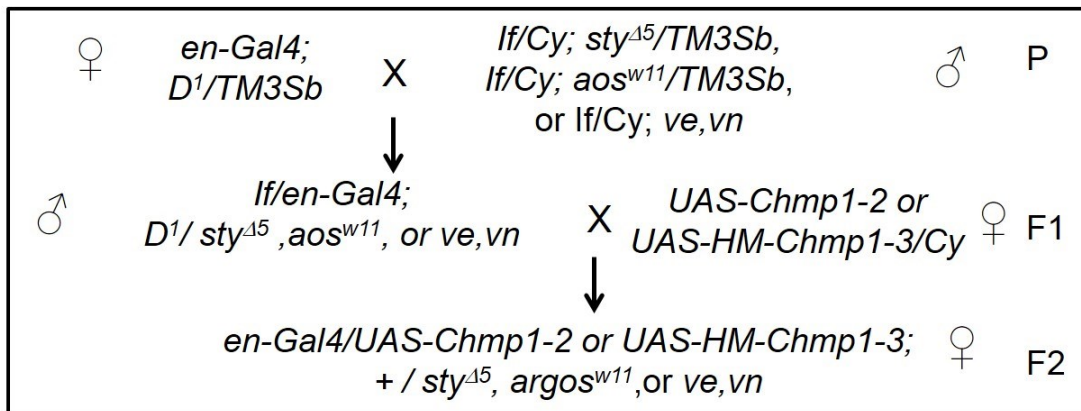


Figure 4.30 Cross design using *Chmp1* over-expression transgenes to test for an interaction between *Chmp1* and DER regulators. P is parental generation, F1 is first filial generation, F2 is second filial generation, F3 is third filial generation. Only the desired genotype from each filial generation is shown.

Expression of *UAS-Chmp1-2* under *en-Gal4* control in a background heterozygous for either *aos* or *rho* and *vn* resulted in similar phenotypes. In both cases, minor deltas were observed and the posterior wing was smaller, indicated by a slight curving to the posterior of the wing (Figure 4.31A and B). Additionally, sporadic and small portions of the L4 wing vein were lost, suggesting that cells adopted an intervein instead of a vein fate (Figure 4.31A and B). Expression of *UAS-HM-Chmp1-3* in a background heterozygous for loss of function alleles for either *aos* or *rho* and *vn* caused minor but specific phenotypes, including loss of the acv and delta formation (Figure 4.31C and D). These phenotypes could indicate a loss of DER activity or a gain of Notch signaling. However, as similar phenotypes were observed when *Chmp1* was over-expressed in wings heterozygous for loss of function alleles for both positive and negative regulators of DER signaling, this effect does not seem specific. This suggests that over-expression of *Chmp1* has no significant effect on DER signaling and thus a precise dosage of *Chmp1* is not crucial for normal DER signaling in wing vein development.

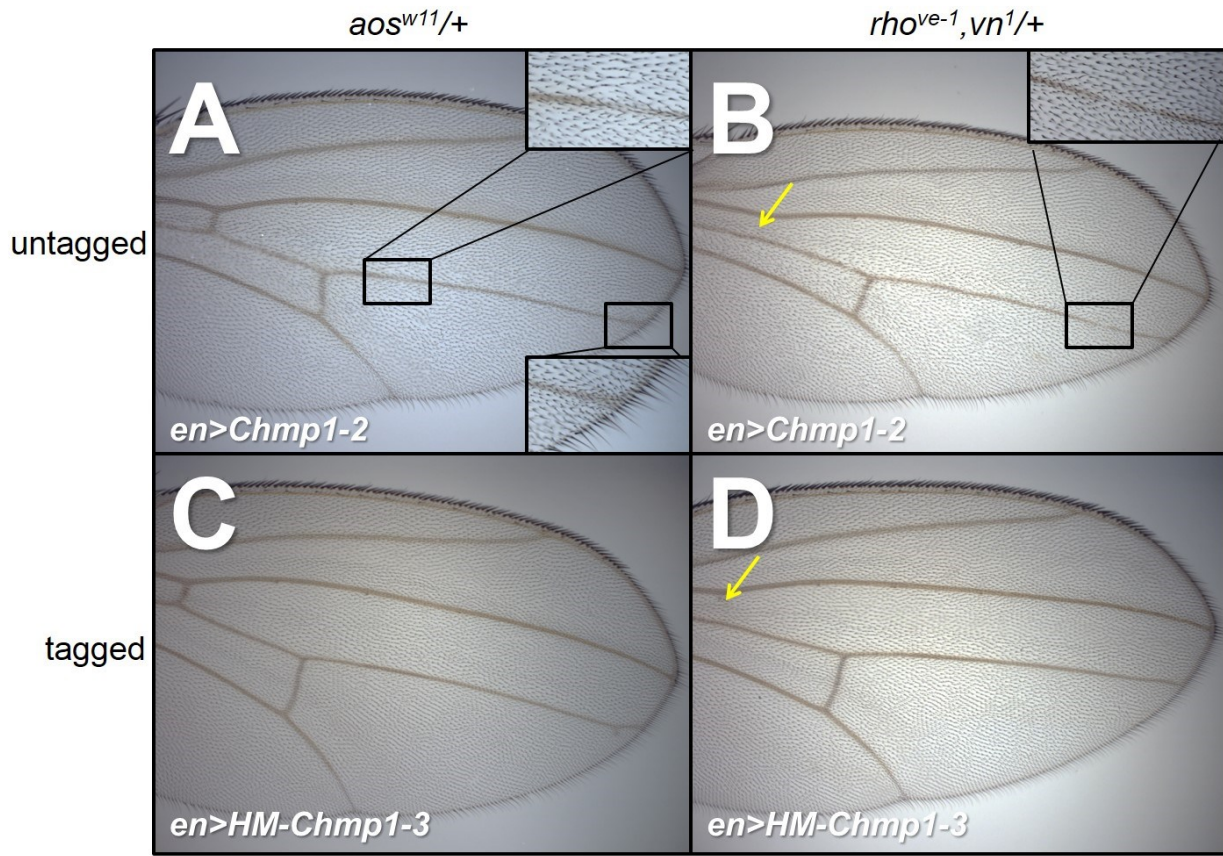


Figure 4.31 *Chmp1* over-expression and DER regulators. Light micrographs of adult female wings grown at 30°C. Distal is right, anterior is uppermost. **A.** *en-Gal4/UAS-Chmp1-2*; *aos^{w11}/+*. **B.** *en-Gal4/UAS-Chmp1-2*; *rho^{ve-1}, vn¹/+*. **C.** *en-Gal4/UAS-HM-Chmp1-3*; *aos^{w11}/+*. **D.** *en-Gal4/UAS-HM-Chmp1-3*; *rho^{ve-1}, vn¹/+*. Yellow arrows indicate loss of the anterior cross vein (acv).

VIII. *Chmp1* knockdown in the eye disrupts ommatidia

Chmp1 knockdown experiments suggested that *Chmp1* negatively regulates DER signaling in the *Drosophila* wing. To investigate whether this was true for other *Drosophila* tissues, and to gain more insight into the function of *Chmp1* in the developing organism, *Chmp1* was knocked down in the fly eye (Figure 4.32). During eye development, DER signaling is involved in specifying photoreceptors of the ommatidia. Loss of DER signaling usually results in loss of photoreceptors, while gain in DER signaling generally causes recruitment of additional

photoreceptors. So if *Chmp1* negatively regulates DER signaling, then *Chmp1* knockdown might cause an increase in the number of photoreceptors within ommatidia.

To test this, two different drivers were used to drive *Chmp1* knockdown in the eye: *sevenless-Gal4* (*sev-Gal4*), which drives Gal4 expression in R cell and cone cell precursors, and *eyeless-Gal4* (*ey-Gal4*), which drives Gal4 expression anterior to the morphogenetic furrow in the eye disc during larval development (see Chapter 1 Section I.C for description of eye development) [2]. *sev-Gal4* or *ey-Gal4* males were crossed to *UAS-Chmp1RNAi-TRiP* virgin females and the progeny were grown at 25°C, 28°C, or 30°C. The heads from the progeny were fixed, dehydrated, embedded in plastic, sectioned, stained and imaged on a light microscope (see Chapter 3 Section VII for methods).

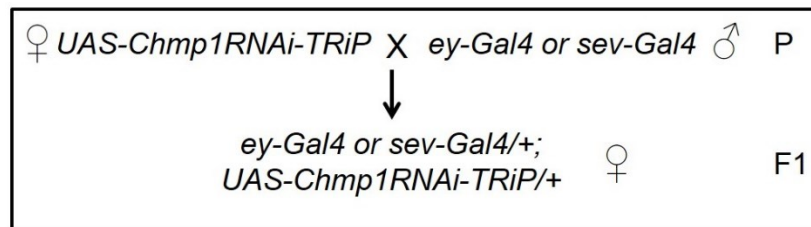


Figure 4.32 Cross design for *Chmp1* knockdown in the *Drosophila* eye. The F1 generation was grown at 25°C, 28°C, or 30°C. P is parental generation, F1 is first filial generation. All progeny were of the desired genotype.

Driving *Chmp1* knockdown with *sev-Gal4* resulted in eyes that were largely wild-type, with the exception that rare defects were observed at 30°C, such as symmetrical ommatidia and loss of photoreceptor cells (Figure 4.33B). Symmetrical, or non-chiral ommatidia have either two R3 or two R4 photoreceptors, instead of one R3 and one R4. Chirality is determined by the position of the R3 and R4 photoreceptors within an ommatidium and is specified by the Notch and Fz PCP signaling pathways [133, 134]. Therefore the presence of symmetrical ommatidia could indicate faulty Notch or Fz PCP signaling.

At 25°C a largely wild-type phenotype was observed when *Chmp1* was knocked down under the control of *ey-Gal4*. But at 28°C and 30°C, *Chmp1* knockdown caused major defects in ommatidial development (Figures 4.33C-E). These defects were usually severe enough to make it difficult to determine the site of the equator of the eye, or to determine the chirality of individual ommatidia. One common defect observed when *Chmp1* knockdown was driven with *ey-Gal4* was misaligned ommatidia. In wild-type eyes, ommatidia are perfectly aligned with each other within each half of the eye (Figure 4.33A). In eyes with *Chmp1* knockdown, misaligned ommatidia were observed, which suggests that ommatidial rotation during eye development was impaired (Figures 4.33D and E). Misrotation of ommatidia is a classic problem associated with both under- and over-active DER signaling [133]. In rare cases, symmetrical ommatidia were observed, which again could indicate faulty Notch or Fz PCP signaling. However, as symmetrical ommatidia were quite rare, and since chirality, when observable, was normal, it appears *Chmp1* knockdown has only a minor effect on these pathways.

By far the most common abnormality observed in eyes with *Chmp1* knockdown was loss of photoreceptor cells. Over-active DER signaling is known to cause recruitment of extra photoreceptors, suggesting that loss of photoreceptors might indicate a loss of DER signal. This would seem to contradict the results from the wing, which suggest that *Chmp1* knockdown increases DER signaling. However, DER *ellipse* alleles (e.g., *EGFR^{ElpB1}* – an amino acid substitution in kinase domain that activates tyrosine kinase activity and causes ligand-independent signaling) are gain of function alleles that cause loss of photoreceptors, similar to the phenotype observed with reduced *Chmp1* activity [127, 135, 136]. Since constitutively active DER and *Chmp1* knockdown result in similar phenotypes, it appears that *Chmp1* knockdown is equivalent to over-active DER. If *Chmp1* knockdown disrupts the incorporation of the DER into

MVBs, this could result in persistent DER signaling since the DER would still be able to signal to the cytoplasm.

Chmp1 was also over-expressed in the eye using the *sev-Gal4* and *ey-Gal4* drivers at 25°C, 28°C, and 30°C. However, a wild-type phenotype was observed. This absence of a *Chmp1* over-expression phenotype in the eye and the weak phenotype observed in the wing may suggest that a precise dosage of *Chmp1* in the cell is not critical for its normal activity.

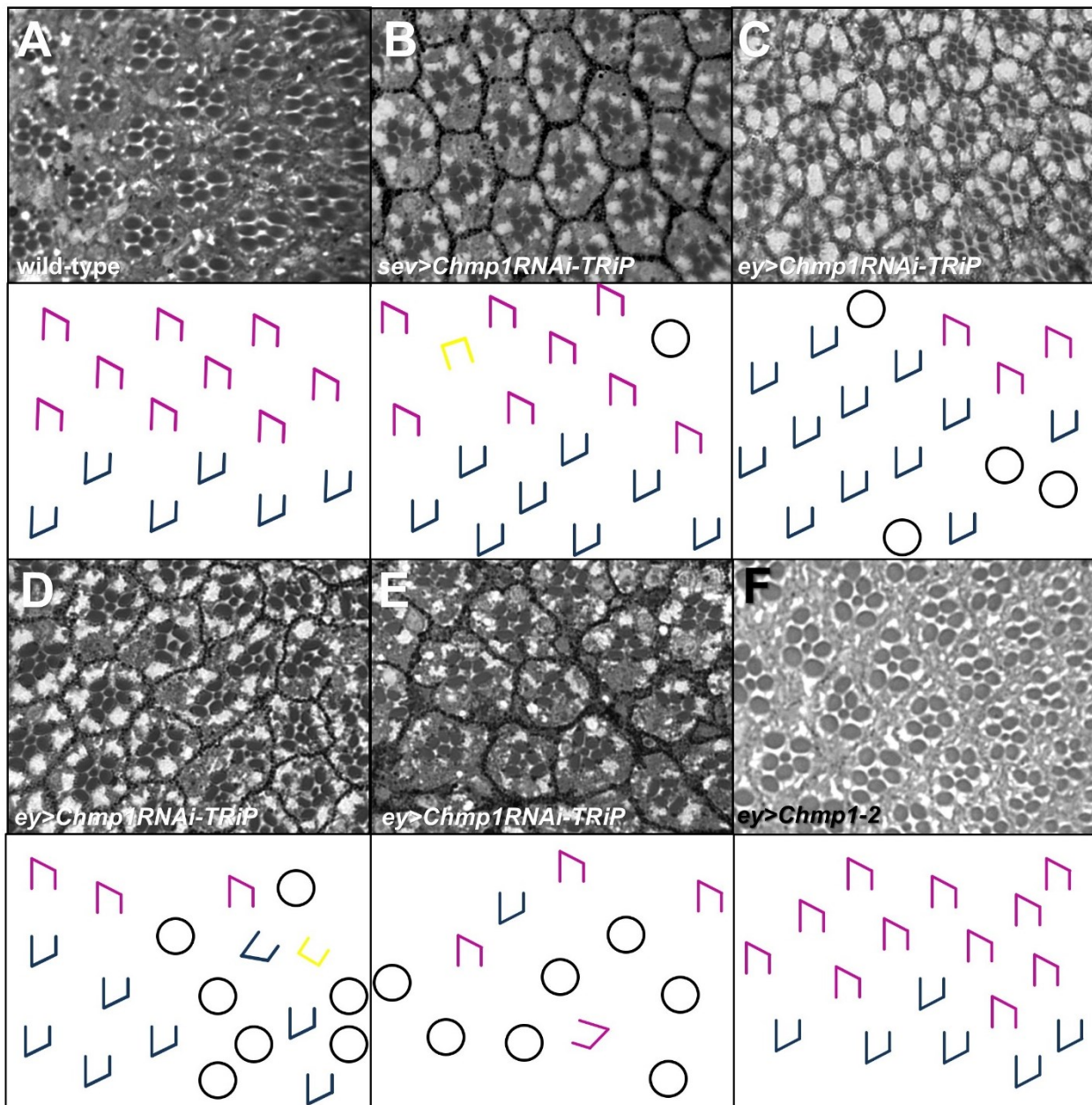


Figure 4.33 *Chmp1* knockdown and over-expression in the *Drosophila* eye. Light microscope images of one micron thick tangential sections of adult *Drosophila* eyes. Images were taken at the equator of the eye, when possible. **A.** *Oregon R*. **B.** *Chmp1* knockdown at 30°C, (*sev-Gal4/+; UAS-Chmp1RNAi-TRiP/+*). **C.** *Chmp1* knockdown at 28°C, (*ey-Gal4/+; UAS-Chmp1RNAi-TRiP/+*). **D. and E.** *Chmp1* knockdown at 30°C, (*ey-Gal4/+; UAS-Chmp1RNAi-TRiP/+*). **F.** *Chmp1* over-expression at 30°C, (*ey-Gal4/UAS-Chmp1-2*). Schematics below each panel show the arrangement of each ommatium, including chirality and rotation. Ommatidia with dorsal chirality marked in purple, ommatidia with ventral chirality marked in blue, and symmetrical ommatidia are marked in yellow. Open black circles indicate ommatidia with fewer R cells than wild-type and thus chirality was undeterminable.

IX. *Drosophila* Chmp1 localizes apically and to the cell membrane

Most studies on the subcellular localization of Chmp1 have been performed in cell culture rather than in developing tissues, and different studies show different localizations for Chmp1. Reports in cultured mammalian cells and *Aspergillus nidulans* show Chmp1 localization to both the early and late endosome, localizations that are consistent with a role for Chmp1 as a component of ESCRT-III [86, 97]. Other reports in cultured mammalian cells, zebrafish, and *Nicotiana benthamiana* show localization to the nucleus [81, 85, 91, 95]. In mammalian cell culture, the localization of Chmp1 seemed to vary by cell treatment and type, a finding that was also observed in the zebrafish brain [91, 95]. Since the *Chmp1* and *HM-Chmp1* over-expression lines appeared to have some normal Chmp1 activity (shown in Chapter 4 Section II), and over-expression of *Chmp1* caused only weak localized phenotypes, the *UAS-HM-Chmp1* fly line provided a suitable way to study the subcellular localization of the Chmp1 protein in cells of a developing tissue. Epithelial cells in embryos and wing imaginal discs were used to investigate the localization of Chmp1. Embryos were tried first because it is normally easy to collect large numbers (i.e., from a single embryo collection hundreds can be collected) and fairly straightforward to prepare for immunostaining. *en-Gal4*, which expresses Gal4 in the anterior of each parasegment, was used to drive expression of HM-Chmp1 and GFP. Therefore cells

expressing HM-Chmp1 were marked by GFP expression. To achieve this, *en-Gal4, UAS-GFP* homozygous virgin females were crossed to *UAS-HM-Chmp1-1/TM6TbSb* males (Figure 4.34). Embryos were fixed, an anti-c-Myc antibody was used to detect HM-Chmp1, and the embryos were mounted in Vectashield mounting media with DAPI. Only embryos that showed both GFP and c-Myc staining were imaged using a confocal microscope.

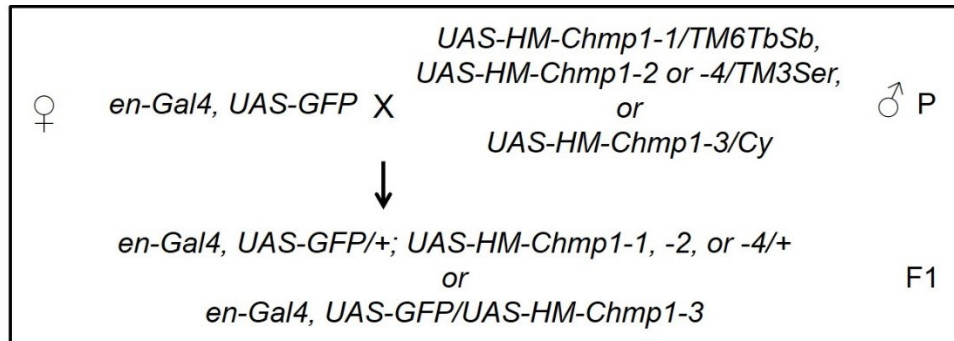


Figure 4.34 Cross design for HM-Chmp1 expression in both the anterior of embryonic parasegments and the posterior wing disc in larvae. P is parental generation, F1 is first filial generation. Only desired genotypes are shown in the F1 generation.

In embryos expressing HM-Chmp1 and GFP under *en-Gal4* control, c-Myc staining was observed specifically in GFP-expressing cells and no c-Myc staining was visible in the non-GFP-expressing cells. This suggested that the c-Myc antibody was specific for HM-tagged Chmp1. HM-Chmp1 localized mostly to the apical plasma membrane of the embryonic epithelial cells (Figure 4.35). Nuclear HM-Chmp1 was not detected, despite the presence of an NLS sequence in *Drosophila* Chmp1, and the fact that previous reports describe Chmp1 localizing to the nucleus.

The subcellular localization of Chmp1 was also investigated in epithelial cells of the imaginal wing disc. The *en-Gal4* driver was used again to drive expression of HM-Chmp1 and GFP in the posterior wing disc. To achieve this, *en-Gal4, UAS-GFP* homozygous virgin females were crossed to males carrying a *UAS-HM-Chmp1* insertion on either the second or third

chromosome (Figure 4.34). Larvae were grown at 18°C. At a lower temperature, the UAS-Gal4 system is less active, so HM-Chmp1 is expected to be lower than at higher temperatures. This reduces the possibility of excessive over-expression resulting in aberrant localization of the protein. Third instar wing discs were dissected and an anti-c-Myc antibody was used to detect HM-Chmp1 in the discs. The discs were mounted onto a microscope slide in Vectashield with DAPI, and discs that showed both GFP and c-Myc staining were of the correct genotype and so were imaged with a confocal microscope.

HM-Chmp1 consistently localized to the apical plasma membrane in the third instar larval wing disc when expressed from multiple independent HM-Chmp1 transgene insertions (Figure 4.35). These results suggest that the apical membrane localization observed is the genuine localization of HM-Chmp1, as multiple independent HM-Chmp1 transgene insertions in two separate tissues showed similar HM-Chmp1 localizations.

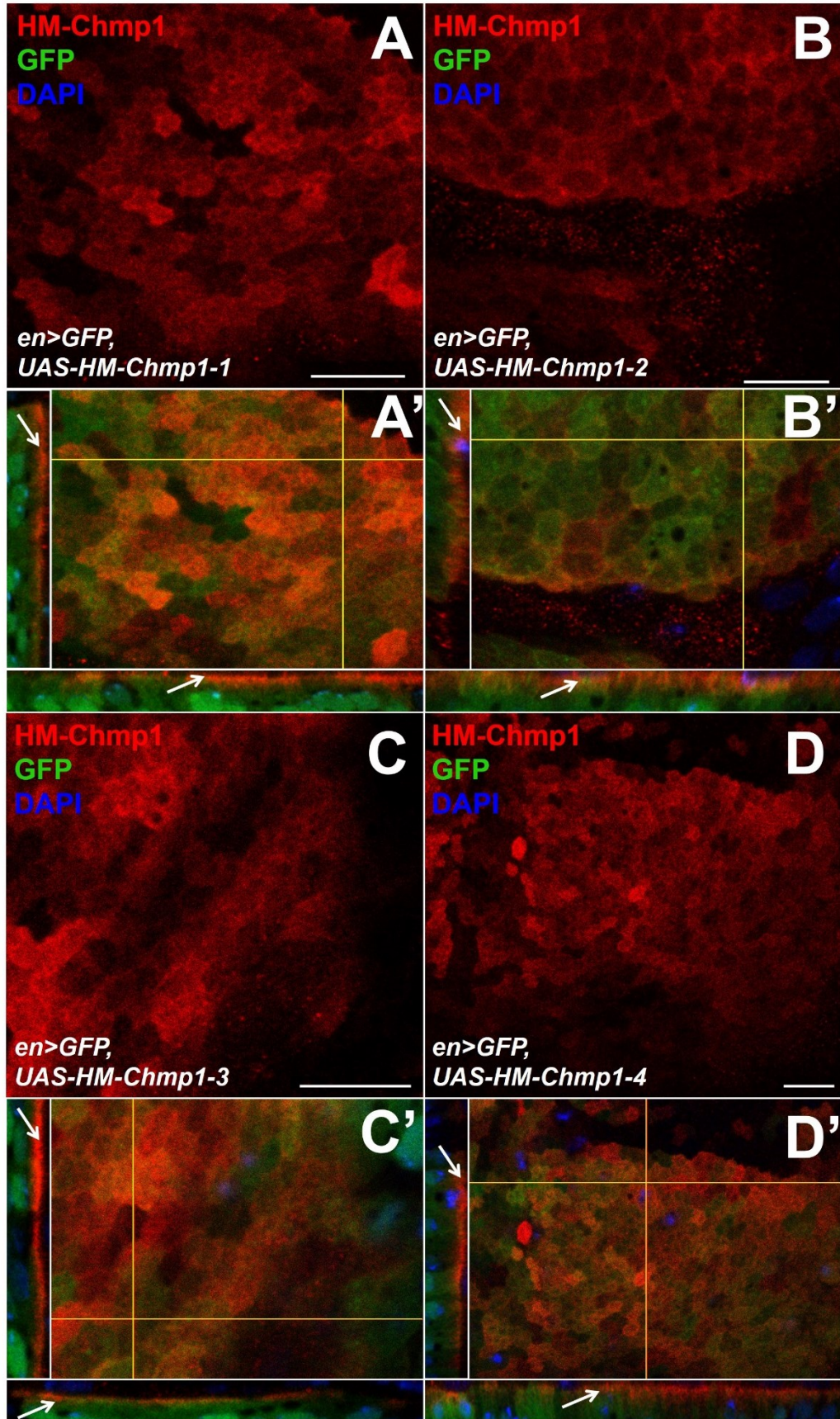


Figure 4.35 Localization of HM-Chmp1 in wing imaginal discs. All images from *en-Gal4,UAS-GFP/+; UAS-HM-Chmp1/+* or *en-Gal4,UAS-GFP/UAS-HM-Chmp1* flies. Confocal Z-series showing HM-Chmp1 localization (red) in wing discs. The Z-series began just above apical region of the columnar epithelial cells of the disc proper. HM-Chmp1 expression was driven under the control of the *en-Gal4* driver using four independent HM-Chmp1 transgene insertions. Cells expressing HM-Chmp1 were marked with GFP (green). Scale bar is 10 μ m. **A-D.** Wing discs were immunostained with anti-c-Myc for HM-Chmp1 (red). One section from a Z-series is shown. **A'-D'.** Images A-D merged with GFP (green) and nuclear (blue) images. Orthogonal X and Y sections, indicated by yellow lines, are below and to the left of the image respectively. White arrows indicate the apical localization of HM-Chmp1. The position of the orthogonal sections is indicated by yellow lines. Z-series depth for A' was 11.78 μ m, B' was 6.38 μ m, C' was 9.64 μ m, and D' was 14.25 μ m.

X. Chmp1 localizes to the late endosome

If *Drosophila* Chmp1 regulates DER signaling through its function in the ESCRT complexes during MVB biogenesis, then Chmp1 should localize to the endosome. Localization of HM-Chmp1 at the early endosome was investigated by looking for co-localization of HM-Chmp1 and the early endosome marker, Rab5. HM-Chmp1 and GFP were expressed in the anterior of parasegments in embryos under the control of the *en-Gal4* driver (Figure 4.34). Embryos were collected and immunostained for HM-Chmp1 using anti-c-Myc and for Rab5 using anti-Rab5. No apparent co-localization was observed between HM-Chmp1 and Rab5, suggesting that HM-Chmp1 does not localize to the early endosome (Figure 4.37A). Co-localization between Chmp1 and its known binding partner, Vps4, was investigated as well. Using an antibody to detect Vps4, no obvious co-localization between Vps4 and HM-Chmp1 was observed (Figure 4.37C). Although Chmp1 has been shown to bind Vps4 in yeast, humans, and *Drosophila* this binding is likely transient [72, 73], which could explain the lack of co-localization [82, 97, 110].

Localization of HM-Chmp1 at the late endosome was investigated by looking for co-localization of HM-Chmp1 and the late endosome marker, Rab9. HM-Chmp1 was expressed in

embryos, along with YFP-tagged Rab9 under the control of the *en-Gal4* driver (Figure 4.36).

If/Cy; D¹/TM3Ser virgin females were mated to *UAS-YFP-Rab9* males. From the progeny of that cross, males that were *Cy* and *Ser*, but not *If* or *Sb* (*UAS-YFP/Cy; TM3Ser/+*), were collected and crossed to *If/Cy; UAS-HM-Chmp1-1/TM6TbSb* virgin females. From the offspring of this cross, males that were *UAS-YFP-Rab9/Cy; UAS-HM-Chmp1/TM3Ser* were collected and crossed to *en-Gal4, UAS-GFP* virgin females. Embryos were collected at 18°C, immunostained with an anti-c-Myc antibody to detect HM-Chmp1, and imaged with a confocal microscope. YFP expression, driven by the *en-Gal4* driver, was only detected the anterior of each parasegment, along with GFP and HM-Chmp1. Additionally, only a proportion of embryos (~ 25% expected) had all three transgenes, so only a proportion of embryos expressed Chmp1, GFP, and YFP-Rab9.

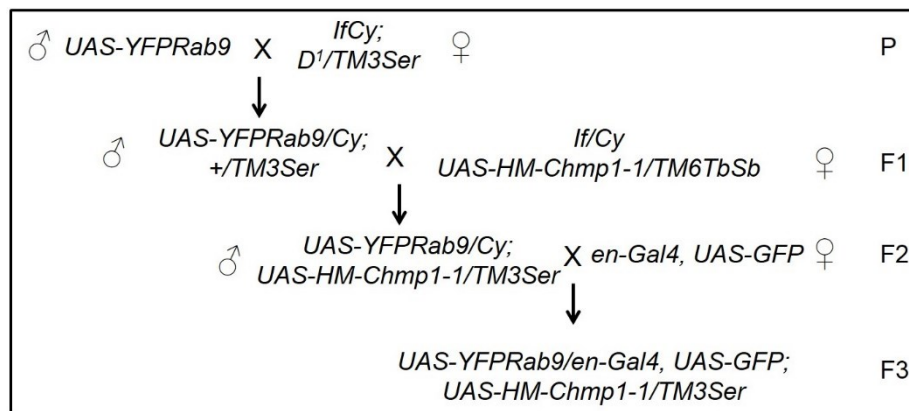


Figure 4.36 Cross design for HM-Chmp1 and YFP-Rab9 expression in the anterior of embryonic parasegments. P is parental generation, F1 is first filial generation, F2 is second filial generation, F3 is third filial generation. Only the desired genotypes in filial generations are shown.

Although the fluorescent signals from YFP-Rab9 and HM-Chmp1 did not completely overlap, some co-localization was apparent (Figure 4.37B). This implies that Chmp1 localizes to the late endosome and suggests that Chmp1 is functioning there. In light of the literature, this localization is likely a function of the role of Chmp1 as a component of the ESCRT-III complex

in MVB generation. This suggests that the negative regulation of DER signaling by *Drosophila* Chmp1 may well be due to its function in MVB biogenesis. So, when *Chmp1* is knocked down, MVB formation is incomplete, resulting in persistent DER signaling due to a failure to separate the DER from the cytoplasm.

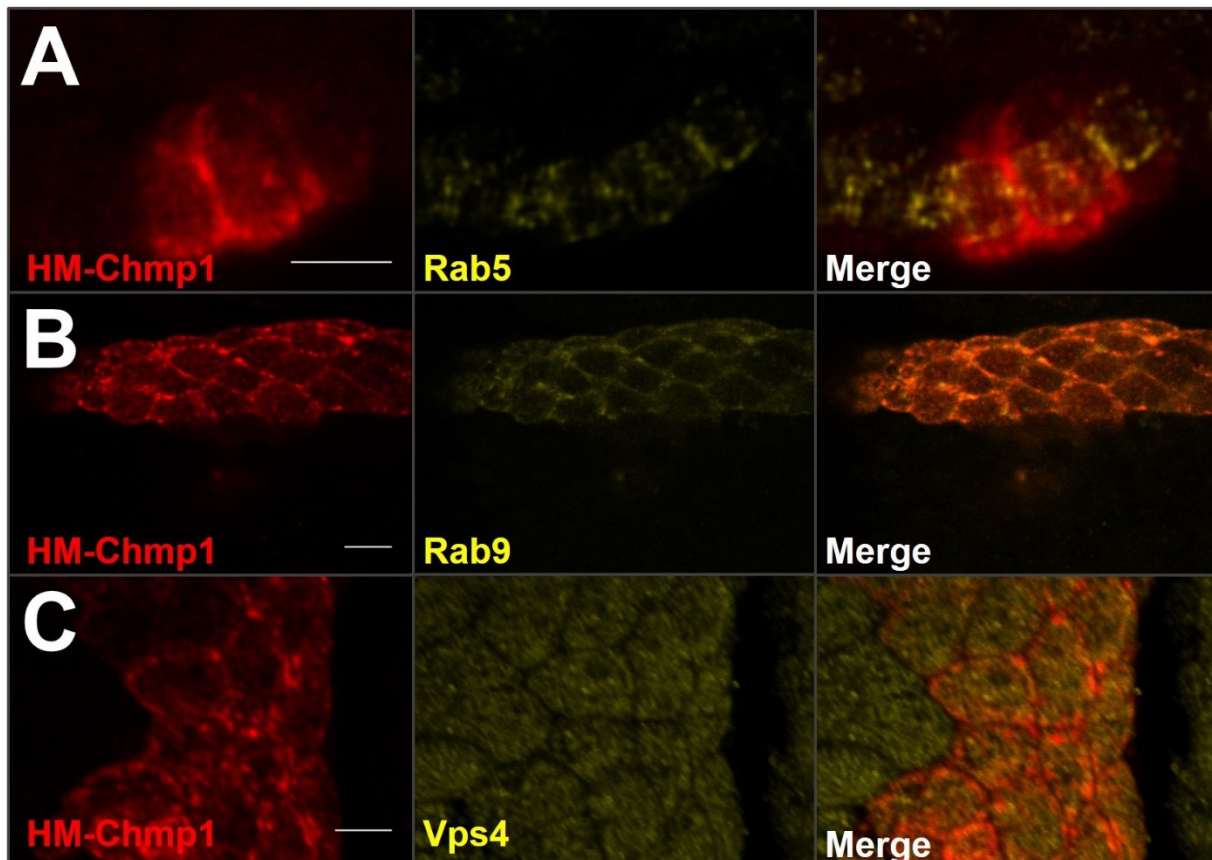


Figure 4.37 Relative subcellular localizations of HM-Chmp1 with endosome markers and Vps4. Confocal images of embryos driving *UAS-HM-Chmp1-1* expression under the control of the *en-Gal4* driver. Embryos were immunostained with anti-c-Myc for HM-Chmp1 (red). One section from a confocal Z-series showing HM-Chmp1 localization is shown. Scale bar is 5 μm. A. Localization of HM-Chmp1 (red) and Rab5 (yellow) and merged image, (*en-Gal4,UAS-GFP/+; UAS-HM-Chmp1-1/+*). B. Localization of HM-Chmp1 and YFP-Rab9 (yellow) and merged image, (*en-Gal4,UAS-GFP/UAS-YFPRab9; UAS-HM-Chmp1-1/+*). C. Localization of HM-Chmp1 and Vps4 (yellow) and merged image, (*en-Gal4,UAS-GFP/+; UAS-HM-Chmp1-1/+*).

CHAPTER 5

DISCUSSION

Many cell signaling pathways share a common cascade structure in which activation is initiated by the binding of a ligand to a transmembrane receptor. The activated receptor then transmits the signal to signaling components in the cellular cytoplasm. This usually leads to a change in gene expression, which alters the activity of the cell. Down-regulation of cellular signaling pathways is crucial for proper function of a cell and persistent signaling can result in severe problems, such as deregulated growth. One method of down-regulating cell signaling pathways is degradation of activated transmembrane receptors through the multivesicular body (MVB) pathway. The ESCRT (Endosomal Sorting Complexes Required for Transport) -0, -I, -II, and -III complexes mediate MVB generation, by which receptors are sequestered from the cytoplasm into intraluminal vesicles (ILVs) of the MVB, thereby silencing the signal. ESCRT function during MVB generation is required for the down-regulation of many signaling pathways, including EGFR and Notch [58-61]. This study investigated the function of the Chmp1 protein, a component of ESCRT-III. The ESCRT-III protein complex provides the core function of ESCRT activity: the scission of the neck of the ILV, completing MVB formation.

Previous studies in a variety of organisms have implicated Chmp1 in MVB biogenesis, protein sorting, mitosis, and both positive and negative regulation of growth [69, 81, 86-89, 91, 92, 100]. As most studies on Chmp1 have been performed in single cell culture, *Drosophila* provided a useful model for investigating Chmp1 function in developing tissues. The research presented in this dissertation suggests that Chmp1 negatively regulates DER signaling and wing vein cell fate in the *Drosophila* wing. This is likely a result of the role of Chmp1 in the ESCRT-

III complex, which mediates the down-regulation of activated DERs via the MVB pathway and lysosomal degradation.

I. Chmp1 is essential

This is the first published investigation of Chmp1 function in invertebrates. *Drosophila* provides a useful model for investigating Chmp1 function as it expresses a single Chmp1 protein that shares all the functional domains identified in the vertebrate Chmp1 protein. Also, the well-established genetic tools available in *Drosophila* allow the fine control of *Chmp1* expression during tissue development. Fly lines expressing RNAi targeted at the *Chmp1* transcript were used to investigate the effect of loss of *Chmp1* on survival. Ubiquitous knockdown of *Chmp1* during fly development was lethal, suggesting that *Chmp1* is an essential gene for *Drosophila* development. This is consistent with the finding that Chmp1 is essential in *Arabidopsis thaliana*, but contrasts with studies in *Nicotiana benthamiana*, and *Aspergillus nidulans*, in which Chmp1 was not essential for survival [85-87]. It appears, therefore, that loss of Chmp1 is not necessarily cell or tissue lethal. However, the deregulation of cell signaling resultant from loss of Chmp1 activity can cause inviability in some organisms. This suggests that, although Chmp1 activity, e.g., its molecular interactions and functional domains, appears to be conserved, the downstream consequences of Chmp1 loss differs between species. When compared in a dendrogram showing the evolutionary relationships between Chmp1 proteins, *Drosophila* Chmp1 is more closely related to mammalian Chmp1 than to Chmp1 in plants or yeast [92]. So, like most *Drosophila* proteins, it appears that Chmp1 function is better conserved between flies and humans, than between flies and plants.

II. Chmp1 regulates the wing vein cell fate decision

The UAS-Gal4 system provided a way to limit *Chmp1* knockdown to a specific tissue, avoiding the lethality associated with ubiquitous *Chmp1* knockdown. Thus, *Chmp1* was knocked down in the wing, one of the best characterized adult structures of the fly and a non-essential tissue for survival. When *Chmp1* knockdown was limited to the wing, thickened wing veins resulted. Ideally, the strength of the knockdown, i.e., the difference in protein levels between wild-type and *Chmp1* knockdown flies, would have been measured. As no antibody has been generated against *Drosophila* Chmp1, Chmp1 protein levels could not be detected via immunoblot. Additionally, as RT-PCR would assay mRNA levels, it would not necessarily give a valid indication of protein levels. However, expression of RNAi against *Chmp1* caused a reproducible and specific wing phenotype using multiple drivers and two independent RNAi lines, strongly suggesting that the thickened wing veins were caused by reduced Chmp1 expression.

Thickened wing veins are classically associated with a cell fate change from intervein to vein in the wing [14]. Therefore, the thickened wing veins observed with *Chmp1* knockdown were likely caused by a change in wing cell fate, rather than increased proliferation of wing vein cells, suggesting that Chmp1 promotes intervein cell fate over vein cell fate. Supporting this conclusion, the number of intervein cells between the thickened veins on a *Chmp1* knockdown wing appeared reduced, suggesting a change in cell fate, rather than over-growth of vein cells. A cell fate change associated with loss of Chmp1 has not been reported previously in animal studies, although in *Zea mays* loss of *Chmp1* caused extra layers of aleurone cells to form [92]. This phenotype was likely caused by increased specification of aleurone cells from endosperm, driven by failure to down-regulate transmembrane receptors through the MVB pathway [92, 93].

The finding that *Chmp1* regulates cell fate in plants is consistent with the finding that *Chmp1* regulates wing vein cell fate in flies, and suggests a conserved role for *Chmp1* in regulating cell fate decisions.

III. *Chmp1* and DER signaling

DER signaling is required to promote wing vein development. Loss of DER signaling causes loss of wing veins and gain of DER signaling causes wing vein thickening and formation of extra wing veins [17, 36]. So it was possible that the thick veins observed with *Chmp1* knockdown could be caused by a gain of DER signaling. This would mean that *Chmp1* negatively regulates DER signaling. This is consistent with previous reports showing that other ESCRT components are required for down-regulation of DER signaling [59, 137].

Genetic interactions between *Chmp1* and regulators of the DER signaling suggest a role for *Chmp1* in the regulation of the DER. Reduced activity of negative regulators of DER signaling in *Chmp1* knockdown wings enhanced the *Chmp1* knockdown phenotype. Additionally, reducing the expression of *Vn*, a positive regulator of DER signaling, in *Chmp1* knockdown wings partially suppressed the *Chmp1* knockdown phenotype. This finding showed that loss of *Vn* activity caused a loss of DER activation that partially counter-acted the gain in DER activation caused by *Chmp1* knockdown. Interestingly, the *Chmp1* knockdown phenotype was not suppressed by decreased activity of *Rho*, another positive regulator of DER signaling. A genetic interaction between *Chmp1* and *Vn* but not *Rho* is surprising, especially as *Vn* and *Rho* appear to have synergistic roles in the wing [121, 122, 138]. This may be explained by considering the functional roles of *Vn* and *Rho* in DER signaling. *Vn* is a ligand secreted by intervein tissue that directly binds and activates the DER, while *Rho* is a membrane bound protease that cleaves and activates the DER ligands, *Spitz* and *Keren*. *Spitz* and *Keren* act

redundantly in the wing and only loss of activity of both alters wing vein patterning [15, 139]. Perhaps losing one copy of *rho* does not affect levels of DER activation even when *Chmp1* is reduced, as there is still enough Rho protein to cleave and activate the Spitz and Keren ligands. Since Rho is an enzyme, it most likely can repeatedly cleave substrate. In contrast Vn is not reused. Additionally, it is thought that Vn provides a low, constant activation of the DER, while Rho is a strong DER activator [17, 140]. Thus, reducing the activity of Rho would have less effect on DER signaling than reducing the activity of Vn. Another possibility is that there is a different timing requirement for Vn and Rho during wing development. An interaction between *Chmp1* knockdown and Vn, rather than Rho could indicate a later requirement for Vn than Rho in the final determination of vein fate [15, 138]. However, since Rho is required late into wing morphogenesis, this appears unlikely [17].

Loss of MAPK activity caused by altered activity of a single regulator of DER signaling usually does not result in a vein-less wing. Instead, only portions of veins are lost, suggesting that regulation of DER signaling in vein formation differs in different parts of the wing. Over-expression of the negative DER regulator *aos* causes loss of the distal portions of the L4 and L5 wing veins due to loss of DER signaling in these regions. Interestingly, when *Chmp1* was knocked down dorsally in wings over-expressing *aos*, the distal L4 and L5 were still lost, but the remaining wing veins were thickened. Although *Chmp1* knockdown caused thickening of the wing veins, it appeared that *Chmp1* knockdown could not reverse the loss of vein cell fate specification caused by *aos* over-expression. This finding is consistent with a model in which *Chmp1* regulates DER signaling downstream of receptor activation and may suggest that *Aos* can no longer inhibit DER signaling in vein cell specification beyond a certain time point during development. After this time, loss of *Chmp1* could still activate DER signaling, but *Aos* would

no longer be able to down-regulate the DER. The idea of a switch in DER signaling during wing development is supported by previous studies. For example, over-expression of *aos* at different times during wing development has different phenotypic effects. *Argos* over-expression during the pupal stage of development causes extra veins to form, while over-expression during larval stages causes vein suppression [138]. Similarly, DER signaling promotes vein specification and is active in the wing veins throughout most of wing development. However, from about 28 to 33 hours after pupal formation (hAPF), MAPK activity, an indicator of DER signaling, is lost in the veins and increased in the intervein [138, 141, 142]. The importance of this event and its implications for wing development are not well understood. It has been proposed that DER activation is required to allow for maintenance of Dpp signaling in the vein, which is required for wing vein differentiation, but that the late shift of DER signaling to the intervein is required for the specification of intervein fates [138, 143].

To quantify the ability of the regulators of DER to modify the *Chmp1* knockdown phenotype, wing vein areas were measured. The area of wing veins was much more variable in the wings with *Chmp1* knockdown and altered DER activity compared to *Chmp1* knockdown alone. In *Chmp1* knockdown wings that were also heterozygous for loss of function alleles of DER regulators, small numbers of wings measured had wing vein areas that were comparable to those of *Chmp1* knockdown alone, while others were well above *Chmp1* knockdown measurements. This variability may have been caused by fluctuations in temperature during fly development. As *Chmp1* knockdown was driven with the UAS-Gal4 system, the *Chmp1* knockdown phenotype was sensitive to temperature. In some cases, a developmental temperature of two degrees (from 28°C to 30°C) was a difference between wings with slightly wider wing veins and wings that were almost entirely wing vein. Minor fluctuations in temperature within

the incubator in which the flies were grown could contribute to the differences observed. Also, though the wings measured were all from flies of the same known genotype, there may be variation in the genetic background between individual flies that results in differences in gene expression. Therefore, individual flies may experience different levels of *Chmp1* knockdown in the wing that was not apparent from the *Chmp1* knockdown phenotype, but is amplified in a different genetic background. Nevertheless, for each genotype, the mean wing vein area was a good representation of the wing vein thickness that was generally observed. Additionally, reduction of all DER suppressors tested enhanced the *Chmp1* knockdown phenotype, whereas reduction of DER enhancers either suppressed or did not significantly alter the *Chmp1* phenotype. The consistent directionality of the interactions between DER regulators and *Chmp1* is good evidence that *Chmp1* negatively regulates DER signaling.

Interestingly, no interaction was detected between *Chmp1* and DER regulators when *Chmp1* was over-expressed in wings heterozygous for loss of function alleles of positive or negative regulators of DER signaling. In light of the *Chmp1* knockdown studies, this may suggest that excessive *Chmp1* protein in the cell has little or no effect on DER signaling during wing vein development. *Chmp1* knockdown, but not *Chmp1* over-expression, results in phenotypes in the fly, showing that while the cell does require *Chmp1* for proper function and signaling, an over-abundance of *Chmp1* does not significantly alter cellular function. This could offer support for *Drosophila Chmp1* as a component of the ESCRT complex when regulating DER signaling, rather than acting directly as a regulator of gene expression. It also suggests that *Chmp1* is not a limiting component of ESCRT function.

Studies in mammalian cell culture show that *Chmp1* regulates cell growth [88, 89, 91]. In contrast, the studies presented here did not indicate a role for *Drosophila Chmp1* regulation of

growth, but rather in regulation of DER signaling in cell fate specification. However, human pancreatic [89] and renal [88] tumor cells show a loss of Chmp1A activity, and a gain of EGFR signaling is often observed in cancerous cells [144-146]. So it is possible that an increase in EGFR signaling caused by loss of Chmp1A activity could contribute to tumorigenesis. Therefore, the *Drosophila* wing may provide a good model for assaying the activity of ESCRT components to better understand their role in tumor formation.

IV. Clones of *Chmp1* knockdown in the wing

Chmp1 interacted genetically with DER signaling components, suggesting that Chmp1 negatively regulates DER signaling. If Chmp1 negatively regulates DER signaling, downstream targets of the DER should be affected by loss of Chmp1 activity. Clones of *Chmp1* knockdown were generated in the developing wing to assess the effect of *Chmp1* knockdown on expression of Bs, which is negatively regulated by DER signaling. Unexpectedly, small clones of *Chmp1* knockdown in the third instar wing disc had no effect on Bs expression. However, Bs expression was decreased in large clones (>120 cells) that spanned wing vein and intervein regions. Large clones of *Chmp1* knockdown were rare, which may mean that *Chmp1* knockdown clones were unhealthy and died or grew slowly when generated early in wing development. If this is the case, it would suggest that Chmp1 is required for proper cellular function in *Drosophila* wings in addition to its role in DER signaling. Another possible explanation for seeing few large clones is cell competition. In the wing, cells of a specific genotype may not survive as wing clones, even though they can make a perfectly formed wing by themselves, as they are “out-competed” by surrounding wild-type cells [147]. *Chmp1* knockdown clones in the wing may be out-competed and thus rare in the developing wing.

Clones of *Chmp1* knockdown were also generated for analysis in the adult wing. In the majority of *Chmp1* knockdown clones located within intervein regions, clusters of cells within the clone adopted vein cell fate. On the other hand, some clones within intervein tissue had no effect on wing cell fate. When *Chmp1* knockdown clones overlapped wing veins, thickening of the wing vein occurred, though the wing vein thickness was only increased by a few cells' width, similar to knockdown in the entire wing, and not throughout the entire clone. Thus, not every *Chmp1* knockdown cell adopts a vein fate. This suggests that other factors, such as the location of the clone within the wing, are involved in determining vein or intervein cell fate in *Chmp1* knockdown clones. However, there is still the question of why intervein cells can adopt a vein fate in *Chmp1* knockdown clones but not when *Chmp1* knockdown is driven with *MS1096-Gal4* and other drivers. It could just be a case of stronger knockdown of *Chmp1* in the clones than with drivers. For example, the FLP/FRT-Gal4 system uses an *actin* promoter to drive expression of Gal4 constantly and at a fairly high rate. In contrast, promoters of developmental genes, such as *engrailed* (*en-Gal4*) and *patched* (*ptc-Gal4*), may have variable expression over time or stop expressing early.

If *Chmp1* acted upstream of the DER signaling pathway, by either directly repressing or activating the DER or one of its regulators, *Chmp1* knockdown clones might have induced vein cell fate regardless of their location on the wing. However, this was not the case. Instead, receptor deregulation caused by loss of *Chmp1* may just alter the balance of signaling between pathways involved in vein specification, i.e., the DER signaling pathway, making a cell more likely to adopt a vein fate. This is consistent with a role for *Chmp1* downstream of the DER, suggesting that *Chmp1* knockdown does not in itself activate DER signaling. Rather, *Chmp1* regulates the active DER signaling pathway. If the DER is not activated, then presumably loss of

Chmp1 can have no effect on the DER signal. However, when the DER is active loss of Chmp1 might boost the signal to a level that induces vein formation in the wing.

V. Chmp1 and Notch signaling

In these studies, experiments using *Chmp1* knockdown to investigate Chmp1 regulation of Notch signaling were inconclusive. No strong evidence for Chmp1 as a regulator of Notch signaling was obtained. However, a possible minor genetic interaction was observed between Chmp1 and the Notch regulator, Deltex. When *Chmp1* was knocked down in a wing over-expressing Deltex, a minor but consistent loss of wing bristle was observed in the wing.

Transgenic fly lines were created that allowed for expression of either a wild-type or HM-tagged Chmp1 protein, enabling investigation into the effects of *Chmp1* over-expression, as well as Chmp1 protein localization. All of these lines expressed an active Chmp1 protein, as they were able to partially or fully rescue the *Chmp1* knockdown phenotype. *Chmp1* over-expression in the wing resulted in widening of the distal tip of the wing vein, or deltas, suggesting that Chmp1 may regulate Notch signaling. Wing vein deltas are also observed when activity of the Notch ligand, Delta, is lost. Although this effect was weak, it is consistent with previous literature showing that ESCRT machinery regulates Notch signaling. For example, in a genome-wide study to identify modifiers of Notch signaling in *Drosophila*, Chmp1 was identified as a possible negative regulator of Notch [115]. *Chmp1* knockdown with an RNAi line from the VDRC in the thorax caused notum migration malformation, which was likely due to upregulation of Notch signaling [115]. Additionally, loss of *Drosophila* ESCRT-II component Vps25 caused endosomal accumulation of the Notch receptor and enhanced Notch signaling [61].

If Chmp1 negatively regulated Notch signaling in *Drosophila*, then *Chmp1* over-expression in the wing might cause reduced Notch signaling, which could result in the deltas

observed. One possible explanation for this finding is that *Chmp1* over-expression caused increased processing of Notch into the ILV. This would imply that Notch normally signals after it has been endocytosed, which is consistent with previous studies showing that the Notch Intracellular Domain is cleaved at the endosome. The deltas observed under *Chmp1* over-expression could also be caused defects in the processing of Delta, rather than Notch. Delta, as well as other Notch ligands, requires monoubiquitination and endocytosis, followed by either degradation or recycling back to the membrane for proper activity [148].

If Chmp1 negatively regulates Notch signaling, then loss of Chmp1 activity should increase Notch signaling. In the wing, phenotypes associated with increased Notch activity could include loss of wing veins, or ectopic wing margin and bristles. These phenotypes were not apparent when *Chmp1* was knocked down in the wing, suggesting that Notch activity is not increased. However, the findings presented here do not rule out a role for Chmp1 in regulation of Notch signaling. It is possible that Chmp1 regulates Notch signaling during wing development, but *Chmp1* knockdown conditions were not sufficient to generate a Notch-related phenotype.

VI. HM-Chmp1 localization

In the light of previous literature, it seems likely that the regulation of DER signaling by Chmp1 is a result of its activity in MVB generation as a part of the ESCRT-III complex. This would place Chmp1 at the endosome, which has been verified in mammalian cultured cells, Arabidopsis, and yeast [86, 93, 97]. The HM-tagged version of *Drosophila* Chmp1 is active and localized to the apical plasma membrane. Similar localization was observed in both embryonic and imaginal disc epithelial cells, and with several independent *UAS-HM-Chmp1* fly lines, suggesting that it is the genuine subcellular localization for HM-Chmp1. When comparing the subcellular localization of Chmp1 across published studies, it becomes apparent that Chmp1

localization varies between cell types [91, 95, 97]. However, the membrane localization observed for HM-Chmp1 is similar to the localization observed for Chmp1A observed in mouse acinar pancreatic tumor cells (CRL-2151) in a paper published on the effects of all-trans retinoic acid (ATRA) and Chmp1A in pancreatic tumor cells [95].

Co-localization was not observed between HM-Chmp1 and the early endosome marker, Rab5. However, HM-Chmp1 did show some co-localization with a late endosomal marker, Rab9. This suggests that a proportion of Chmp1 localizes to the late endosome, but not to the early endosome in *Drosophila*. This contrasts with reports that Chmp1 was detected at both early and late endosomes in *Aspergillus nidulans* and mammalian cell culture [86, 97]. However, the late endosomal localization of Chmp1 is supported by studies in yeast, showing that ESCRT-III components are only present on the endosomal membrane late in MVB biogenesis [72, 73]. The localization of *Drosophila* Chmp1 to the late endosome is compatible with a role for Chmp1 in MVB biogenesis, and supports the idea that this is the mechanism for down-regulating the DER.

There is published evidence supporting a role for ESCRT function in the nucleus. For example, in cultured human cells the ESCRT-I component Tsg101 has been reported to repress the cyclin-dependent kinase p21 by directly binding its promoter [149]. Tsg101 may also act as a cofactor in regulating gene expression in cultured mammalian cells [150, 151]. Several studies report a role for Chmp1 in the nucleus, and the few mechanistic studies on Chmp1 pin the effects observed under *Chmp1* mis-expression to its nuclear function. [90, 91, 95]. Though Chmp1 was not detected via immunostaining in the nucleus of the *Drosophila* tissues investigated here, the conservation of the NLS suggests that *Drosophila* Chmp1 may play a role in the nucleus. Other studies in mammalian cultured cells have reported that Chmp1 may not always be present in the nucleus, as it is only detectable at specific phases of the cell cycle, or upon certain cell treatments

[81, 90, 95]. Thus it is possible that the nuclear localization of *Drosophila* Chmp1 was not detected because it is transient. Chmp1 appears to recruit BMI1 to condensed chromatin in the nucleus of cultured human cells [81, 91]. This is interesting because BMI1 can work as a part of PRC1, a protein complex which maintains a transcriptional repressive state in many genes by mediating monoubiquitination of histone H2A-K119 [152]. As ESCRTs 0-II can recognize monoubiquitinated proteins, this may explain the presence of ESCRTs in the nucleus. Despite these findings, there is no well established role for ESCRTs in the nucleus. All characterized roles for the ESCRT machinery involve the scission of membranes, but this activity does not explain the localization of Chmp1 to condensed chromatin or its interaction with BMI1. It is possible that the role of Chmp1 in the nucleus is independent of the ESCRT-III complex, or that the ESCRT complexes play a role in the nucleus that has not yet been described. As the role of Tsg101 in the nucleus has not been linked with other ESCRT components or known functions of ESCRTS, it may well be independent from the well-established ESCRT activities.

Co-immunoprecipitation and mass spectroscopy experiments have identified many binding partners for *Drosophila* Chmp1, several of which are regulators of gene expression at the level of translation [2]. In addition, ESCRT-II components interact with ELL proteins, which are elongation factors for RNA polymerase II [153]. Chmp1 may also be involved in the maintenance of chromosome integrity during mitosis [100]. Together, these results suggest diverse functions for ESCRT proteins, many of which are not well characterized. So it remains possible that Chmp1 regulates DER signaling in other ways, in addition to receptor down-regulation through the MVB pathway.

VII. Concluding remarks

When *Chmp1* was knocked down in the *Drosophila* wing, the DER was deregulated, causing wing cells to adopt a vein over an intervein fate. A role for Chmp1 determining in cell fate specification through receptor down-regulation is consistent with the function of Chmp1 in the ESCRT-III complex. Chmp1 binds Vps4, which completes ILV formation at the MVB. If loss of Chmp1 function caused incomplete ILV formation, this might result in retention of transmembrane receptors in the limiting membrane of the endosome, rather than incorporation into the ILV (Figure 5.1). Indeed, in *Arabidopsis thaliana*, *Chmp1* mutation resulted in the presence of membrane proteins in the limiting membrane of the MVB and vacuole [87]. Additionally, in mammalian cultured cells knockdown of UBPY, a binding partner of Chmp1, caused accumulation of the EGFR on endosomes [108]. Loss of ESCRT-III component activity in *Drosophila* also impaired ILV formation [137]. Therefore, the increased DER signaling observed in *Chmp1* knockdown wings may be a consequence of incomplete ILV formation, resulting in a failure to isolate the DER from the cytoplasm and retention of the DER in the limiting membrane of the endosome, where it continues to signal.

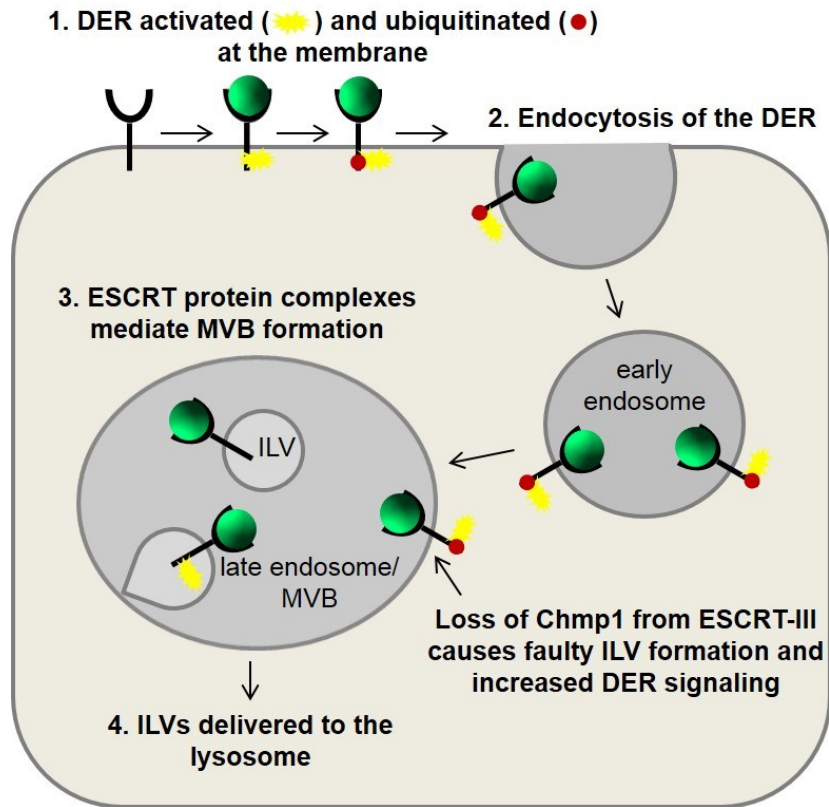


Figure 5.1 Model for Chmp1 regulation of the DER through the MVB pathway. 1.

Activating ligand binds to the extracellular domain of the DER. This activates the DER, which transmits the signal to the cell through the MAPK pathway. The activated DER is ubiquitinated. 2. Ubiquitination of the DER signals endocytosis of the activated receptor. 3. The ESCRT protein complexes normally mediate incorporation of the DER into ILVs of the MVB. 4. The ILVs containing the DER are delivered to the lysosome, where the DER is degraded. Loss of Chmp1 from the ESCRT-III complex causes incomplete scission of the neck of the ILV and causes the DER to accumulate in the limiting membrane of the MVB, so the receptor is still able to signal to the cytoplasm.

VIII. Possible future studies

ESCRT components have been shown to regulate several pathways in *Drosophila*. Investigations into Chmp1 regulation of other pathways in other tissues could be informative. This could be tested similarly to DER signaling components. For example, *Chmp1* could be knocked down in wings heterozygous for regulators of other pathways, such as Dpp or Hh. Additionally, the work on Chmp1 in the eye could be expanded. *Chmp1* knockdown in the eye

caused loss of photoreceptors. This phenotype could be investigated at earlier stages. For example, in the third instar eye imaginal disc immunostaining can be used to identify at what stage the specific photoreceptors are lost during eye development. Additionally, genetic interactions with DER, Notch, and other pathways in the eye could be investigated.

Further testing for interactions between Chmp1 and proteins involved in endocytosis, such as clathrin, could link Chmp1 to its role in the MVB pathway more firmly. For example, *Chmp1* could be knocked down in flies carrying loss of function alleles for proteins involved in endocytosis that have no wing phenotype in the heterozygous state. If the *Chmp1* knockdown phenotype is enhanced in these different genetic backgrounds, then a role for Chmp1 in endosomal trafficking in the wing would be supported.

Chmp1 co-localized with Rab9, a marker for the late endosome. This suggests that Chmp1 functions at the late endosome, probably as a component of the ESCRT-III complex in MVB generation. A next step in Chmp1 research would be tracking the endocytosis of signaling receptors, including the DER or Notch receptor, under *Chmp1* knockdown or over-expression conditions. If *Chmp1* knockdown caused accumulation of the DER or Notch in the endosomal membrane, as identified by co-localization with an endosomal marker, then a role for Chmp1 in regulating these pathways through the MVB pathway would be better supported.

Though no nuclear Chmp1 localization was detected in epithelial cells of the *Drosophila* embryo or imaginal disc, there have been multiple studies showing a nuclear localization and suggesting a nuclear function for Chmp1 [81, 89-91]. In cultured mammalian cells, nuclear Chmp1 was detected at specific stages of the cell cycle or upon certain cell treatments [81, 90, 95]. So it is possible that Chmp1 does localize to the nucleus in *Drosophila* cells, but that it just was not detected. If Chmp1 localizes to the nucleus at specific times during the cell cycle, then it

might be detected in the nucleus upon imaging of live cells, or fixed synchronized cells in culture. Investigation of Chmp1 localization in live cells, e.g., in a cultured imaginal disc, would require the generation of a transgenic fly line that could express fluorescently tagged Chmp1 protein. This would allow live imaging of Chmp1 localization in *Drosophila* tissues.

Unfortunately, fluorescent tags are often large, and there is always the possibility of interference of the tag with the function of the protein. Alternatively, Chmp1 localization could be investigated cultured S2 cells (*Drosophila* cell line), which would allow for synchronization of the cell cycle and observation of Chmp1 localization in fixed cells using a smaller epitope tag on the Chmp1 protein. However, much of the power of using *Drosophila* in the lab is the ease of genetics and the ability to study the tissues of an entire organism. So moving to insect cell culture might be considered a step backwards.

Creation of a *Drosophila*-specific Chmp1 antibody, along with *Chmp1* mutants, would be useful in further studies with Chmp1. Different mutations could be generated to investigate which functional domains or regions of the Chmp1 protein are required for proper function/regulation of DER signaling, and signaling of other pathways in *Drosophila*. Generation of a *Chmp1* mutant with the NLS deleted could be informative about any nuclear function for Chmp1 in *Drosophila*. Additionally, it could be interesting to create a transgenic fly line that allows for expression of Chmp1 from a different species, such as humans. If human Chmp1A could rescue a *Chmp1* mutant phenotype, that would imply that the functions are highly conserved and the findings in *Drosophila* are transferrable.

Clones of *Chmp1* knockdown occasionally caused a cell fate change from intervein to vein cell in the adult wing. Additionally, clones of *Chmp1* knockdown caused an increase in DER signaling and a decrease in Bs expression. However, Chmp1 knockdown did not always

have an effect on Bs expression. Large clones of *Chmp1* knockdown were required to see a change in Bs expression in the wing disc, despite the fact that small clones of *Chmp1* knockdown could generate vein in the adult wing. A more direct readout of DER pathway activation is phosphorylation of ERK. Additionally, Rho expression is indicator of DER activation. In the developing wing, one of the first markers of wing vein cells is Rho expression. So it would be informative to generate clones of *Chmp1* knockdown in the wing disc to see if ERK is phosphorylated in any of the clone cells, or if Rho expression was activated. This would offer more definitive evidence for a role for *Chmp1* in regulation of DER signaling.

The studies presented in this dissertation suggest that the choice of vein or intervein cell fate in the *Drosophila* wing is a good model for investigating the activity of ESCRT components. Thus, the activity of other ESCRT components in regulation of cell signaling pathways involved in vein patterning could be investigated in the wing. Many of the interactions of ESCRT components have only been suggested through biochemical assays. Therefore, genetic interaction studies similar to those used in these studies could be used to establish functional interactions between these pathways/proteins. Genetic screens involving ESCRT components could identify which components are required for ESCRT function in pathways involved in vein development.

CHAPTER 6

PROJECTS INVESTIGATING FRIZZLED (FZ) PLANAR CELL POLARITY (PCP)

SIGNALING IN DROSOPHILA

In addition to DER and Notch signaling, Chmp1 may regulate the Frizzled (Fz) Planar Cell Polarity (PCP) pathway. Investigations of Chmp1 in Fz PCP signaling, as well as contributions made to other Fz PCP signaling projects, are discussed in this chapter.

I. Background on PCP

Cell polarity is established by an asymmetrical distribution of contents within a cell and is critical for cellular specification and diversity. One example of cell polarity is the polarization of epithelial tissues on the apical-basal axis, which gives cells a top and a bottom. However, cells that make up epithelial tissues are not only polarized on the apical-basal axis, but also within the plane of the epithelium. This type of polarity is called PCP. The Fz PCP pathway controls PCP and was first identified for its role in patterning the fruit fly cuticle. It is conserved in vertebrates where it is referred to as a non-canonical Wnt signaling pathway [154, 155]. The Fz PCP pathway is also involved in cell fate specification, as well as cell migration events, including convergent extension movements during gastrulation and neurulation in vertebrates [3, 156]. Mutations in human Fz PCP pathway genes have been linked to neural tube defects such as anencephaly and spina bifida, and also with epileptic seizures [157-161]. Additionally, in humans and mice, defects in Fz PCP have been linked to some cystic kidney diseases, likely related to defects in ciliogenesis [155, 162-166].

Despite the importance of the Fz PCP pathway in human development and disease, it is still incompletely understood. From studies in *Drosophila*, it is known that within each epithelial cell, six Core Fz PCP pathway proteins, Fz, Dishevelled (Dsh), Diego (Dgo), Flamingo (Fmi,

also known as Starry-night, Stan), Strabismus (Stbm, also known as Van-gogh, Vang), and Prickle (Pk), must undergo a series of specific interactions and become asymmetrically localized in order to establish proper PCP. Although much is known about the interactions and subcellular localizations of these proteins, there is no consensus on a global signal that initiates Core PCP protein localization within the cell, how the Core PCP proteins interpret that signal, or how the signal is transduced. The Fz PCP pathway has been best studied in the fruit fly, which provides an easily manipulatable system in which to study this pathway. In these studies, the eye and wing were used to investigate Fz PCP signaling.

II. The Fz PCP pathway in the *Drosophila* wing

With respect to Fz PCP signaling, the wing is the most widely used and best characterized epithelial tissue of the fly (see Chapter 1 section I.B for details on wing development and anatomy). The developing fly wing is composed of an epithelial cell layer of hexagonally packed cells. Each wing cell produces a single distally-pointing wing hair, resulting in an adult wing decorated with a regular array of hairs. Traditionally, the study of PCP in the wing focuses on the formation and polarity of these hairs. Determining the initiation site of hair formation, as well as the number of hairs produced within a cell, are processes that require the proteins of the Fz PCP pathway [167-169]. During the pupal stage of wing development, within each epithelial cell the Fz PCP Core proteins localize apically in the adherens junction (AJ) plane and asymmetrically to the proximal and distal ends of each epithelial cell [170] (Figure 6.1A). Fz, Dsh and Dgo localize to the distal edges of the cell, Stbm and Pk localize to the proximal edges, and Fmi localizes to both proximal and distal edges. The apical and lateral localizations are both crucial for proper PCP, as failure to appropriately localize all six Core PCP proteins results in PCP defects, such as altered hair initiation site, altered hair polarity, and cells carrying

multiple hairs [171-176]. There is no consensus on what global signal initiates the asymmetric localization of Fz PCP pathway components within wing cells and establishes direction in the tissue. One candidate is a group of proteins, including the atypical protocadherins Fat (Ft) and Dachshous (Ds), gradients of which have been proposed to provide a global signal for Fz PCP protein localization and so direct wing cell polarity. This idea is supported by evidence that Ft and Ds play a role in microtubule orientation, and that the subcellular localization of the Core proteins depends upon microtubule-based transport of Fz to the distal end of the cell [173, 177].

Wnts, extracellular proteins that transmit signals into the cell through Frizzled family receptors, have also been proposed as a global cue for establishing polarity. In vertebrates, loss of Wnts can cause PCP defects suggesting that Wnts are involved in Fz PCP [178-180]. In flies evidence for Wnts as a directional cue for Fz PCP signaling is lacking, though recent work suggests Wingless (Wg) and Wnt4 may act redundantly in the wing to establish proper PCP [181-183]. In the wing, the localization of Fz PCP pathway components is correlated with cytoskeletal reorganization and the distal formation of an actin rich hair. It is thought that the position of Fz within the cell is the main determinant of where a wing hair forms, i.e., Fz localizes distally and the wing hair forms at the distal end of the cell [174]. However, the mechanisms by which this occurs are unknown.

III. The Fz PCP pathway in the *Drosophila* eye

In addition to DER signaling, development of the *Drosophila* eye also requires Fz PCP signaling, but in this case it controls a cell fate specification event that is critical for patterning of the eye [3]. The fly eye is a complex structure composed of about 800 ommatidia. The organization of photoreceptors within each ommatidia has a chirality, or handedness, which differs between ommatidia in the dorsal and ventral halves of the eye. This means that ventral

ommatidia are a mirror image of dorsal ommatidia (see Chapter 1 section I.C for eye development and anatomy). Fz PCP signaling is involved in the establishment of the chirality, or handedness of each ommatidium, by specifying which photoreceptors become the R3 and R4 cells (Figure 6.1B). Fz PCP signaling also directs the direction of ommatidial rotation, as the specification of R3 and R4 photoreceptors largely determines the direction of rotation. The R3/R4 precursor cells can differentiate into either R3 or R4. The Fz PCP pathway signals from the future R3 photoreceptor through Fz to Stbm in the future R4 photoreceptor. Fz becomes active and signals from the R3/R4 precursor closest to the equator, which becomes committed to an R3 fate, while the other precursor closer to the pole of the eye adopts the R4 fate. Downstream targets of the Fz PCP pathway drive and reinforce the cell fate decision. For example, Fz signaling promotes Delta activity in future R3 photoreceptors and results in activation of Notch in the future R4 photoreceptors [24, 25]. Thereby the Fz PCP pathway establishes the proper chirality of each ommatidium, as well as the correct direction of rotation. When Fz PCP signaling is disrupted in the eye, resulting phenotypes may include achiral, or symmetric ommatidia, in which the R3 and R4 photoreceptors become either both R3 or both R4, misrotation, in which the ommatidia do not rotate the full 90°, and opposite chirality, in which a ventral ommatidium adopts a dorsal chirality or vice versa.

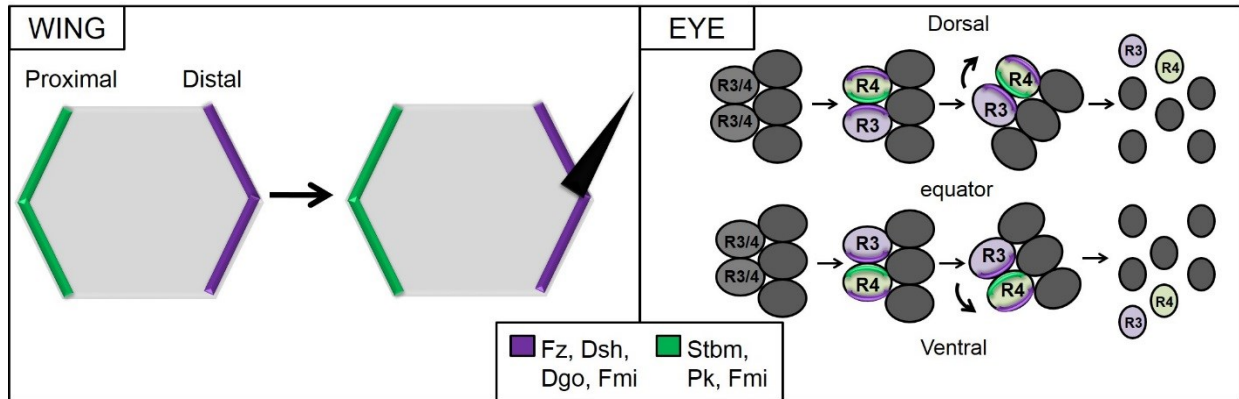


Figure 6.1 The Fz PCP pathway polarizes cells of the *Drosophila* wing and eye. In the wing (left panel), Fz PCP core proteins localize to opposite ends of each cell, polarizing the cell. The wing hair is produced at the distal end of the cell. In the eye (right panel), Fz PCP core proteins localize to the apical membrane bordering the R3 and R4 cell precursors. This leads to the specification of R3 and R4 cells and proper ommatidial rotation within each hemisphere of the eye.

Project 1: Chmp1 may regulate Fz PCP signaling

Introduction: As a component of the ESCRT-III complex, Chmp1 is involved in the regulation of many cellular signaling pathways and processes. Some Fz PCP core proteins undergo endocytosis during signaling, so they may require the ESCRT machinery for proper regulation of signaling [184]. When Fz PCP signaling is disrupted in the wing, classic PCP phenotypes result (i.e., cells carrying multiple hairs, altered hair polarity). Therefore, to determine whether Chmp1 regulates Fz PCP signaling, *Chmp1* was knocked down and over-expressed in the wing. Indeed, *Chmp1* knockdown and over-expression lead to defects in PCP, suggesting that Chmp1 regulates Fz PCP signaling.

Methods: Fly crosses for *Chmp1* knockdown and over-expression are described in Chapter 4, Figures 4.3 and 4.18 respectively. To test for interactions between Chmp1 and Fz PCP signaling components, *Chmp1* was also knocked down in wings heterozygous for loss of function alleles of Fz PCP Core genes, *fz* (fz^{P21}), *stbm* (*Vang^l*), and *pk* ($pk^{pk-sple14}$). Wings from

females with *Chmp1* knockdown, and *Chmp1* knockdown in a background heterozygous for loss of function alleles of Fz PCP genes were mounted in GMM onto a glass slide and imaged with a light microscope.

Results and Discussion: Ubiquitous knockdown of *Chmp1* in the dorsal wing under the control of the *MS1096-Gal4* driver caused thickening of dorsal wing veins (Figures 4.3 and 4.7), but gave no classical Fz PCP phenotypes, e.g., altered hair polarity or cells carrying multiple hairs. However, localized *Chmp1* knockdown caused Fz PCP phenotypes at the boundary of *Chmp1* knockdown and wild-type cells. *Chmp1* knockdown in the posterior wing under the control of the *en-Gal4* driver caused the expected thickening of posterior wing veins (L4 and L5) (Figures 4.4 and 6.2B). Additionally, wings cells carrying multiple hairs were observed adjacent to the anteroposterior (AP) boundary of these wings, which was also the boundary of *Chmp1* knockdown (Figure 6.2B). The wing hairs in this region adopted an anterior rather than a distal hair polarity, while the wing hairs in the rest of the wing remained wild-type (Figure 6.2B). When *Chmp1* was knocked down with *ptc-Gal4*, which has both anterior and posterior boundaries of expression (Figure 4.4), altered hair polarity and additional hairs were again observed at the boundaries of *Chmp1* knockdown and wild-type cells (Figure 6.2C). At the anterior boundary of *ptc-Gal4* expression wing hairs took on an anterior polarity, and at the posterior boundary of *ptc-Gal4* expression wing hairs adopted a posterior polarity. These results indicate that the Fz PCP pathway may have been disrupted, and suggests a possible role for *Chmp1* in regulation of Fz PCP signaling. It seems that a gradient of *Chmp1* activity was required to disrupt wing hair patterning, as the phenotypes were only observed at the boundaries of *Chmp1* knockdown.

The Fz PCP signaling pathway involves cell-to-cell signaling of asymmetrically localized transmembrane proteins. A gradient of *Chmp1* activity may have created a gradient of Fz PCP Core protein activity, possibly due to reduced down-regulation of Fz through the MVB pathway, which would alter cell-cell signaling of Fz PCP components. This could explain why the wing hair defects were only observed at the boundary of knockdown in the wing. A boundary/gradient of *Chmp1* knockdown would not exist in the remaining wing, which kept a wild-type hair polarity. If loss of *Chmp1* activity cause retention of Fz PCP Core proteins in the limiting membrane of the late endosome/MVB, it is possible that the localizations of Fz PCP Core proteins could be changed.

When *Chmp1* was knocked down in a localized pattern, wing hair polarity was reoriented away from the *Chmp1* knockdown region, suggesting that wing hairs point away from low *Chmp1* activity (Figure 6.2B and C). Interestingly, wing hairs point away from low *Stbm* and towards low Fz activity, suggesting a possible role for *Chmp1* in regulation of these proteins [185, 186]. Specifically, *Chmp1* knockdown might cause either low *Stbm* or enhanced Fz activity.

To investigate a role for *Chmp1* in Fz PCP further, *Chmp1* was knocked down in wings heterozygous for loss of function alleles of *fz* (*fz^{P21}*), *stbm* (*vang^{TBS42}*), and *pk* (*pk^{pk-sple14}*). Wings heterozygous for these Fz PCP loss of function alleles appear wild-type, apart from weak hair polarity changes in the proximal part of the wing in *vang^{TBS42}* wings. As previously shown, uniform knockdown of *Chmp1* with *MS1096-Gal4* caused thickened wing veins but no classic Fz PCP phenotypes (Figure 4.7B). However, uniform knockdown of *Chmp1* with *MS1096-Gal4* in *vang^{TBS42}* heterozygous wings caused hair polarity defects as well as multiple hairs (Figure 6.2D). In these wings the PCP defects were mostly observed around thickened wing veins, and

reoriented hairs pointed away from the thickened wing veins. As wing hairs usually point away from low levels of Stbm, this suggests that there is loss of Stbm activity in the thickened wing veins compared to the intervein tissue. This effect was specific for Stbm, as uniform *Chmp1* knockdown in *fz^{P21}* (*MS1096-Gal4/X; UAS-Chmp1RNAi-VDRC/+; fz^{P21}/+*) or *pk^{pk-sple14}* (*MS1096-Gal4; UAS-Chmp1RNAi-VDRC/pk^{pk-sple14}*) heterozygous wings did not cause any significant PCP phenotypes.

An interaction with Stbm and not Fz was surprising, considering that Fz is endocytosed and degraded during signaling, a process that should be affected by loss of ESCRT activity [184]. The specificity of the phenotype to thickened wing veins could suggest that in a *Chmp1* knockdown wing, vein cells are more sensitive to loss of Stbm activity than the remaining wing. However, if loss of *Chmp1* in the wing disrupts the role of the ESCRT-III complex in protein degradation, then heightened Stbm activity due to decreased down-regulation might be expected. Loss of Stbm activity is also possible though, as investigations with ESCRT components have shown that the ESCRT complexes may both positively and negatively regulate signaling pathways, depending upon the context of signaling [187]. More likely, these results suggest an interaction between Stbm and DER signaling in wing development. Results from Chapter 4 indicated that *Chmp1* may negatively regulate DER signaling, which is active in the wing vein. Perhaps there is crosstalk between the DER and Fz PCP signaling pathways during wing development. In fact, both DER and Notch signaling pathways interact with the Fz PCP signaling pathway during eye development [24, 25, 133, 188].

Over-expression of *Chmp1* also caused occasional wing hair phenotypes, including minor hair polarity changes and additional wing hairs, which provides further support of a role for *Chmp1* in regulating Fz PCP signaling. Though a gradient of *Chmp1* knockdown was required to

cause wing hair defects, uniform *Chmp1* over-expression on the dorsal wing with *MS1096-Gal4* was sufficient to cause wing hair phenotypes (Figures 4.18 and 6.2A). The difference in vein phenotypes observed from *Chmp1* knockdown and over-expression suggest that loss of Chmp1 activity has different effects on cellular signaling pathways than *Chmp1* over-expression. This would mean that if *Chmp1* knockdown phenotypes are due to faulty ESCRT function and incomplete MVB generation, then the *Chmp1* over-expression phenotypes may have a different cause. Studies in cultured mammalian cells show that *Chmp1* over-expression causes an increase in phosphorylation, thus activity, of nuclear factors, such as ATM and p53, possibly through Chmp1's nuclear function [89, 90]. If Chmp1 has multiple distinct roles, then it is possible that knockdown and over-expression disrupt different cellular processes. So it is possible that the function of *Drosophila* Chmp1 is not limited to the ESCRT's role in MVB formation, but there might also be a nuclear function despite the fact that this study detected no nuclear localization.

It is also possible that *Chmp1* over-expression has the opposite effect to loss of Chmp1, in that the ESCRT complex becomes hyper-active when *Chmp1* is over-expressed. This could lead to different *Chmp1* knockdown and over-expression phenotypes associated with its role in regulating DER signaling, for example. However, both over-activity and loss of most Core PCP proteins results in PCP phenotypes, e.g., extra hairs and altered hair polarity. Therefore the opposite effects of *Chmp1* knockdown and over-expression on ESCRT activity might result in similar PCP phenotypes.

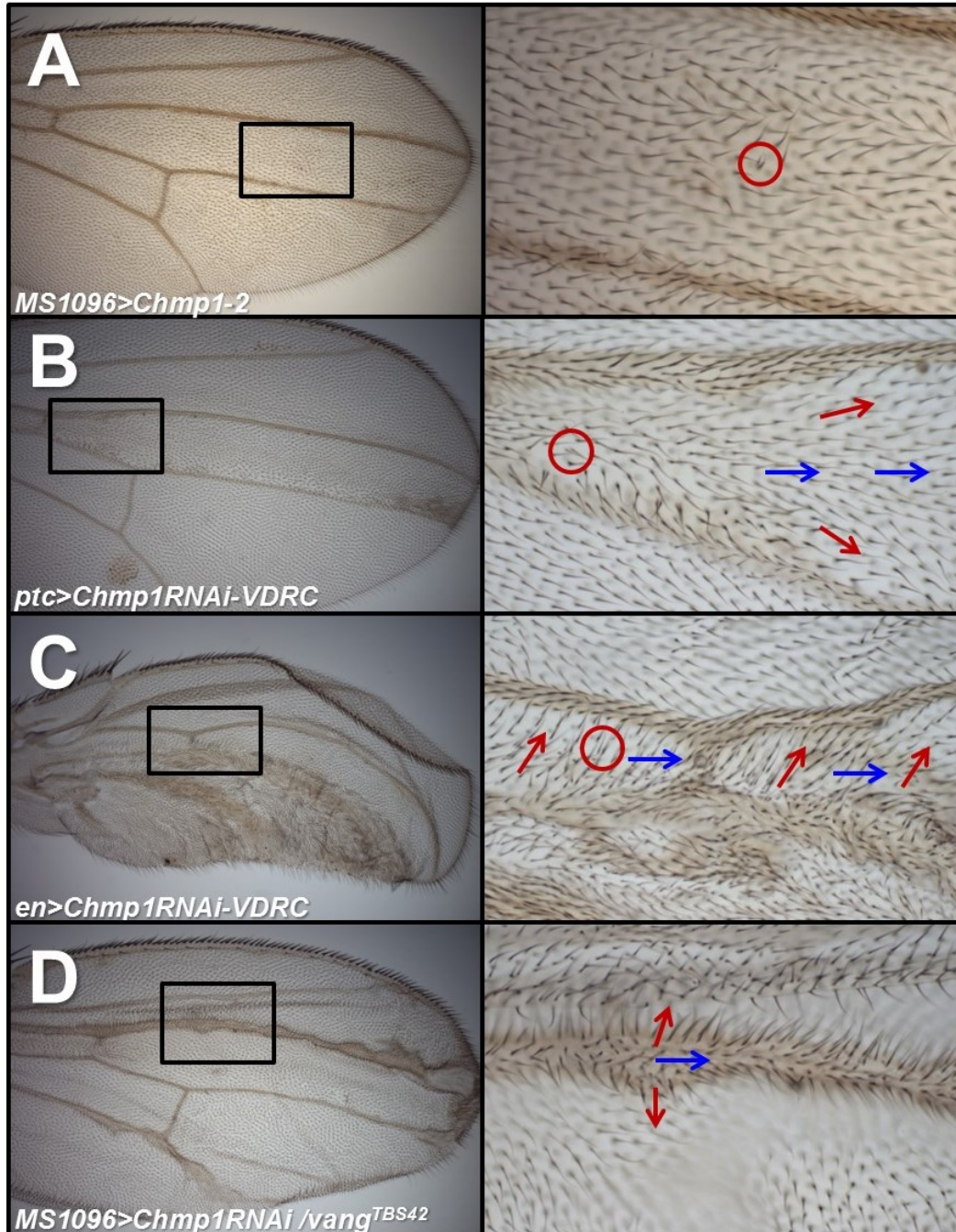


Figure 6.2 Chmp1 may regulate Fz PCP signaling. Light micrographs of wings from adult *Drosophila* females. Distal is right, anterior is uppermost. A. *MS1096-Gal4/X; UAS-Chmp1-2/+*, raised at 30°C. B. *UAS-Chmp1RNAi-VDR/ptc-Gal4*, raised at 28°C. C. *en-Gal4/UAS-Chmp1RNAi-VDR*, raised at 30°C. D. *MS1096-Gal4/X; vang^{TBS42}/UAS-Chmp1RNAi-VDR*, raised at 28°C. Panels to the right are higher magnification images of the boxed in regions of the panels on the left. Red circles around cells carrying additional hairs. Red arrows indicate altered hair polarity; blue arrows indicate wild-type hair polarity.

Project 2: Expression of *pk* and *sple* in pupal wings

Introduction: One of the Core Fz PCP genes, *prickle*, encodes two protein isoforms that are involved in PCP in the fly, Pk and Sple (Figure 6.3). The two isoforms are active in all tissues studied [189]. However, loss of single isoforms affects different epithelial tissues in the fly. Loss of Sple activity results in phenotypes in the eye, abdomen, and legs while loss of Pk activity causes phenotypes in the thorax and wings [189]. Work from the Collier lab indicates that in the wing both Pk and Sple are active but may be required for Fz PCP signaling at different times during pupal wing development [190-192]. Specifically, Sple may be required for an early signaling event at around 18 hours after pupal formation (hAPF), while Pk may be required for a late signaling event at around 32hAPF [191, 193-195].

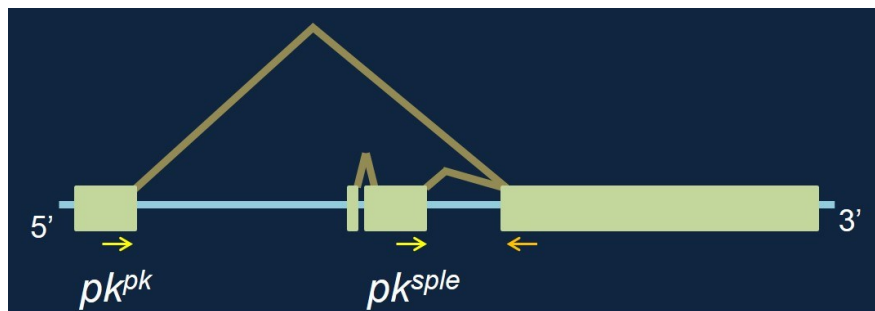


Figure 6.3 Genetic structure of the *prickle* gene. The *pk* gene expresses two transcripts involved in Fz PCP, *pk^{pk}* and *pk^{sple}*, which encode for the Pk and Sple protein isoforms, respectively. Green boxes represent encoded exons, brown lines indicate splicing of exons. The *pk* and *sple* transcripts share a large 3' region, but contain different 5' exons and have independent promoters. Yellow arrows indicate the position of primers used to amplify fragments of *pk* and *sple* cDNA.

If Pk and Sple are required at different time points during development, then this might be reflected in the regulation of their expression, i.e., Sple would be expressed at the 18hAPF time point, and Pk would be expressed at the 32hAPF time point. To test this hypothesis, the presence of *pk* and *sple* mRNA was analyzed at these two time points in the developing fly wing.

Methods: Wild-type flies were grown in large bottles. Developing flies were collected at the pre-pupal stage and separated into two groups - one was aged for 18 hours and the other for 32 hours. At 18 or 32hAPF, the pupae were dissected from their pupal cases and the left and right wings were removed. Immediately after dissection, the total mRNA was collected from the pupal wings with a Qiagen QIAshredder kit. cDNA from the pupal wing mRNA was generated by reverse transcription (RT) using the ImProm-II Reverse Transcription System (Promega) and polyT primers (Invitrogen). The RT reaction was run at 37°C for one hour. Pk, Sple, and Actin control cDNA generated from RT was PCR amplified using custom primers (Invitrogen) (Table 6.1 and Figure 6.3). The control RTPCR reaction omitted addition of reverse transcriptase. Optimal annealing temperatures for *pk*, *sple*, and *actin* primers were determined by temperature gradient PCR reactions using cDNA generated from embryo RNA extractions. The parameters for the PCR reactions were as follows: an initial denaturing step at 94°C for 4 minutes, followed by 35 cycles of denaturing at 94°C for 30 seconds, annealing at 55°C (*pk*) or 60°C (*sple* and *actin*) for 30 seconds, and elongation at 72°C for 1 minute and 30 seconds. Control PCR reactions omitted the addition of template. The PCR product was run on a 1.2% agarose gel for 1 hour at 120V and analyzed on a GelDoc system. PCR reactions were usually successful with as little as two pupal wings from a single fly.

	Forward primer	Reverse primer	Length of amplified fragment (bp)
Pk	GCGCGATTAAAGGAAACAAC	CTGCAGAAGATCCCCACGCT	307
Sple	AAACAGAAGCAGCAGCGTCC	CTGCAGAAGATCCCCACGCT	336
Actin	GGCATGTGCAAGGCCGATTGCCG	CCCAGATCATGTTTCGAGACCTTC	339

Table 6.1 Primers used to amplify *pk*, *sple*, and *actin* cDNA. Primers listed are 5' to 3'.

Results and Discussion: Though amplification of a *pk* cDNA fragment was never optimized it was detectable at both 18 and 32hAPF, as was *sple* (Figure 6.4). This suggested that

the activity of Pk and Sple in Fz PCP signaling in the wing was not controlled by the expression of each isoform at the level of mRNA and suggested that further studies (i.e. optimization of Pk PCR or qPCR) were unnecessary. So it is likely that the activity of Pk and Sple are controlled in ways other than at the level of transcription. For example, it is possible that the Pk and Sple proteins are differentially degraded or stabilized at these time points during development. It is also possible that there is translational control that differs at different time points. Additionally, it is possible that expression of Pk and/or Sple is regulated by microRNAs with incomplete complementarity to the mRNA transcripts, which would mean that translation of Pk and Sple mRNA transcripts would be stalled and differences in expression may not be reflected in mRNA levels [196]. It is also possible that Sple and Pk are both expressed throughout Fz PCP signaling, but that the protein structure of Sple and Pk is altered by binding other proteins, or that they are modified in a way that activates or deactivates them depending on the requirement for Fz PCP signaling. In fact, there is evidence of *Drosophila* Pk phosphorylation, which is important for localization and endosomal trafficking of Pk, as well as its prenylation *in vivo*, which is important for its recruitment to the membrane and proteosomal degradation [197-199].

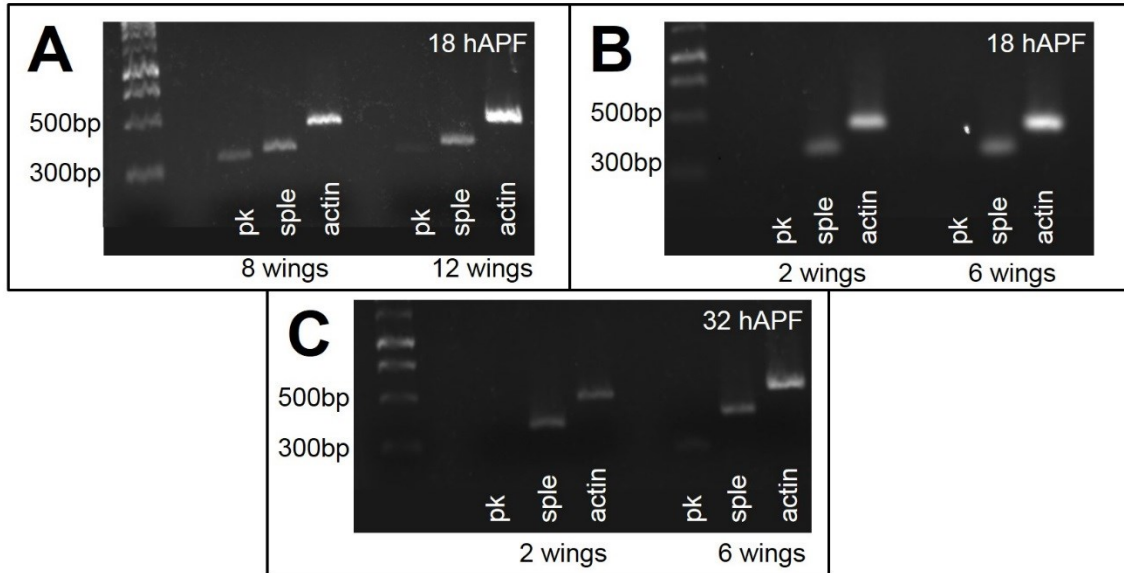


Figure 6.4 Amplification of *pk*, *sple*, and *actin* cDNA fragments. PCR products were run on a 1.2% gen containing ethidium bromide at 120V for 1 hour alongside a 1kb DNA ladder. A and B are from pupal wings at 18hAPF. C is from pupal wings at 32hAPF.

Project 3: Pk and Sple protein isoforms in patterning of the Drosophila eye

Introduction: Patterning of the fly cuticle requires the Fz PCP pathway. The polarity of hairs may be considered as a ‘readout’ of Fz PCP signaling events that occurred during development. As mentioned above, the two isoforms of the Prickle protein, Pk and Sple, are active in the epithelial tissues of the fly, but loss of Pk causes PCP defects in some epithelial tissues, while loss of Sple affects others [189]. This suggests that the Fz PCP pathway has a differential requirement for Prickle isoforms depending upon the tissue. Unpublished studies from the Collier lab suggest that in the fly cuticle, Pk and Sple actually have opposite effects on the direction of (or the hair polarity established by) Fz PCP signaling. In fact, ubiquitous over-expression of *pk* or *sple* in flies mutant for *pk* and *sple* (*pksple¹⁴*) results in opposite hair polarities over most of the cuticle. Though the eye develops in a different manner from the rest of the cuticle, we wondered whether Pk and Sple had opposite effects on eye development as

well. Specifically, that ommatidia in an eye expressing only Pk would have an opposite chirality to ommatidia in an eye expressing only Sple.

Methods: *pk* or *sple* transcripts were over-expressed in a *pksple*¹⁴ background.

*pksple*¹⁴/*pksple*¹⁴; *tub-Gal4/UAS-Sple* flies over-express Sple ubiquitously under the control of the *tub-Gal4* driver in flies lacking active Pk and Sple. *pksple*¹⁴/*pksple*¹⁴, *act5c-myc-pk* flies express myc-tagged Pk ubiquitously under the control of an actin promoter in flies lacking active Pk and Sple. myc-Pk can rescue the *pk* phenotype, suggesting that the myc tag does not inhibit normal Pk activity. Eyes were prepared as described in Chapter 3, Section VIII.

Results and Discussion: Expression of Sple in *pksple*¹⁴ flies resulted in nearly wild-type eyes (Figure 6.5C). The equator was easily identified and most ommatidia were of the correct chirality and rotated properly. Occasionally symmetrical, or achiral, ommatidia were present. Also, occasional ommatidia had the opposite chirality or misrotation; however these ommatidia were uncommon (Figure 6.5C). This shows that the eye can develop almost normally in the absence of the Pk isoform and ubiquitous expression of Sple, suggesting that the Sple isoform is sufficient for eye development, which is consistent with other published work [189]. It also suggests that the spatial or temporal control of Sple expression is not important.

Expression of Pk in *pksple*¹⁴ flies caused severe defects in eye patterning (Figure 6.5B). The site of the equator was uncertain in these eyes. This means that large numbers of ommatidia in each hemisphere of the eye had chirality opposite to wild-type, and appear to have rotated in the opposite direction as wild-type. Additionally, ommatidia were present with incomplete rotation. However, because the position of the equator was unknown in these eyes, making any judgment about the numbers of ommatidia with opposite chirality from normal was difficult. In order to obtain a more useful result, this experiment needs to be repeated with a marker of the

equator. The best way forward may be to study the eye imaginal disc. The position of the equator is known in the eye disc. If the developing photoreceptors are labeled, for example with an antibody against the neuronal marker *Elav*, in combination with a marker for the R3 or R4, such as the transgene *E(spl)mdelta0.5lacZ*, which marks the R4 with β -galactosidase expression, the chirality and rotation of ommatidia in each half of the eye can be compared more reliably.

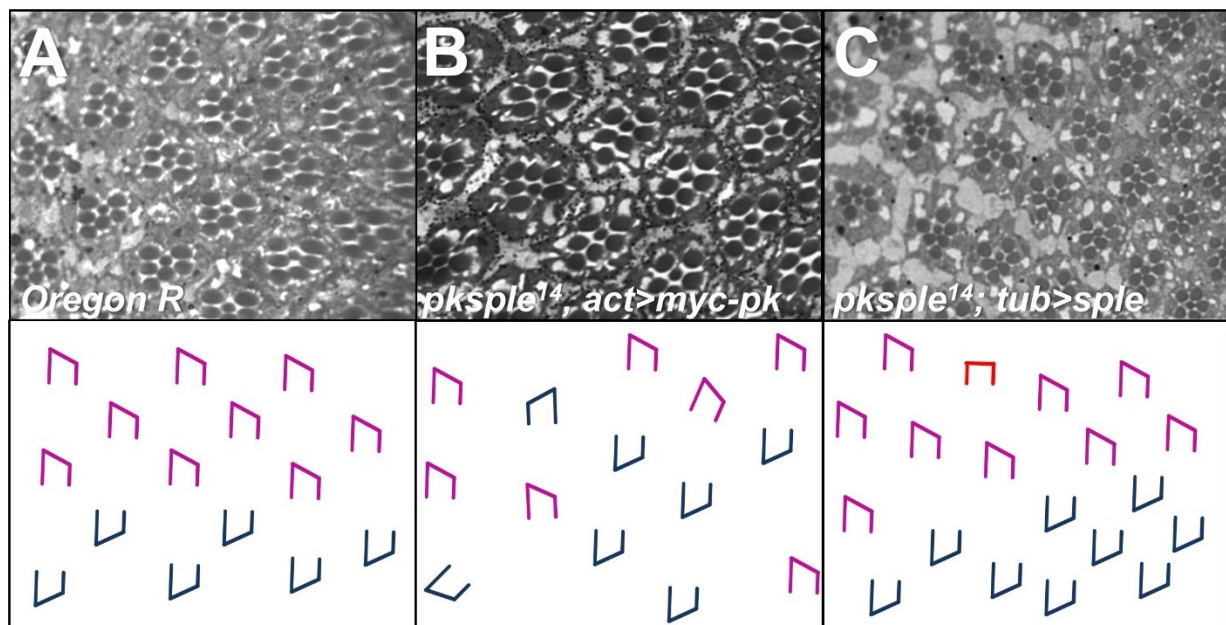


Figure 6.5 Pk and Sple in Fz PCP signaling in the Drosophila eye. Light micrographs of one micron thick tangential sections of the Drosophila eye with cartoon interpretation below. Dorsal-type ommatidia are indicated in purple, ventral-type ommatidia are indicated in blue, achiral ommatidia in red. A. *Oregon R*. B. *act5c-myc-pk, pksple¹⁴/pksple¹⁴*. C. *pksple¹⁴/pksple¹⁴; tub-Gal4/UAS-sple*.

Project 4: Localization of the Sple isoform in pupal wing cells

Introduction: In the Drosophila wing, Fz, Dsh, Dgo, and Fmi localize to the distal edge of developing wing cells, while Pk, Stan, and Fmi localize to the proximal edge. As previously mentioned, the Core Fz PCP protein, Prickle is expressed as two isoforms relevant for PCP, Pk and Sple. It is well documented that the localization of Fz PCP Core proteins is crucial for proper Fz PCP signaling. However, while the localization of the Pk isoform has been characterized,

Sple localization remained uninvestigated. Though Sple is known to have some activity in Fz PCP signaling in the wing, its function is poorly understood [189]. Work from the Collier lab suggests an early requirement for Sple in Fz PCP signaling [190]. Determining the subcellular localization of Sple, will provide more information on its function.

Methods: One problem in visualizing the subcellular localization of membrane proteins is that when the protein localizes to a cell-cell boundary, it is not normally possible to know whether it is present in just one cell or both. Expression clones can overcome this problem because they allow for visualization of all edges (anterior, posterior, proximal, and distal) of clone cells that are adjacent to cells that do not express the protein. To investigate the localization of Sple, clones expressing Sple tagged with an N-terminal myc epitope (myc-Sple) were generated. The myc-Sple protein could rescue loss of Sple activity (*sple^l*), suggesting that it was active and the myc tag did not inhibit its function. The localization of myc-Sple was investigated in wings lacking Pk activity (*pk³⁰* mutant).

Clones of myc-Sple were induced in a *pk³⁰* background (see Chapter 1 section 2D and 2E for information on generating clones). To achieve this, an *act>STOP>myc-sple* fly line was used. This fly line carries a *myc-sple* transgene that is downstream of an Actin promoter, but separated from the promoter by a polyA stop sequence flanked by two FRT sites (>). *hs-flp; pk³⁰* virgin females were crossed to *pk³⁰, act>STOP>myc-sple* males. The F1 generation was heat shocked at 37°C for one hour at 4-5 days (120-144 hours) into development to induce Flippase (Flp) expression and removal of the PolyA stop sequence in a subset of cells. First, female larvae, identified by their genitalia (*hs-flp/X; pk³⁰, act>STOP>myc-sple/pk³⁰*), were collected and wing imaginal discs were dissected and fixed (for method, see Chapter 3 section VI) to ensure that clones were being generated. Clones were identified as small groups of cells within the

imaginal disc that exhibited localization of myc-Sple to the membrane as detected with an anti-myc antibody. Next, female pre-pupa from the same cross were collected and aged for 32 hours. After aging, each pupa was removed from its pupal case. The posterior and anterior ends of the pupae were cut with forceps to allow for fixative penetration, and the insides of the pupae were washed out with 1X PBS. The pupae were then immediately transferred to a fixative solution (8% paraformaldehyde, 200mM sodium cacodylate, 100mM sucrose, 40mM potassium acetate, 10mM EGTA), where the wings were dissected off and the pupal sacs removed. The wings were rinsed in 0.01% PBS-TritonX (PBST) and blocked in 5% BSA in 0.01% PBS-TritonX (BSA-PBST) for 20 minutes. They were then incubated with an anti-c-myc antibody (1:500, diluted in BSA-PBST) at 4°C overnight. The primary antibody was removed and the pupal wings were rinsed 3 times and washed 3 times for 10 minutes each in PBST. Wings were blocked again for 20 minutes in BSA-PBST, followed by incubation with an anti-mouse Alexa-488 antibody (1:500, diluted in BSA-PBST) for 3 hours protected from light. The pupal wings were rinsed 3 times and washed 3 times for 10 minutes each in PBST. The wings were incubated in rhodamine phalloidin (1:100, diluted in PBST) for 30 minutes. They were then rinsed 3 times and washed 3 times for 10 minutes each in PBST at room temperature and finally mounted on a glass microscope slide in Vectashield mounting media with DAPI. Wings were imaged on a confocal microscope.

Results and Discussion: myc-Sple localized to the opposite edge of the cell as the wing hair. This is likely the same localization as Pk, and opposite of the expected localization of Fz, although this has never been tested in these wings [197]. This is consistent with a recent study showing that Sple localized to the opposite edge of the cell as the wing hair [197]. The similar localizations of Pk and Sple with respect to hair formation show that the difference in Pk and

Sple function may not be due to different localizations. *sple* over-expression reverses hair polarity in the wing, i.e., hairs point proximally, rather than distally. It could be that Sple localizes proximally like Pk, and so directs hair formation to the proximal edge of the cell. Alternatively, a distal Sple localization could drive a proximal site of hair formation. These results support the latter, as Sple localized opposite to the site of hair formation. These results suggest that the relationship between the site of hair formation and localization is the same for Pk and Sple. However, Pk and Sple may very well have different localizations with respect to Fz localization.

The results above (Project 2) showed that *pk* and *sple* transcripts are both detected during the two Fz signaling events, suggesting that their activity in Fz PCP signaling is not regulated by their transcription. Instead, the functional differences may lie in binding partners or modifications. The Pk and Sple proteins are identical in amino acid sequence, except in the N-terminal regions. Pk has 13 N-terminal amino acids that are not critical to its function. On the other hand, the Sple protein has a large N-terminal region that appears to be almost entirely unique, with the exception of a small (30 amino acid) region that is shared with other arthropods, but not with vertebrates. This region may facilitate interaction with proteins with which Pk does not interact. Alternatively, it could inhibit interaction with proteins with which Pk binds. Another possibility is that Sple is needed to form and localize protein complexes important in controlling the direction of Fz PCP signaling. If Sple does bind proteins that Pk does not, these binding partners may modify the Sple structure to change its function. A useful future study for investigating Sple function would be to identify proteins that the N-terminal region binds in *Drosophila* cells. This would help characterize the function of Sple in Fz PCP signaling.

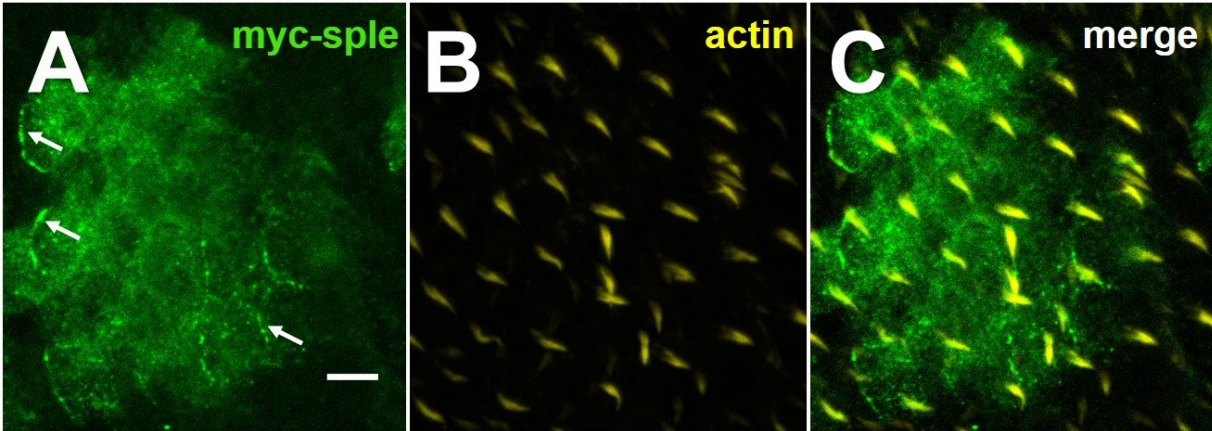


Figure 6.6 Splice localization in the *Drosophila* pupal wing. A clone expressing myc-Sple in the posterior wing of a female of the genotype *hs-flp/X; pk³⁰, act>STOP>myc-sple/pk³⁰*. Max projections of confocal Z-series. A. Detection of myc-Sple (green) with anti-myc. White arrows show localization to the edge of the cell. B. The prehairs are composed of Actin, which was detected with rhodamine phalloidin. C. Merge of A and B, showing localization of myc-Sple to the opposite edge of the cell as the prehair.

APPENDIX

IRB APPROVAL LETTER



Office of Research Integrity

February 10, 2014

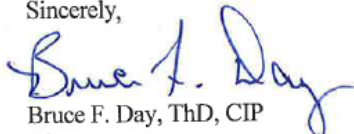
Meagan Valentine
6 Seminole Rd.
Huntington, WV 25705

Dear Ms. Valentine:

This letter is in response to the submitted dissertation abstract entitled "*CHMP1 Negatively Regulates Epidermal Growth Factor Signaling in the Drosophila Wing.*" After assessing the abstract it has been deemed not to be human subject research and therefore exempt from oversight of the Marshall University Institutional Review Board (IRB). The Code of Federal Regulations (45CFR46) has set forth the criteria utilized in making this determination. Since the study does not involve human subjects as defined in DHHS regulation 45 CFR §46.102(f) it is not considered human subject research. If there are any changes to the abstract you provided then you would need to resubmit that information to the Office of Research Integrity for review and determination.

I appreciate your willingness to submit the abstract for determination. Please feel free to contact the Office of Research Integrity if you have any questions regarding future protocols that may require IRB review.

Sincerely,



Bruce F. Day, ThD, CIP
Director

WE ARE... **MARSHALL**™

401 11th Street, Suite 1300 • Huntington, West Virginia 25701 • Tel 304/696-7320
A State University of West Virginia • An Affirmative Action/Equal Opportunity Employer

REFERENCES

1. Butler, M.J., et al., *Discovery of genes with highly restricted expression patterns in the Drosophila wing disc using DNA oligonucleotide microarrays*. *Development*, 2003. **130**(4): p. 659-70.
2. Marygold, S.J., et al., *FlyBase: improvements to the bibliography*. *Nucleic Acids Res*, 2013. **41**(Database issue): p. D751-7.
3. Jenny, A., *Planar cell polarity signaling in the Drosophila eye*. *Curr Top Dev Biol*, 2010. **93**: p. 189-227.
4. Adams, M.D., et al., *The genome sequence of Drosophila melanogaster*. *Science*, 2000. **287**(5461): p. 2185-95.
5. Pandey, U.B. and C.D. Nichols, *Human disease models in Drosophila melanogaster and the role of the fly in therapeutic drug discovery*. *Pharmacol Rev*, 2011. **63**(2): p. 411-36.
6. Bier, E., *Drosophila, the golden bug, emerges as a tool for human genetics*. *Nat Rev Genet*, 2005. **6**(1): p. 9-23.
7. Fortini, M.E., et al., *A survey of human disease gene counterparts in the Drosophila genome*. *J Cell Biol*, 2000. **150**(2): p. F23-30.
8. Reiter, L.T., et al., *A systematic analysis of human disease-associated gene sequences in Drosophila melanogaster*. *Genome Res*, 2001. **11**(6): p. 1114-25.
9. Stephenson, R. and N.H. Metcalfe, *Drosophila melanogaster: a fly through its history and current use*. *J R Coll Physicians Edinb*, 2013. **43**(1): p. 70-5.
10. Rubin, G.M. and E.B. Lewis, *A brief history of Drosophila's contributions to genome research*. *Science*, 2000. **287**(5461): p. 2216-8.
11. *Basic Methods of Culturing Drosophila, Bloomington Stock Center*. 2007 [cited 2013 07/09]; Available from: <http://flystocks.bio.indiana.edu/FlyWork/culturing.htm#stockkeeping>.
12. Gilbert, S.F., *Developmental biology*. 6th ed. 2000, Sunderland, Mass.: Sinauer Associates. xviii, 749 p.

13. Bownes, M., *A photographic study of development in the living embryo of Drosophila melanogaster*. J Embryol Exp Morphol, 1975. **33**(3): p. 789-801.
14. De Celis, J.F., *Pattern formation in the Drosophila wing: The development of the veins*. Bioessays, 2003. **25**(5): p. 443-51.
15. Blair, S.S., *Wing vein patterning in Drosophila and the analysis of intercellular signaling*. Annu Rev Cell Dev Biol, 2007. **23**: p. 293-319.
16. Biehs, B., M.A. Sturtevant, and E. Bier, *Boundaries in the Drosophila wing imaginal disc organize vein-specific genetic programs*. Development, 1998. **125**(21): p. 4245-57.
17. Sturtevant, M.A., M. Roark, and E. Bier, *The Drosophila rhomboid gene mediates the localized formation of wing veins and interacts genetically with components of the EGF-R signaling pathway*. Genes Dev, 1993. **7**(6): p. 961-73.
18. Diaz-Benjumea, F.J. and E. Hafen, *The sevenless signalling cassette mediates Drosophila EGF receptor function during epidermal development*. Development, 1994. **120**(3): p. 569-78.
19. de Celis, J.F., S. Bray, and A. Garcia-Bellido, *Notch signalling regulates veinlet expression and establishes boundaries between veins and interveins in the Drosophila wing*. Development, 1997. **124**(10): p. 1919-28.
20. Huppert, S.S., T.L. Jacobsen, and M.A. Muskavitch, *Feedback regulation is central to Delta-Notch signalling required for Drosophila wing vein morphogenesis*. Development, 1997. **124**(17): p. 3283-91.
21. de Celis, J.F., M. Llimargas, and J. Casanova, *Ventral veinless, the gene encoding the Cfla transcription factor, links positional information and cell differentiation during embryonic and imaginal development in Drosophila melanogaster*. Development, 1995. **121**(10): p. 3405-16.
22. Freeman, M., *Reiterative use of the EGF receptor triggers differentiation of all cell types in the Drosophila eye*. Cell, 1996. **87**(4): p. 651-60.
23. Dominguez, M., J.D. Wasserman, and M. Freeman, *Multiple functions of the EGF receptor in Drosophila eye development*. Curr Biol, 1998. **8**(19): p. 1039-48.
24. Cooper, M.T. and S.J. Bray, *Frizzled regulation of Notch signalling polarizes cell fate in the Drosophila eye*. Nature, 1999. **397**(6719): p. 526-30.

25. Fanto, M. and M. Mlodzik, *Asymmetric Notch activation specifies photoreceptors R3 and R4 and planar polarity in the Drosophila eye*. Nature, 1999. **397**(6719): p. 523-6.
26. Muller, H.J., *Genetic Variability, Twin Hybrids and Constant Hybrids, in a Case of Balanced Lethal Factors*. Genetics, 1918. **3**(5): p. 422-99.
27. Brand, A.H. and N. Perrimon, *Targeted gene expression as a means of altering cell fates and generating dominant phenotypes*. Development, 1993. **118**(2): p. 401-15.
28. Dietzl, G., et al., *A genome-wide transgenic RNAi library for conditional gene inactivation in Drosophila*. Nature, 2007. **448**(7150): p. 151-6.
29. *The Transgenic RNAi Project at Harvard Medical School* <http://www.flyrnai.org/TRiP-HOME.html> [cited 2013 10/18].
30. Golic, K.G. and S. Lindquist, *The FLP recombinase of yeast catalyzes site-specific recombination in the Drosophila genome*. Cell, 1989. **59**(3): p. 499-509.
31. Shilo, B.Z., *Signaling by the Drosophila epidermal growth factor receptor pathway during development*. Exp Cell Res, 2003. **284**(1): p. 140-9.
32. Neuman-Silberberg, F.S. and T. Schupbach, *The Drosophila dorsoventral patterning gene gurken produces a dorsally localized RNA and encodes a TGF alpha-like protein*. Cell, 1993. **75**(1): p. 165-74.
33. Freeman, M., *The spitz gene is required for photoreceptor determination in the Drosophila eye where it interacts with the EGF receptor*. Mech Dev, 1994. **48**(1): p. 25-33.
34. Rutledge, B.J., et al., *The Drosophila spitz gene encodes a putative EGF-like growth factor involved in dorsal-ventral axis formation and neurogenesis*. Genes & Development, 1992. **6**(8): p. 1503-1517.
35. Tio, M., C. Ma, and K. Moses, *spitz, a Drosophila homolog of transforming growth factor-alpha, is required in the founding photoreceptor cells of the compound eye facets*. Mech Dev, 1994. **48**(1): p. 13-23.
36. Urban, S., J.R. Lee, and M. Freeman, *A family of Rhomboid intramembrane proteases activates all Drosophila membrane-tethered EGF ligands*. EMBO J, 2002. **21**(16): p. 4277-86.

37. Lee, J.R., et al., *Regulated intracellular ligand transport and proteolysis control EGF signal activation in Drosophila*. Cell, 2001. **107**(2): p. 161-71.
38. Reich, A. and B.Z. Shilo, *Keren, a new ligand of the Drosophila epidermal growth factor receptor, undergoes two modes of cleavage*. EMBO J, 2002. **21**(16): p. 4287-96.
39. Schnepp, B., et al., *Vein is a novel component in the Drosophila epidermal growth factor receptor pathway with similarity to the neuregulins*. Genes Dev, 1996. **10**(18): p. 2302-13.
40. Yarnitzky, T., L. Min, and T. Volk, *The Drosophila neuregulin homolog Vein mediates inductive interactions between myotubes and their epidermal attachment cells*. Genes Dev, 1997. **11**(20): p. 2691-700.
41. Galindo, M.I., et al., *Leg patterning driven by proximal-distal interactions and EGFR signaling*. Science, 2002. **297**(5579): p. 256-9.
42. Simcox, A.A., et al., *Molecular, phenotypic, and expression analysis of vein, a gene required for growth of the Drosophila wing disc*. Dev Biol, 1996. **177**(2): p. 475-89.
43. Schweitzer, R., et al., *Inhibition of Drosophila EGF receptor activation by the secreted protein Argos*. Nature, 1995. **376**(6542): p. 699-702.
44. Klein, D.E., et al., *Argos inhibits epidermal growth factor receptor signalling by ligand sequestration*. Nature, 2004. **430**(7003): p. 1040-4.
45. Ghiglione, C., *Mechanism of inhibition of the Drosophila and mammalian EGF receptors by the transmembrane protein Kekkon 1*. Development, 2003. **130**(18): p. 4483-4493.
46. Ghiglione, C., et al., *The transmembrane molecule kekkon 1 acts in a feedback loop to negatively regulate the activity of the Drosophila EGF receptor during oogenesis*. Cell, 1999. **96**(6): p. 847-56.
47. Casci, T., J. Vinos, and M. Freeman, *Sprouty, an intracellular inhibitor of Ras signaling*. Cell, 1999. **96**(5): p. 655-65.
48. Brunner, D., et al., *The ETS domain protein pointed-P2 is a target of MAP kinase in the sevenless signal transduction pathway*. Nature, 1994. **370**(6488): p. 386-9.

49. O'Neill, E.M., et al., *The activities of two Ets-related transcription factors required for Drosophila eye development are modulated by the Ras/MAPK pathway*. Cell, 1994. **78**(1): p. 137-47.
50. Hurley, J.H., *The ESCRT complexes*. Crit Rev Biochem Mol Biol, 2010. **45**(6): p. 463-87.
51. Raiborg, C. and H. Stenmark, *The ESCRT machinery in endosomal sorting of ubiquitylated membrane proteins*. Nature, 2009. **458**(7237): p. 445-52.
52. Morita, E. and W.I. Sundquist, *Retrovirus budding*. Annu Rev Cell Dev Biol, 2004. **20**: p. 395-425.
53. McDonald, B. and J. Martin-Serrano, *No strings attached: the ESCRT machinery in viral budding and cytokinesis*. J Cell Sci, 2009. **122**(Pt 13): p. 2167-77.
54. Lee, J.A. and F.B. Gao, *Neuronal Functions of ESCRTs*. Exp Neurobiol, 2012. **21**(1): p. 9-15.
55. Roxrud, I., H. Stenmark, and L. Malerod, *ESCRT & Co*. Biol Cell, 2010. **102**(5): p. 293-318.
56. Langelier, C., et al., *Human ESCRT-II complex and its role in human immunodeficiency virus type 1 release*. J Virol, 2006. **80**(19): p. 9465-80.
57. Morita, E., et al., *Human ESCRT and ALIX proteins interact with proteins of the midbody and function in cytokinesis*. EMBO J, 2007. **26**(19): p. 4215-27.
58. Chin, L.S., et al., *Hrs interacts with sorting nexin 1 and regulates degradation of epidermal growth factor receptor*. J Biol Chem, 2001. **276**(10): p. 7069-78.
59. Jekely, G. and P. Rorth, *Hrs mediates downregulation of multiple signalling receptors in Drosophila*. EMBO Rep, 2003. **4**(12): p. 1163-8.
60. Moberg, K.H., et al., *Mutations in erupted, the Drosophila ortholog of mammalian tumor susceptibility gene 101, elicit non-cell-autonomous overgrowth*. Dev Cell, 2005. **9**(5): p. 699-710.
61. Vaccari, T. and D. Bilder, *The Drosophila tumor suppressor vps25 prevents nonautonomous overproliferation by regulating notch trafficking*. Dev Cell, 2005. **9**(5): p. 687-98.

62. Katzmann, D.J., M. Babst, and S.D. Emr, *Ubiquitin-dependent sorting into the multivesicular body pathway requires the function of a conserved endosomal protein sorting complex, ESCRT-I*. Cell, 2001. **106**(2): p. 145-55.
63. Piper, R.C. and J.P. Luzio, *Ubiquitin-dependent sorting of integral membrane proteins for degradation in lysosomes*. Curr Opin Cell Biol, 2007. **19**(4): p. 459-65.
64. Fabrikant, G., et al., *Computational model of membrane fission catalyzed by ESCRT-III*. PLoS Comput Biol, 2009. **5**(11): p. e1000575.
65. Boura, E., et al., *Solution structure of the ESCRT-I and -II supercomplex: implications for membrane budding and scission*. Structure, 2012. **20**(5): p. 874-86.
66. Ghazi-Tabatabai, S., et al., *Structure and disassembly of filaments formed by the ESCRT-III subunit Vps24*. Structure, 2008. **16**(9): p. 1345-56.
67. Hanson, P.I., et al., *Plasma membrane deformation by circular arrays of ESCRT-III protein filaments*. J Cell Biol, 2008. **180**(2): p. 389-402.
68. Lata, S., et al., *Helical structures of ESCRT-III are disassembled by VPS4*. Science, 2008. **321**(5894): p. 1354-7.
69. Bajorek, M., et al., *Structural basis for ESCRT-III protein autoinhibition*. Nat Struct Mol Biol, 2009. **16**(7): p. 754-62.
70. Wollert, T., et al., *Membrane scission by the ESCRT-III complex*. Nature, 2009. **458**(7235): p. 172-7.
71. Hurley, J.H. and P.I. Hanson, *Membrane budding and scission by the ESCRT machinery: it's all in the neck*. Nat Rev Mol Cell Biol, 2010. **11**(8): p. 556-66.
72. Babst, M., et al., *Escrt-III: an endosome-associated heterooligomeric protein complex required for mvb sorting*. Dev Cell, 2002. **3**(2): p. 271-82.
73. Babst, M., et al., *The Vps4p AAA ATPase regulates membrane association of a Vps protein complex required for normal endosome function*. EMBO J, 1998. **17**(11): p. 2982-93.
74. Lin, Y., et al., *Interaction of the mammalian endosomal sorting complex required for transport (ESCRT) III protein hSnf7-1 with itself, membranes, and the AAA+ ATPase SKD1*. J Biol Chem, 2005. **280**(13): p. 12799-809.

75. Tsang, H.T., et al., *A systematic analysis of human CHMP protein interactions: additional MIT domain-containing proteins bind to multiple components of the human ESCRT III complex*. Genomics, 2006. **88**(3): p. 333-46.
76. Muziol, T., et al., *Structural basis for budding by the ESCRT-III factor CHMP3*. Dev Cell, 2006. **10**(6): p. 821-30.
77. Yang, D., et al., *Structural basis for midbody targeting of spastin by the ESCRT-III protein CHMP1B*. Nat Struct Mol Biol, 2008. **15**(12): p. 1278-86.
78. Shim, S., L.A. Kimpler, and P.I. Hanson, *Structure/function analysis of four core ESCRT-III proteins reveals common regulatory role for extreme C-terminal domain*. Traffic, 2007. **8**(8): p. 1068-79.
79. Zamborlini, A., et al., *Release of autoinhibition converts ESCRT-III components into potent inhibitors of HIV-1 budding*. Proc Natl Acad Sci U S A, 2006. **103**(50): p. 19140-5.
80. von Schwedler, U.K., et al., *The protein network of HIV budding*. Cell, 2003. **114**(6): p. 701-13.
81. Stauffer, D.R., et al., *CHMP1 is a novel nuclear matrix protein affecting chromatin structure and cell-cycle progression*. J Cell Sci, 2001. **114**(Pt 13): p. 2383-93.
82. Obita, T., et al., *Structural basis for selective recognition of ESCRT-III by the AAA ATPase Vps4*. Nature, 2007. **449**(7163): p. 735-9.
83. Scott, A., et al., *Structure and ESCRT-III protein interactions of the MIT domain of human VPS4A*. Proc Natl Acad Sci U S A, 2005. **102**(39): p. 13813-8.
84. Stuchell-Breteron, M.D., et al., *ESCRT-III recognition by VPS4 ATPases*. Nature, 2007. **449**(7163): p. 740-4.
85. Yang, K.S., et al., *Molecular characterization of NbCHMP1 encoding a homolog of human CHMP1 in Nicotiana benthamiana*. Mol Cells, 2004. **17**(2): p. 255-61.
86. Hervas-Aguilar, A., et al., *Characterization of Aspergillus nidulans DidB Did2, a non-essential component of the multivesicular body pathway*. Fungal Genet Biol, 2010. **47**(7): p. 636-46.
87. Spitzer, C., et al., *The ESCRT-related CHMP1A and B proteins mediate multivesicular body sorting of auxin carriers in Arabidopsis and are required for plant development*. Plant Cell, 2009. **21**(3): p. 749-66.

88. You, Z., et al., *Chmp1A acts as a tumor suppressor gene that inhibits proliferation of renal cell carcinoma*. Cancer Lett, 2012. **319**(2): p. 190-6.
89. Li, J., et al., *Chmp1A functions as a novel tumor suppressor gene in human embryonic kidney and ductal pancreatic tumor cells*. Cell Cycle, 2008. **7**(18): p. 2886-93.
90. Manohar, S., et al., *Chromatin modifying protein 1A (Chmp1A) of the endosomal sorting complex required for transport (ESCRT)-III family activates ataxia telangiectasia mutated (ATM) for PanC-1 cell growth inhibition*. Cell Cycle, 2011. **10**(15): p. 2529-39.
91. Mochida, G.H., et al., *CHMPIA encodes an essential regulator of BMI1-INK4A in cerebellar development*. Nat Genet, 2012. **44**(11): p. 1260-4.
92. Shen, B., et al., *sall1 determines the number of aleurone cell layers in maize endosperm and encodes a class E vacuolar sorting protein*. Proc Natl Acad Sci U S A, 2003. **100**(11): p. 6552-7.
93. Tian, Q., et al., *Subcellular localization and functional domain studies of DEFECTIVE KERNEL1 in maize and Arabidopsis suggest a model for aleurone cell fate specification involving CRINKLY4 and SUPERNUMERARY ALEURONE LAYER1*. Plant Cell, 2007. **19**(10): p. 3127-45.
94. Maemoto, Y., H. Shibata, and M. Maki, *Identification of Phosphorylation Sites in the C-Terminal Region of Charged Multivesicular Body Protein 1A (CHMPIA)*. Biosci Biotechnol Biochem, 2013. **77**(6): p. 1317-9.
95. Li, J., et al., *Chmp 1A is a mediator of the anti-proliferative effects of all-trans retinoic acid in human pancreatic cancer cells*. Mol Cancer, 2009. **8**: p. 7.
96. Nickerson, D.P., M. West, and G. Odorizzi, *Did2 coordinates Vps4-mediated dissociation of ESCRT-III from endosomes*. J Cell Biol, 2006. **175**(5): p. 715-20.
97. Howard, T.L., et al., *CHMPI functions as a member of a newly defined family of vesicle trafficking proteins*. J Cell Sci, 2001. **114**(Pt 13): p. 2395-404.
98. Lottridge, J.M., et al., *Vta1p and Vps46p regulate the membrane association and ATPase activity of Vps4p at the yeast multivesicular body*. Proc Natl Acad Sci U S A, 2006. **103**(16): p. 6202-7.
99. Zhong, Q., et al., *Perturbation of TSG101 protein affects cell cycle progression*. Cancer Res, 1998. **58**(13): p. 2699-702.

100. Morita, E., et al., *Human ESCRT-III and VPS4 proteins are required for centrosome and spindle maintenance*. Proc Natl Acad Sci U S A, 2010. **107**(29): p. 12889-94.
101. Reid, E., et al., *The hereditary spastic paraplegia protein spastin interacts with the ESCRT-III complex-associated endosomal protein CHMP1B*. Hum Mol Genet, 2005. **14**(1): p. 19-38.
102. Dimaano, C., et al., *Ist1 regulates Vps4 localization and assembly*. Mol Biol Cell, 2008. **19**(2): p. 465-74.
103. Rue, S.M., et al., *Novel Ist1-Did2 complex functions at a late step in multivesicular body sorting*. Mol Biol Cell, 2008. **19**(2): p. 475-84.
104. Xiao, J., et al., *Structural basis of Ist1 function and Ist1-Did2 interaction in the multivesicular body pathway and cytokinesis*. Mol Biol Cell, 2009. **20**(15): p. 3514-24.
105. Azmi, I.F., et al., *ESCRT-III family members stimulate Vps4 ATPase activity directly or via Vta1*. Dev Cell, 2008. **14**(1): p. 50-61.
106. Shim, S., S.A. Merrill, and P.I. Hanson, *Novel interactions of ESCRT-III with LIP5 and VPS4 and their implications for ESCRT-III disassembly*. Mol Biol Cell, 2008. **19**(6): p. 2661-72.
107. Xiao, J., et al., *Structural basis of Vta1 function in the multivesicular body sorting pathway*. Dev Cell, 2008. **14**(1): p. 37-49.
108. Row, P.E., et al., *The MIT domain of UBPY constitutes a CHMP binding and endosomal localization signal required for efficient epidermal growth factor receptor degradation*. J Biol Chem, 2007. **282**(42): p. 30929-37.
109. Yorikawa, C., et al., *Human calpain 7/PalBH associates with a subset of ESCRT-III-related proteins in its N-terminal region and partly localizes to endocytic membrane compartments*. J Biochem, 2008. **143**(6): p. 731-45.
110. Guruharsha, K.G., et al., *A protein complex network of Drosophila melanogaster*. Cell, 2011. **147**(3): p. 690-703.
111. Guruharsha, K.G., et al., *Drosophila protein interaction map (DPiM): a paradigm for metazoan protein complex interactions*. Fly (Austin), 2012. **6**(4): p. 246-53.
112. Schneider, C.A., W.S. Rasband, and K.W. Eliceiri, *NIH Image to ImageJ: 25 years of image analysis*. Nat Methods, 2012. **9**(7): p. 671-5.

113. Graveley, B.R., et al., *The developmental transcriptome of Drosophila melanogaster*. Nature, 2011. **471**(7339): p. 473-9.
114. Jiang, H., et al., *Natalisin, a tachykinin-like signaling system, regulates sexual activity and fecundity in insects*. Proc Natl Acad Sci U S A, 2013. **110**(37): p. E3526-34.
115. Mummery-Widmer, J.L., et al., *Genome-wide analysis of Notch signalling in Drosophila by transgenic RNAi*. Nature, 2009. **458**(7241): p. 987-92.
116. Dobzhansky, T., *A Homozygous Translocation in Drosophila Melanogaster*. Proc Natl Acad Sci U S A, 1929. **15**(8): p. 633-8.
117. Fristrom, D., et al., *Blistered: a gene required for vein/intervein formation in wings of Drosophila*. Development, 1994. **120**(9): p. 2661-71.
118. Valentine, M., *The role of Chmp1 in Drosophila melanogaster*, 2010.
119. Babst, M., et al., *Mammalian tumor susceptibility gene 101 (TSG101) and the yeast homologue, Vps23p, both function in late endosomal trafficking*. Traffic, 2000. **1**(3): p. 248-58.
120. Lloyd, T.E., et al., *Hrs regulates endosome membrane invagination and tyrosine kinase receptor signaling in Drosophila*. Cell, 2002. **108**(2): p. 261-9.
121. Garcia-Bellido, A., F. Cortes, and M. Milan, *Cell interactions in the control of size in Drosophila wings*. Proc Natl Acad Sci U S A, 1994. **91**(21): p. 10222-6.
122. Diaz-Benjumea, F.J. and A. Garcia-Bellido, *Behaviour of cells mutant for an EGF receptor homologue of Drosophila in genetic mosaics*. Proc Biol Sci, 1990. **242**(1303): p. 36-44.
123. Roch, F., et al., *Genetic interactions and cell behaviour in blistered mutants during proliferation and differentiation of the Drosophila wing*. Development, 1998. **125**(10): p. 1823-32.
124. Milan, M., F.J. Diaz-Benjumea, and S.M. Cohen, *Beadex encodes an LMO protein that regulates Apterous LIM-homeodomain activity in Drosophila wing development: a model for LMO oncogene function*. Genes Dev, 1998. **12**(18): p. 2912-20.
125. Bachmann, A. and E. Knust, *Positive and negative control of Serrate expression during early development of the Drosophila wing*. Mech Dev, 1998. **76**(1-2): p. 67-78.

126. Panin, V.M., et al., *Fringe modulates Notch-ligand interactions*. Nature, 1997. **387**(6636): p. 908-12.
127. Weber, U., C. Eroglu, and M. Mlodzik, *Phospholipid membrane composition affects EGF receptor and Notch signaling through effects on endocytosis during Drosophila development*. Dev Cell, 2003. **5**(4): p. 559-70.
128. Hori, K., et al., *Drosophila deltex mediates suppressor of Hairless-independent and late-endosomal activation of Notch signaling*. Development, 2004. **131**(22): p. 5527-37.
129. Wilkin, M., et al., *Drosophila HOPS and AP-3 complex genes are required for a Deltex-regulated activation of notch in the endosomal trafficking pathway*. Dev Cell, 2008. **15**(5): p. 762-72.
130. Baron, M., *Endocytic routes to Notch activation*. Semin Cell Dev Biol, 2012. **23**(4): p. 437-42.
131. Sriram, V., K.S. Krishnan, and S. Mayor, *deep-orange and carnation define distinct stages in late endosomal biogenesis in Drosophila melanogaster*. J Cell Biol, 2003. **161**(3): p. 593-607.
132. Akbar, M.A., S. Ray, and H. Kramer, *The SM protein Car/Vps33A regulates SNARE-mediated trafficking to lysosomes and lysosome-related organelles*. Mol Biol Cell, 2009. **20**(6): p. 1705-14.
133. Strutt, H. and D. Strutt, *EGF signaling and ommatidial rotation in the Drosophila eye*. Curr Biol, 2003. **13**(16): p. 1451-7.
134. Zheng, L., J. Zhang, and R.W. Carthew, *frizzled regulates mirror-symmetric pattern formation in the Drosophila eye*. Development, 1995. **121**(9): p. 3045-55.
135. Baker, N.E. and G.M. Rubin, *Effect on eye development of dominant mutations in Drosophila homologue of the EGF receptor*. Nature, 1989. **340**(6229): p. 150-3.
136. Lesokhin, A.M., et al., *Several levels of EGF receptor signaling during photoreceptor specification in wild-type, Ellipse, and null mutant Drosophila*. Dev Biol, 1999. **205**(1): p. 129-44.
137. Vaccari, T., et al., *Comparative analysis of ESCRT-I, ESCRT-II and ESCRT-III function in Drosophila by efficient isolation of ESCRT mutants*. J Cell Sci, 2009. **122**(Pt 14): p. 2413-23.

138. Martin-Blanco, E., et al., *A temporal switch in DER signaling controls the specification and differentiation of veins and interveins in the Drosophila wing*. Development, 1999. **126**(24): p. 5739-47.
139. Brown, K.E., M. Kerr, and M. Freeman, *The EGFR ligands Spitz and Keren act cooperatively in the Drosophila eye*. Dev Biol, 2007. **307**(1): p. 105-13.
140. Schnepp, B., et al., *EGF domain swap converts a drosophila EGF receptor activator into an inhibitor*. Genes Dev, 1998. **12**(7): p. 908-13.
141. Guichard, A., et al., *rhomboid and Star interact synergistically to promote EGFR/MAPK signaling during Drosophila wing vein development*. Development, 1999. **126**(12): p. 2663-76.
142. Marendia, D.R., et al., *MAP kinase subcellular localization controls both pattern and proliferation in the developing Drosophila wing*. Development, 2006. **133**(1): p. 43-51.
143. de Celis, J.F., *Expression and function of decapentaplegic and thick veins during the differentiation of the veins in the Drosophila wing*. Development, 1997. **124**(5): p. 1007-18.
144. Ardito, C.M., et al., *EGF receptor is required for KRAS-induced pancreatic tumorigenesis*. Cancer Cell, 2012. **22**(3): p. 304-17.
145. Bardeesy, N. and R.A. DePinho, *Pancreatic cancer biology and genetics*. Nat Rev Cancer, 2002. **2**(12): p. 897-909.
146. Normanno, N., et al., *Epidermal growth factor receptor (EGFR) signaling in cancer*. Gene, 2006. **366**(1): p. 2-16.
147. Morata, G. and P. Ripoll, *Minutes: mutants of drosophila autonomously affecting cell division rate*. Dev Biol, 1975. **42**(2): p. 211-21.
148. Lai, E.C., et al., *The ubiquitin ligase Drosophila Mind bomb promotes Notch signaling by regulating the localization and activity of Serrate and Delta*. Development, 2005. **132**(10): p. 2319-32.
149. Young, T.W., et al., *Up-regulation of tumor susceptibility gene 101 conveys poor prognosis through suppression of p21 expression in ovarian cancer*. Clin Cancer Res, 2007. **13**(13): p. 3848-54.

150. Li, L. and S.N. Cohen, *Tsg101: a novel tumor susceptibility gene isolated by controlled homozygous functional knockout of allelic loci in mammalian cells*. Cell, 1996. **85**(3): p. 319-29.
151. Hittelman, A.B., et al., *Differential regulation of glucocorticoid receptor transcriptional activation via AF-1-associated proteins*. EMBO J, 1999. **18**(19): p. 5380-8.
152. Li, Z., et al., *Structure of a Bmi-1-Ring1B polycomb group ubiquitin ligase complex*. J Biol Chem, 2006. **281**(29): p. 20643-9.
153. Kamura, T., et al., *Cloning and characterization of ELL-associated proteins EAP45 and EAP20. a role for yeast EAP-like proteins in regulation of gene expression by glucose*. J Biol Chem, 2001. **276**(19): p. 16528-33.
154. Wang, Y. and J. Nathans, *Tissue/planar cell polarity in vertebrates: new insights and new questions*. Development, 2007. **134**(4): p. 647-58.
155. Simons, M. and M. Mlodzik, *Planar cell polarity signaling: from fly development to human disease*. Annu Rev Genet, 2008. **42**: p. 517-40.
156. Yin, C., B. Ciruna, and L. Solnica-Krezel, *Convergence and extension movements during vertebrate gastrulation*. Curr Top Dev Biol, 2009. **89**: p. 163-92.
157. Goto, T. and R. Keller, *The planar cell polarity gene strabismus regulates convergence and extension and neural fold closure in Xenopus*. Dev Biol, 2002. **247**(1): p. 165-81.
158. Carreira-Barbosa, F., et al., *Prickle 1 regulates cell movements during gastrulation and neuronal migration in zebrafish*. Development, 2003. **130**(17): p. 4037-46.
159. Gray, R.S., et al., *The planar cell polarity effector Fuz is essential for targeted membrane trafficking, ciliogenesis and mouse embryonic development*. Nat Cell Biol, 2009. **11**(10): p. 1225-32.
160. Kibar, Z., et al., *Mutations in VANGL1 associated with neural-tube defects*. N Engl J Med, 2007. **356**(14): p. 1432-7.
161. Bassuk, A.G., et al., *A homozygous mutation in human PRICKLE1 causes an autosomal-recessive progressive myoclonus epilepsy-ataxia syndrome*. Am J Hum Genet, 2008. **83**(5): p. 572-81.

162. Ross, A.J., et al., *Disruption of Bardet-Biedl syndrome ciliary proteins perturbs planar cell polarity in vertebrates*. Nat Genet, 2005. **37**(10): p. 1135-40.
163. Simons, M., et al., *Inversin, the gene product mutated in nephronophthisis type II, functions as a molecular switch between Wnt signaling pathways*. Nat Genet, 2005. **37**(5): p. 537-43.
164. Karner, C.M., et al., *Wnt9b signaling regulates planar cell polarity and kidney tubule morphogenesis*. Nat Genet, 2009. **41**(7): p. 793-9.
165. McNeill, H., *Planar cell polarity and the kidney*. J Am Soc Nephrol, 2009. **20**(10): p. 2104-11.
166. Saburi, S., et al., *Loss of Fat4 disrupts PCP signaling and oriented cell division and leads to cystic kidney disease*. Nat Genet, 2008. **40**(8): p. 1010-5.
167. Gubb, D. and A. Garcia-Bellido, *A genetic analysis of the determination of cuticular polarity during development in Drosophila melanogaster*. J Embryol Exp Morphol, 1982. **68**: p. 37-57.
168. Wong, L.L. and P.N. Adler, *Tissue polarity genes of Drosophila regulate the subcellular location for prehair initiation in pupal wing cells*. J Cell Biol, 1993. **123**(1): p. 209-21.
169. Adler, P.N., *Planar signaling and morphogenesis in Drosophila*. Dev Cell, 2002. **2**(5): p. 525-35.
170. Strutt, D.I., *The asymmetric subcellular localisation of components of the planar polarity pathway*. Semin Cell Dev Biol, 2002. **13**(3): p. 225-31.
171. Axelrod, J.D., *Unipolar membrane association of Dishevelled mediates Frizzled planar cell polarity signaling*. Genes Dev, 2001. **15**(10): p. 1182-7.
172. Feiguin, F., et al., *The ankyrin repeat protein Diego mediates Frizzled-dependent planar polarization*. Dev Cell, 2001. **1**(1): p. 93-101.
173. Shimada, Y., et al., *Asymmetric colocalization of Flamingo, a seven-pass transmembrane cadherin, and Dishevelled in planar cell polarization*. Curr Biol, 2001. **11**(11): p. 859-63.
174. Strutt, D.I., *Asymmetric localization of frizzled and the establishment of cell polarity in the Drosophila wing*. Mol Cell, 2001. **7**(2): p. 367-75.
175. Tree, D.R., et al., *Prickle mediates feedback amplification to generate asymmetric planar cell polarity signaling*. Cell, 2002. **109**(3): p. 371-81.

176. Bastock, R., H. Strutt, and D. Strutt, *Strabismus is asymmetrically localised and binds to Prickle and Dishevelled during Drosophila planar polarity patterning*. *Development*, 2003. **130**(13): p. 3007-14.
177. Harumoto, T., et al., *Atypical cadherins Dachshous and Fat control dynamics of noncentrosomal microtubules in planar cell polarity*. *Dev Cell*, 2010. **19**(3): p. 389-401.
178. Gros, J., O. Serralbo, and C. Marcelle, *WNT11 acts as a directional cue to organize the elongation of early muscle fibres*. *Nature*, 2009. **457**(7229): p. 589-93.
179. Le Grand, F., et al., *Wnt7a activates the planar cell polarity pathway to drive the symmetric expansion of satellite stem cells*. *Cell Stem Cell*, 2009. **4**(6): p. 535-47.
180. Qian, D., et al., *Wnt5a functions in planar cell polarity regulation in mice*. *Dev Biol*, 2007. **306**(1): p. 121-33.
181. Chen, W.S., et al., *Asymmetric homotypic interactions of the atypical cadherin flamingo mediate intercellular polarity signaling*. *Cell*, 2008. **133**(6): p. 1093-105.
182. Lawrence, P.A., J. Casal, and G. Struhl, *Towards a model of the organisation of planar polarity and pattern in the Drosophila abdomen*. *Development*, 2002. **129**(11): p. 2749-60.
183. Wu, J., et al., *Wg and Wnt4 provide long-range directional input to planar cell polarity orientation in Drosophila*. *Nat Cell Biol*, 2013. **15**(9): p. 1045-55.
184. Strutt, H. and D. Strutt, *Differential stability of flamingo protein complexes underlies the establishment of planar polarity*. *Curr Biol*, 2008. **18**(20): p. 1555-64.
185. Taylor, J., et al., *Van Gogh: a new Drosophila tissue polarity gene*. *Genetics*, 1998. **150**(1): p. 199-210.
186. Adler, P.N., R.E. Krasnow, and J. Liu, *Tissue polarity points from cells that have higher Frizzled levels towards cells that have lower Frizzled levels*. *Curr Biol*, 1997. **7**(12): p. 940-9.
187. Chanut-Delalande, H., et al., *The Hrs/Stam complex acts as a positive and negative regulator of RTK signaling during Drosophila development*. *PLoS One*, 2010. **5**(4): p. e10245.
188. Weber, U., et al., *Combinatorial signaling by the Frizzled/PCP and Egfr pathways during planar cell polarity establishment in the Drosophila eye*. *Dev Biol*, 2008. **316**(1): p. 110-23.

189. Gubb, D., et al., *The balance between isoforms of the prickle LIM domain protein is critical for planar polarity in Drosophila imaginal discs*. *Genes Dev*, 1999. **13**(17): p. 2315-27.
190. Doyle, K., et al., *The Frizzled Planar Cell Polarity signaling pathway controls Drosophila wing topography*. *Dev Biol*, 2008. **317**(1): p. 354-67.
191. Hogan, J., et al., *Two frizzled planar cell polarity signals in the Drosophila wing are differentially organized by the Fat/Dachsous pathway*. *PLoS Genet*, 2011. **7**(2): p. e1001305.
192. Valentine, M. and S. Collier, *Planar cell polarity and tissue design: Shaping the Drosophila wing membrane*. *Fly (Austin)*, 2011. **5**(4): p. 316-21.
193. Adler, P.N., J. Taylor, and J. Charlton, *The domineering non-autonomy of frizzled and van Gogh clones in the Drosophila wing is a consequence of a disruption in local signaling*. *Mech Dev*, 2000. **96**(2): p. 197-207.
194. Strutt, H. and D. Strutt, *Nonautonomous planar polarity patterning in Drosophila: dishevelled-independent functions of frizzled*. *Dev Cell*, 2002. **3**(6): p. 851-63.
195. Strutt, D. and H. Strutt, *Differential activities of the core planar polarity proteins during Drosophila wing patterning*. *Dev Biol*, 2007. **302**(1): p. 181-94.
196. Filipowicz, W., S.N. Bhattacharyya, and N. Sonenberg, *Mechanisms of post-transcriptional regulation by microRNAs: are the answers in sight?* *Nat Rev Genet*, 2008. **9**(2): p. 102-14.
197. Strutt, H., V. Thomas-MacArthur, and D. Strutt, *Strabismus promotes recruitment and degradation of farnesylated prickle in Drosophila melanogaster planar polarity specification*. *PLoS Genet*, 2013. **9**(7): p. e1003654.
198. Maurer-Stroh, S., et al., *Towards complete sets of farnesylated and geranylgeranylated proteins*. *PLoS Comput Biol*, 2007. **3**(4): p. e66.
199. Daulat, A.M., et al., *Mink1 regulates beta-catenin-independent Wnt signaling via Prickle phosphorylation*. *Mol Cell Biol*, 2012. **32**(1): p. 173-85.